

DRAFT

NOAA OAR Special Report

PMEL Tsunami Forecast Series: Vol. 7

A Tsunami Forecast Model for Kahului, Hawaii

Liujuan Tang^{1,2}, Christopher D. Chamberlin^{1,2}, and Vasily V. Titov²

¹Joint Institute for the Study of the Atmosphere and Ocean (JISAO), University of Washington, Seattle, WA

²NOAA/Pacific Marine Environmental Laboratory (PMEL), Seattle, WA

June 2011



**UNITED STATES
DEPARTMENT OF COMMERCE**

**Gary Locke
Secretary**

**NATIONAL OCEANIC AND
ATMOSPHERIC ADMINISTRATION**

Jane Lubchenco
Under Secretary for Oceans
and Atmosphere/Administrator

Office of Oceanic and
Atmospheric Research

Craig McLean
Assistant Administrator

NOTICE from NOAA

Mention of a commercial company or product does not constitute an endorsement by NOAA/OAR. Use of information from this publication concerning proprietary products or the tests of such products for publicity or advertising purposes is not authorized. Any opinions, findings, and conclusions or recommendations expressed in this material are those of the authors and do not necessarily reflect the views of the National Oceanic and Atmospheric Administration.

Contribution No. 3352 from NOAA/Pacific Marine Environmental Laboratory
Contribution No. 1773 from Joint Institute for the Study of the Atmosphere and Ocean (JISAO)

Also available from the National Technical Information Service (NTIS)
(<http://www.ntis.gov>)

Contents

List of Figures	v
List of Tables	vii
Foreword	ix
Abstract	1
1 Background and Objective	1
2 Forecast Methodology	3
2.1 Construction of a tsunami source based on DART observations and tsunami source functions	3
2.2 Real-time coastal predictions by high-resolution forecast models	5
3 Model Development	7
3.1 Forecast area	7
3.2 Tsunami data and history	7
3.3 Bathymetry and topography	8
3.4 Model setup	12
4 Results and Discussion	15
4.1 Sensitivity study of model output to model setup	15
4.1.1 Sensitivity of modeled time series to grid resolutions and computational domains	15
4.1.2 Sensitivity of modeled inundation to friction coefficients .	15
4.2 Validation, verification, and testing of the forecast model	17
4.2.1 Validation	17
4.2.2 Verification	20
4.2.3 Robustness and stability tests	20
4.3 Tsunami hazard assessment from simulated magnitudes 7.5, 8.2, 8.7, and 9.3 tsunamis	20
5 Summary and Conclusions	23
6 Acknowledgments	24
7 References	25
FIGURES	29
Appendix A	61
A1. Reference model *.in file for Kahului, Hawaii	61
A2. Forecast model *.in file for Kahului, Hawaii	61
Appendix B Propagation Database: Pacific Ocean Unit Sources	63
Appendix C Synthetic Testing Report	101

C1. Purpose	103
C2. Testing Procedure	104
C3. Results	105

List of Figures

1	Overview of the Tsunami Forecast System.	31
2	Population density, Maui. (Source: 2000 Census)	32
3	A chart of Kahului.	33
4	An aerial photo of Kahului.	34
5	Forecast inundation model setups in Hawaii.	35
6	Bathymetric and topographic data source overview.	36
7	Grid setup of the reference inundation model for Kahului.	37
8	Tsunami time series computed from different grid setups at Kahului tide gauge for the 3 May 2006 Tonga tsunami.	38
9	Sensitivity of inundation and time series of tsunami amplitudes computed by the Kahului forecast model to Manning coefficients.	38
10	Observed and modeled time series of wave amplitudes at Kahului tide gauge for 17 past tsunamis.	39
11	Observed and modeled time series of wave amplitudes and wavelet-derived amplitude spectra at Kahului tide gauge up to 24 hr since tsunami generation for 17 past tsunamis.	43
12	Error of the maximum wave height, and peak wave period from observations and results computed by the Kahului forecast model. . . .	49
13	Computed maximum amplitude and current by the Kahului reference model and forecast model for the 16 past tsunamis.	50
14	Modeled tsunami time series by the Kahului reference and forecast models for 18 synthetic magnitude 9.3 tsunamis.	56
15	Maximum water elevation computed by the Kahului reference model and forecast model for 18 synthetic magnitude 9.3 tsunamis.	57
16	Maximum water elevation at 4951-m water depth offshore Kahului from the propagation database (magnitude 7.5) and at Kahului tide station computed by the forecast model at approximately 2 m water depth for synthetic magnitude 7.5, 8.2, 8.7, and 9.3 tsunamis.	58
17	Computed maximum water elevation at offshore deep water (4951 m) and Kahului tide station (~2 m) in logarithmic and Cartesian coordinates.	59
B1	Aleutian-Alaska-Cascadia Subduction Zone unit sources.	65
B2	Central and South America Subduction Zone unit sources.	71
B3	Eastern Philippines Subduction Zone unit sources.	79
B4	Kamchatka-Kuril-Japan-Izu-Mariana-Yap Subduction Zone unit sources.	81
B5	Manus-Oceanic Convergent Boundary Subduction Zone unit sources.	87
B6	New Guinea Subduction Zone unit sources.	89
B7	New Zealand-Kermadec-Tonga Subduction Zone unit sources.	91
B8	New Britain-Solomons-Vanuatu Subduction Zone unit sources.	95
B9	Ryukyu-Kyushu-Nankai Subduction Zone unit sources.	99

List of Tables

1	Tsunami source functions in the Pacific, Atlantic, and Indian oceans.	4
2	Historical events used for model validation for Kahului, Hawaii.	9
3	Data sources used for grid development.	10
4	MOST setup of the reference and forecast models for Kahului, Hawaii	13
5	Model speed and accuracy for different setups in Fig. 8 for Kahului for the May 2006 Tonga tsunami.	16
6	Simulated tsunamis for hazard assessment study for Kahului.	21
B1	Earthquake parameters for Aleutian-Alaska-Cascadia Subduction Zone unit sources	66
B2	Earthquake parameters for Central and South America Subduction Zone unit sources.	72
B3	Earthquake parameters for Eastern Philippines Subduction Zone unit sources.	80
B4	Earthquake parameters for Kamchatka-Kuril-Japan-Izu-Mariana-Yap Subduction Zone unit sources.	82
B5	Earthquake parameters for Manus-Oceanic Convergent Boundary Subduction Zone unit sources.	88
B6	Earthquake parameters for New Guinea Subduction Zone unit sources	90
B7	Earthquake parameters for New Zealand-Kermadec-Tonga Subduction Zone unit sources.	92
B8	Earthquake parameters for New Britain-Solomons-Vanuatu Subduction Zone unit sources.	96
B9	Earthquake parameters for Ryukyu-Kyushu-Nankai Subduction Zone unit sources.	100
C1	Synthetic forecast model scenarios for Kahului, Hawaii.	105
C2	Maximum and minimum amplitudes at the Kahului, Hawaii, warning point for synthetic and historical events tested using SIFT.	106

Foreword

Tsunamis have been recognized as a potential hazard to United States coastal communities since the mid-twentieth century, when multiple destructive tsunamis caused damage to the states of Hawaii, Alaska, California, Oregon, and Washington. In response to these events, the United States, under the auspices of the National Oceanic and Atmospheric Administration (NOAA), established the Pacific and Alaska Tsunami Warning Centers, dedicated to protecting United States interests from the threat posed by tsunamis. NOAA also created a tsunami research program at the Pacific Marine Environmental Laboratory (PMEL) to develop improved warning products.

The scale of destruction and unprecedented loss of life following the December 2004 Sumatra tsunami served as the catalyst to refocus efforts in the United States on reducing tsunami vulnerability of coastal communities, and on 20 December 2006, the United States Congress passed the “Tsunami Warning and Education Act” under which education and warning activities were thereafter specified and mandated. A “tsunami forecasting capability based on models and measurements, including tsunami inundation models and maps...” is a central component for the protection of United States coastlines from the threat posed by tsunamis. The forecasting capability for each community described in the *PMEL Tsunami Forecast Series* is the result of collaboration between the National Oceanic and Atmospheric Administration office of Oceanic and Atmospheric Research, National Weather Service, National Ocean Service, National Environmental Satellite, Data, and Information Service, the University of Washington’s Joint Institute for the Study of the Atmosphere and Ocean, National Science Foundation, and United States Geological Survey.

NOAA Center for Tsunami Research

PMEL Tsunami Forecast Series: Vol. 7

A Tsunami Forecast Model for Kahului, Hawaii

L. Tang^{1,2}, C.D. Chamberlin^{1,2}, and V.V. Titov²

Abstract. This study describes the development, validation, and testing of a tsunami forecast model for Kahului, Hawaii. Based on the Method of Splitting Tsunamis (MOST) model, the forecast model is capable of simulating 4 hr of tsunami wave dynamics at a resolution of 2 arc sec (~ 60 m) in 10 min of computational time. A reference inundation model of higher resolution of 1/3 arc sec (~ 10 m) was also developed in parallel, to provide modeling references for the forecast model. Both models were tested for 17 past tsunamis and a set of 18 synthetic magnitude 9.3 tsunamis.

Based on 14 historical tsunami water level records at Kahului tide station, the accuracy of the maximum wave height computed by the forecast model is greater than 80% when the observed maximum wave height is greater than 1.0 m, and 50% while the observation is between 0.3 and 1.0 m. The error of the modeled arrival time of the first peak is within 3% of the travel time. Wavelet analyses indicate that the peak wave period at the station mainly falls into one of three local resonant periods: near 16, 24, or 34 min (± 2 min). The peak wave period is relevant to the geographic location of the tsunami sources. The good agreement between the model computations and observations, along with the numerical consistency between the model results for the maximum amplitude and velocity, provide a quantitative validation and reliable robustness and stability testing of the forecast model.

The validated Kahului forecast model was further applied to hazard assessment from 1,884 scenarios of synthetic magnitude 7.5, 8.2, 8.7, and 9.3 tsunamis based on subduction zone earthquakes in the Pacific. The results show an impressive local variability of tsunami amplitudes even for far-field tsunamis, and indicate the complexity of forecasting tsunami amplitudes at a coastal location. It is essential to use high-resolution models in order to provide accuracy that is useful for coastal tsunami forecasts for practical guidance.

1. Background and Objective

The Center for Tsunami Research at the National Oceanic and Atmospheric Administration (NOAA)'s Pacific Marine Environmental Laboratory (PMEL) has developed a tsunami forecasting system for operational use by NOAA's two Tsunami Warning Centers located in Hawaii and Alaska (Titov *et al.*, 2005; Titov, 2009). The forecast system combines real-time deep-ocean tsunami measurements from Deep-ocean Assessment and Reporting of Tsunamis (DART) stations (González *et al.*, 2005; Bernard *et al.*, 2006; Bernard and Titov, 2007) with the Method of Splitting Tsunamis (MOST) model, a suite of finite difference numerical codes based on nonlinear long-wave approximation (Titov and Synolakis, 1998; Titov and González, 1997; Synolakis *et al.*, 2008) to produce real-time forecasts of tsunami arrival time, heights, periods, and inundation. To achieve accurate and detailed forecasts of tsunami impact for specific sites, high-resolution tsunami forecast models are under development for United States coastal communities at risk (Tang *et al.*, 2009a;b). The resolution of these models has to be high enough to resolve the dynamics of a tsunami inside a particular harbor, including influences of major harbor structures such as

¹Joint Institute for the Study of the Atmosphere and Ocean, University of Washington, Seattle, WA

²NOAA, Pacific Marine Environmental Laboratory, Seattle, WA

breakwaters. These models have been integrated as crucial components into the forecast system.

Presently, a system of 41 (33 U.S.-, 1 Russian-, 1 Chilean-, and 6 Australian-owned) DART stations is monitoring tsunami activity in the Pacific Ocean. Globally, the network consists of 52 stations deployed in the Atlantic Ocean, the Pacific Ocean, and the Gulf of Mexico. The precomputed propagation models currently have 1,106 scenarios to cover Pacific tsunami sources (1,691 globally), and the high-resolution forecast inundation models are now set up for 67 U.S. coastal communities. The fully implemented system will use real-time data from the DART network to provide high-resolution tsunami forecasts for at least 75 communities in the U.S. by 2013 (Titov, 2009). Since its first testing in the 17 November 2003 Rat Island tsunami, the forecast system has produced experimental real-time forecasts for 18 tsunamis in the Pacific and Indian oceans (Titov *et al.*, 2005; Wei *et al.*, 2008; Titov, 2009; National Center for Tsunami Research, 2010). The forecast methodology has also been tested with the data from nine additional events that produced the deep-ocean data.

Kahului, Hawaii, is located on the north shore of the island of Maui, the third largest in the Hawaiian Island chain. With a population greater than 20,000 (2000 census), Kahului is the largest community on Maui, whose entire resident population is estimated at greater than 145,000 (quickfacts.census.gov/qfd/states/15/15009.html). **Figure 2** details the population density of Kahului, indicating a high concentration of people living along the coast and inland alike, in contrast to the major population centers of Kahana, Lahaina, and Kihei, whose populations reside predominately along the coast. In addition to a large resident population, Kahului hosts Maui's main airport, Kahului Airport, as well as the deep-draft Kahului harbor, Maui's shopping center, and various tourist attractions. A bathymetric chart showing basic Kahului infrastructure and offshore bathymetry, including the extensive offshore reef, is shown in **Figure 3**. An aerial photo of the region is shown in **Figure 4**.

This report describes the development, testing, and application of the Kahului forecast model. The objective in developing this model is to provide NOAA's Tsunami Warning Centers with the ability to assess danger posed to Kahului following tsunami generation in the Pacific Ocean Basin in order to produce accurate and timely forecasts, enabling the community to respond appropriately. A secondary objective is to explore the potential tsunami impact on the city of Kahului from earthquakes at major subduction zones in the Pacific using the developed forecast model. Wavelet analysis was applied to investigate Kahului harbor and local responses to tsunami waves.

The report is organized as follows. Section 2 briefly introduces NOAA's tsunami forecast methodology. Section 3 describes the model development. Section 4 presents the results and discussion, which includes sensitivity of the forecast model to model setup and friction coefficients, model validation, verification, and testing for past and synthetic tsunamis, and a tsunami hazard assessment study using the validated forecast model. Section 5 provides a summary and conclusion.

2. Forecast Methodology

NOAA's real-time tsunami forecasting scheme is a process comprised of two steps: (1) constructing a tsunami source via inversion of DART observations with precomputed tsunami source functions, and (2) generating coastal predictions by running high-resolution forecast models in real time (Titov *et al.*, 1999; 2005; Tang *et al.*, 2009b). The DART-constrained tsunami source, the corresponding offshore scenario from the tsunami source function database, and the high-resolution forecast models cover the evolution of earthquake-generated tsunamis (generation, propagation, and coastal inundation), providing a complete tsunami forecast capability.

2.1 Construction of a tsunami source based on DART observations and tsunami source functions

Several real-time data sources, including seismic, coastal tide gauge, and deep-ocean data, have been used for tsunami warning and forecast (Satake *et al.*, 2008; Whitmore, 2003; Titov, 2009). NOAA's strategy for real-time forecasting is to use deep-ocean measurements at DART stations as the primary data source because of several key features: (1) Unlike the indirect seismic data, DART stations provide a direct measure of tsunami waves. (2) The deep-ocean tsunami measurements are, in general, the earliest tsunami information available, since tsunamis propagate much faster in the deep ocean than in shallow coastal areas, where coastal tide gauges are used for tsunami measurements. (3) Compared to coastal tide gauges, DART data with a high signal-to-noise ratio can be obtained without interference from harbor and local shelf effects. (4) Wave dynamics of tsunami propagation in deep ocean are assumed to be linear, allowing application of efficient inversion schemes (Liu, 2009).

Time series of tsunami observations in the deep ocean can be decomposed into a linear combination of a set of tsunami source functions in the time domain by a linear least squares method. We call coefficients obtained through this inversion process tsunami-derived source coefficients. The magnitude computed from the sum of the moment of tsunami source functions multiplied by the corresponding coefficients is referred to as the tsunami-derived moment magnitude (to distinguish it from the seismic moment magnitude M_w , which is the magnitude of the associated earthquake source). While the seismic and tsunami sources are in general not the same, this approach provides a link between the seismically derived earthquake magnitude and the observation-derived tsunami magnitude.

During real-time tsunami forecasts, seismic waves propagate much faster than tsunami waves, so the initial seismic magnitude can be estimated before the DART measurements are available. Since time is of the essence, the initial tsunami forecast is based only on the seismic magnitude. The magnitude will

Table 1: Tsunami source functions in the Pacific, Atlantic, and Indian oceans.

Subduction Zone			Tsunami Source Functions	
No.	Abbr.	Name	Line/Zone	Numbers
1	ACSZ	Aleutian-Alaska-Canada-Cascadia	BAZYXW	184
2	CSSZ	Central-South America	BAZYX	382
3	EPSZ	East Philippines	BA	44
4	KISZ	Kamchatka-Kuril-Japan Trench-Izu Bonin-Marianas-Yap	BAZYXWV	222
5	MOSZ	Manus Ocean Convergence Boundary	BA	34
6	NVSZ	New Britain-Solomons-Vanuatu	BA	74
7	NGSZ	North New Guinea	BA	30
8	NTSZ	New Zealand-Kermadec-Tonga	BA	78
9	NZSZ	South New Zealand	BA	14
10	RNSZ	Ryukyu-Kyushu-Nankai	BA	44
			Subtotal:	1106
11	ATSZ	Atlantic	BA	214
12	SSSZ	South Sandwich	BA	22
			Subtotal:	236
13	IOSZ	Adam-Nicobar-Sumatra-Java	BAZYXW	307
14	MKSZ	Makran	BA	20
15	WPSZ	West Philippines	BA	22
			Subtotal:	349
			Total:	1691

update the forecast when it is available via DART inversion using the tsunami source function database.

Titov *et al.* (1999; 2001) conducted sensitivity studies on far-field deep-water tsunamis to different parameters of the elastic deformation model described in Gusiakov (1978) and Okada (1985). The results showed that source magnitude and location essentially define far-field tsunami signals for a wide range of subduction zone earthquakes. Other parameters have secondary influence and can be pre-defined during forecast. Based on these results, tsunami source function databases for the Pacific, Atlantic, and Indian oceans have been built using pre-defined source parameters, length = 100 km, width = 50 km, slip = 1 m, rake = 90, and rigidity = 4.5×10^{10} N/m². Other parameters are location-specific; details of the databases are described in Gica *et al.* (2008). Each tsunami source function is equivalent to a tsunami from a typical Mw 7.5 earthquake with defined source parameters. Locations of tsunami source functions in the Pacific Ocean are shown in the **Figure 1** overview of the tsunami forecast system map.

The database can provide offshore forecasts of tsunami amplitudes and all other wave parameters immediately once the inversion is complete. The tsunami source, which combines real-time tsunami measurements with tsunami source functions, provides an accurate offshore tsunami scenario without additional time-consuming model runs.

2.2 Real-time coastal predictions by high-resolution forecast models

High-resolution forecast models are designed for the final stage of the evolution of tsunami waves: coastal runup and inundation. Once the DART-constrained tsunami source is obtained (as a linear combination of tsunami source functions), the precomputed time series of offshore wave height and depth-averaged velocity from the model propagation scenario are applied as the dynamic boundary conditions for the forecast models. This saves the simulation time of basin-wide tsunami propagation. Tsunami inundation is a highly nonlinear process; therefore, a linear combination would not, in general, provide accurate solutions. A high-resolution model is also required to resolve shorter tsunami wavelengths nearshore with accurate bathymetric/topographic data. The forecast models are constructed with the Method of Splitting Tsunamis (MOST) model, a finite difference tsunami inundation model based on nonlinear shallow-water wave equations (Titov and González, 1997). Each forecast model contains three telescoping computational grids with increasing resolution, covering regional, intermediate, and nearshore areas. Runup and inundation are computed at the coastline. For example, **Figure 5** shows forecast model setup for several tsunami forecast models in Hawaii, detailing the telescoping grids used:

1. One regional grid of 2-arc-min (~3600 m) resolution covers the main Hawaiian Islands (**Figure 5a**).
2. Four intermediate grids of 12 to 18 arc sec (~360–540 m) for four natural geographic areas (**Figures 5b, 1–4**):
 - (a) Ni’ihau, Ka’ula Rock, and Kauai (Kauai complex);
 - (b) Oahu;
 - (c) Molokai, Maui, Lanai, and Kaho’olawe (the Maui Complex);
 - (d) Hawaii.
3. Each intermediate grid contains 2-arc-sec (~60 m) nearshore grids (**Figures 5c, 1–4**).

The highest-resolution grid includes the population center and tide stations for forecast verification. The grids are derived from the best available bathymetric/topographic data at the time of development, and will be updated as new survey data become available.

The forecast models are optimized for speed and accuracy. By reducing the computational areas and grid resolutions, each model is optimized to provide 4-hr event forecasting results in minutes of computational time using a single processor while still providing good accuracy for forecasting. To ensure forecast accuracy at every step of the process, the model outputs are validated with historical tsunami records and compared to numerical results from a reference inundation model with higher resolutions and larger computational domains. In order to provide warning guidance for a long duration during a tsunami event, each forecast model has been tested to output up to 24-hr of simulation since tsunami generation.

3. Model Development

3.1 Forecast area

The main Hawaiian Islands are the younger, southern portion of the Hawaii Archipelago. From northwest to southeast, the islands form four natural geographic groups by shared channels and inter-island shelves, including

1. Ni'ihau, Ka'ula Rock, and Kauai (Kauai complex);
2. Oahu;
3. Molokai, Maui, Lanai, and Kaho'olawe (the Maui Complex); and
4. Hawaii.

The coastal geological features around the Island of Maui are complex. Separated by three channels, the smaller islands of Molokai, Lanai, and Kaho'olawe are located northwest, west, and south of Maui, respectively (**Figure 7b**). The three channels Pailolo, Auau, and Alalakeiki have narrow widths of 12.9 km (8 mi), 15 km (9.2 mi), and 11 km (7 mi), respectively. Most places along the channels are shallow, with water depth less than 300 m. Sections of the Auau Channel, connecting Maui and Lanai, are less than 50 m deep. To the southeast, the 48-km-wide (26 mi), 2-km-deep Alenuihaha Channel separates Maui from the Island of Hawaii. Maui is unprotected against waves from the north and northeast.

The Kahului nearshore is gently embayed, with an average slope of 0.016 from the 0- to 500-m depth contour. On the land, the two volcanoes that are Maui's dominant geological features, the East Haleakala and the West Maui Mountains, are united by a narrow flat isthmus. The isthmus is 11 km (7 mi) across and no higher than 40 m. Most of the northern coast of Maui consists of cliffs. Coral reefs in water of 0.3 to 0.9 m (1 to 3 ft) are as much as 1.8-km (1.2 mi) wide in the study area, which covers the coastal communities of Kahului, Wailuku, and Waiehu along the north shore of central Maui, Hawaii. The location of the Kahului tide station, identified on the map in **Figure 3**, is chosen as the warning point.

3.2 Tsunami data and history

Established 19 December 1946 in Kahului Harbor, Kahului tide station has provided valuable records of historical tsunamis (**Table 2**). A gas-purging pressure tide gauge, also known as the bubbler gauge, was installed in 1946. In the mid-1970s this equipment was replaced with an ADR (Analog to Digital Recorder) that recorded the height of water level at 6-min intervals. In February 1989, Kahului gauge was then replaced with the Next Generation Water Level Measurement System. The new primary water level sensor is an air acoustic measurement device. It is self-calibrating for variations in the speed of sound, and

can be leveled directly to a local benchmark that provides absolute measurements referenced to local water-level datum. It employs a less restrictive protective well with parallel plates, which only screens out waves with a period shorter than 2–3 sec. The new system's data sampling procedures in conjunction with the open protective well is a significant improvement over the old (NOAA/NOS, 1991). In 2005, the Kahului tide station was named one of the tsunami-capable tide stations by NOS/CO-OPS, with new hardware and software to enable collection and dissemination of 1-min water-level sample data (<http://tidesandcurrents.noaa.gov/1mindata.shtml>). The stations also sample 15-sec data, which can be downloaded as needed. The mean high water (MHW) at the Kahului tide station is 1.313 m and the mean sea level (MSL) is 1.075 m on the station datum (<http://tidesandcurrents.noaa.gov/>). The mean tide range is 0.478 m.

Kahului has a long history of destructive tsunamis. The earliest recorded tsunami at Kahului was on 7 November 1837, when the sea first receded horizontally 36 m before a wall of returning water generated by a wave originating in southern Chile engulfed inhabitants who were collecting stranded fish, killing two (Pararas-Carayannis, 1969). Twenty-six grass houses were swept 240 m inland. Since 1813, 54 tsunamis have been observed in Kahului. Many of them caused significant damage.

On 3 February 1923, a tsunami originated from East Kamchatka caused “heavy damage in Kahului and the east coast of Maui.” (Pararas-Carayannis, 1969) The 1 April 1946 Unimak Island tsunami marked the highest tsunami runup records in the study area. Coral blocks as large as 1.2 m (4 ft) in diameter were thrown on shore just east of the breakwater (Shepard *et al.*, 1950). At Spreckelsville, the wave reached an elevation of 8.5 m (28 ft) and swept inland as much as 244 m (800 ft). On 4 November 1952 “the Kahului-Spreckelsville region suffered the greatest damage” from a tsunami originating in East Kamchatka (Pararas-Carayannis, 1969). On 9 March 1957, the Andrianov tsunami event exceeded the Kahului gauge limit of 1.7 m, resulting in considerable damage along the northeast of the Island of Maui (Salsman, 1959; Fraser *et al.*, 1959). Then, on 22 May 1960, the maximum wave height of the South Chile tsunami exceeded the new gauge limit of 2.8 m (Pararas-Carayannis, 1969), and on 28 March 1964, the Alaska-generated tsunami produced a maximum wave height of 3.35 m at the Kahului gauge, flooding a waterfront shopping center and causing \$52,590 worth of damage to Kahului (Pararas-Carayannis, 1969).

As a population center that has repeatedly been affected by Pacific tsunamis, Kahului is in need of a forecast model to aid site-specific evacuation decisions.

3.3 Bathymetry and topography

Tsunami inundation modeling requires accurate topography and bathymetry in coastal and nearshore areas. Two gridded digital elevation models (DEMs) were developed: a bathymetric DEM at medium resolution (6 arc sec) for wave transformation from the open ocean to coastal areas, and a high-resolution (1/3-arc-sec) topography and bathymetry DEM for modeling wave runup and

Table 2: Historical events used for model validation for Kahului, Hawaii.

Event	Earthquake information				Tsunami information		
	USGS Epicenter	Date Time (UTC)	CMT Centroid	Date Time (UTC)	Magnitude Mw	Tsunami Magnitude ¹	Subduction Zone
1–2011 Japan	11 Mar 05:46:23 38.322° N 142.369° E	11 Mar 03:47:32.8 37.52° S 143.05° E	9.1	8.8	Kamchatka-Kuril-Japan-Izu-Mariana-Yap (KISZ)	34.66 × b24 + 12.23 × b25 + 26.31 × a26	
2–2010 Chile	27 Feb 06:34:14 35.909° S 72.733° W	27 Feb 06:35:15.4 35.95° S 73.15° W	2.8.8	8.8	Central-South America (CSSZ)	+ 21.27 × b26 + 22.75 × a27 + 4.98 × b27	
3–2009 Samoa	29 Sep 17:48:10 15.509° S 172.034° W	29 Sep 17:48:26.8 15.13° S 171.97° W	2.8.1	8.1	New Zealand-Kermadec-Tonga (NTSZ)	3 a88 × 17.24 + a90 × 8.82 + b88 × 11.86	
4–2007 Peru	15 Aug 23:40:57 13.354° S 76.509° W	15 Aug 23:41:57.9 13.73° S 77.04° W	2.8.0	8.1	Central-South America (CSSZ)	+ b89 × 18.39 + b90 × 16.75 + z88 × 20.78	
5–2007 Kuril	13 Jan 04:23:20 46.272° N 154.455° E	13 Jan 04:23:48.1 46.17° N 154.80° E	2.8.1	7.9	Kamchatka-Kuril-Japan-Izu-Mariana-Yap (KISZ)	+ z90 × 7.06	
6–2006 Kuril	15 Nov 11:14:16 46.607° N 153.230° E	15 Nov 11:15:08 46.71° N 154.33° E	2.8.3	8.1	Kamchatka-Kuril-Japan-Izu-Mariana-Yap (KISZ)	3.96 × a34 + 3.96 × b34	
7–2006 Tonga	03 May 15:26:39 20.13° S 174.164° W	03 May 15:27:03.7 20.39° S 173.47° W	2.8.0	8.0	New Zealand-Kermadec-Tonga (NTSZ)	3.41 × a9 + 4.32 × b9	
8–2003 Rat Island	17 Nov 06:43:07 51.13° N 178.74° E	17 Nov 06:43:31.0 51.14° N 177.86° E	2.7.7	7.8	Aleutian-Alaska-Cascadia (ACSZ)	-3.64 × b13	
9–2003 Hokkaido	25 Sep 19:50:06 41.775° N 143.904° E	25 Sep 19:50:38.2 42.21° N 143.84° E	2.8.3	8.0	Kamchatka-Kuril-Japan-Izu-Mariana-Yap (KISZ)	3.4 × a12 + 0.5 × b12 + 2 × a13 + 1.5 × b13	
10–2001 Peru	23 Jun 20:33:14 16.265° S 73.641° W	23 Jun 20:34:23.3 17.28° S 72.71° W	2.8.4	8.2	Central-South America (CSSZ)	6.6 × b29	
11–1996 Andeanov	10 Jun 04:03:35 51.56° N 175.39° W	10 Jun 04:04:03.4 51.10° N 177.41° W	2.7.9	7.8	Aleutian-Alaska-Cascadia (ACSZ)	3.281 × b11	
12–1994 East Kuril	04 Oct 13:22:58 43.73° N 147.321° E	04 Oct 13:23:28.5 43.60° N 147.63° E	2.8.3	8.1	Kamchatka-Kuril-Japan-Izu-Mariana-Yap (KISZ)	3.6 m × (100 × 100 km)	
13–1964 Alaska	28 Mar 03:36:00 61.02° N 147.65° W	28 Mar 03:36:14 61.10° N 147.50° W	4.9.2	9.0	Aleutian-Alaska-Cascadia (ACSZ)	109#rake, 20#dip, 230#strike, 25 m depth	
14–1960 Chile	22 May 19:11:14 38.29° S 73.05° W	22 May 19:11:14 39.50° S 74.50° W	4.9.5		Central-South America (CSSZ)	5.7 × a15 + 2.9 × b16 + 1.98 × a16	
15–1957 Andeanov	09 Mar 14:22:31 51.56° N 175.39° W	09 Mar 14:22:31.9 51.292° N 175.629° W	4.8.6	8.7	Aleutian-Alaska-Cascadia (ACSZ)	2.40 × a15 + 0.80 × b16	
16–1952 Kamchatka	04 Nov 16:58:26.0 52.76° N 160.06° E	04 Nov 16:58:26.0 52.75° N 159.50° E	4.9.0	8.7	Kamchatka-Kuril-Japan-Izu-Mariana-Yap (KISZ)	—	
17–1946 Unimak	01 Apr 12:28:56 52.75° N 163.50° W	01 Apr 12:28:56 53.32° N 163.19° W	5.8.5	8.5	Aleutian-Alaska-Cascadia (ACSZ)	31.4 × a15 + 10.6 × a16 + 12.2 × a17	

¹Preliminary source—Derived from deep-ocean observations except the 2003 Hokkaido tsunami and the five tsunamis from 1946 to 1964.²Global CMT catalog (<http://www.globalcmt.org/CMTsearch.html>)³Tsunami source was obtained in real time and applied to the forecast⁴United States Geological Survey (USGS)⁵López and Okal (2006)

Table 3: Data sources used for grid development.

Data Provider	Data Type	Survey Dates	Description
Joint Airborne Lidar Bathymetry Technical Center of Expertise (JALBTCX)	Points	1999–2000	Nearshore bathymetry and topography from SHOALS airborne LIDAR. 1–5-m horizontal resolution.
Monterey Bay Aquarium Research Institute (MBARI)	Grid	1998	Multibeam bathymetric surveys. 10–30-m horizontal resolution.
USGS Pacific Seafloor Mapping Project	Grid	1998	Multibeam bathymetric surveys. 8-m resolution.
Japan Agency for Marine-Earth Science and Technology (JAMSTEC)	Grid	1998–2002	Multibeam bathymetric surveys. 150-m horizontal resolution. Multibeam track-lines at varying resolutions.
United States Navy	Point	2000	Multibeam surveys, south and west sides of Oahu.
United States Army Corps of Engineers, Honolulu District (USACE)	Point	2000–2005	Digital echosounder surveys in USACE harbor project areas.
National Geophysical Data Center (NGDC)	Point	1968–1992	Bathymetric survey data. Multiple technologies, including lead line, digital echosounder, and multibeam.
National Ocean Service (NOS)	Point	1979–1989, 2005	Older bathymetric data points digitized from NOS nautical charts. Recent points imported from Electronic Navigational Charts (ENCs).
Smith and Sandwell (1997)	Point	1997	2-min resolution bathymetry derived from satellite altimetry and ship track-lines.
USGS Geological Long-Range Inclined Asdic (GLORIA)	Point	1986–1988	Sidescan sonar bathymetric surveys in deep-water regions of Hawaii's EEZ.
NOAA Coastal Services Center	Grid	2005	IfSAR (radar altimetry) topographic survey. Gridded to 5-m horizontal resolution.
USGS National Elevation Dataset	Grid	Varies	10-m resolution topographic data derived from USGS DEMs

inundation onto dry land. The grids were constructed using data available from several sources. An overview of the spatial extent covered by all data used in the construction of the Kahului tsunami forecast model is provided in **Figure 6**. In areas where multiple datasets overlapped, newer and higher-resolution datasets were preferred, and superseded datasets were used for comparison and verification. **Table 3** is an overview of the data sources used. Source details for the datasets incorporated into the model grids:

- Joint Airborne Lidar Bathymetry Technical Center of Expertise (JALBTCX), U.S. Army Corps of Engineers, Mobile District. Online reference: http://shoals.sam.usace.army.mil/hawaii/pages/Hawaii_Data.htm.
- Monterey Bay Aquarium Research Institute (MBARI) Hawaii Multibeam Survey, Version 1. Online reference: <http://www.mbari.org/data/mapping/hawaii/>.
- USGS Pacific Seafloor Mapping Project. Online reference: <http://walrus.wr.usgs.gov/pacmaps/data.html>.

- Japan Agency for Marine-Earth Science and Technology (JAMSTEC) 1998–1999 multibeam bathymetric surveys. Published in: Takahashi, E. *et al.* (eds.) (2002): *Hawaiian Volcanoes: Deep Underwater Perspectives*. American Geophysical Union Monograph 128.
JAMSTEC trackline data was recorded by the R/V *Mirai* during transits in 1999 and 2002. Online reference: http://www.jamstec.go.jp/mirai/index_eng.html.
- United States Army Corps of Engineers (USACE), Honolulu District. Online reference: <http://www.poh.usace.army.mil/>.
- NOAA National Geophysical Data Center (NGDC). Online reference: http://www.ngdc.noaa.gov/mgg/gdas/gd_sys.html.
- NOAA National Ocean Service (NOS). Sounding points were digitized from NOS nautical charts 19347, 19358, 19359, 19364, 19366, 19342, 19381, and 19324. Sounding data from electronic chart (ENC) 19357 was used. This data was included in relatively shallow regions where other data sources were sparse or unavailable, or for quality control of other sources.
- Smith, W.H.F., and D.T. Sandwell, Global seafloor topography from satellite altimetry and ship depth soundings, *Science*, 277, 1957–1962, 26 September 1997. Online reference: http://topex.ucsd.edu/WWW_html/mar_topo.html.
- USGS Geological Long-Range Inclined Asdic (GLORIA) surveys. Online data reference: <http://walrus.wr.usgs.gov/infobank/>.
- NOAA Coastal Services Center. <http://www.csc.noaa.gov/>. The IfSAR topographic data was collected and processed for CSC by Intermap Technologies Inc. The data is subject to a restrictive license agreement and is not publicly available.
- USGS National Elevation Dataset. Online reference: <http://seamless.usgs.gov/>.

The SHOALS LIDAR project, which provides high-resolution unified topographic and bathymetric data for the nearshore areas of several Hawaiian Islands, including all of Maui, was essential for accurate modeling of reef and intertidal regions where conventional bathymetric survey data is usually coarse or unavailable. Quality data in this region is especially essential because bathymetric inaccuracies have a great impact on tsunami wave dynamics in shallow water. The 2005 NOAA CSC IfSAR survey of Maui provided similarly valuable high-resolution topography for the entire island, ensuring confidence in the prediction of the extent of inundation. The USGS National Elevation Dataset (NED) was used on islands outside of the study area.

High-resolution gridded datasets derived from multibeam surveys are available for many parts of the archipelago and were used wherever available. In deep water, where high-resolution multibeam data was not available, the grid was developed by interpolation of a combination of USGS GLORIA surveys and the Smith and Sandwell 2-min global seafloor dataset.

All selected input datasets were converted to the MHW vertical datum as necessary. Bathymetric datasets were converted from the survey tidal datum (usually MLLW or MSL) using offset surfaces interpolated from NOS tide gauges

at Kahului, Kawaihae (Hawaii), and Kaunakakai (Molokai). The CSC IfSAR topographic data as obtained was vertically referenced to the GRS80 ellipsoid. It was converted to MHW using an offset surface interpolated from seven National Geodetic Survey (NGS) benchmark stations on Maui that had ellipsoid and tidal heights recorded.

Raw data sources were imported to ESRI ArcGIS-compatible file formats. Horizontal positions were re-projected, where necessary, to the WGS84 horizontal geodetic datum using ArcGIS. In the point datasets, single sounding points that differed substantially from neighboring data were removed. Gridded datasets were checked for extreme values by examination of contour lines, and, where available, by comparison with other data sources.

To compile the multiple data sources into a single grid, subsets of the source data were created in the priority order described above. A triangulated irregular network (TIN) was created from the detided vector point data (geodas, usace, csc_lidar). Also added to the TIN were points taken from the edges of the gridded data regions to ensure a smooth interpolated transition between areas with different data sources. This TIN was linearly interpolated using ArcGIS 3D Analyst to produce an intermediate 1-arc-sec and 6-arc-sec raster grid. The gridded datasets were then bilinearly resampled to these resolutions and overlaid on top of the intermediate grids.

3.4 Model setup

By subsampling the digital elevation models described in section 3.2, two sets of computational grids were derived: the Kahului reference model, for which grid extents are shown in **Figure 7**, and the optimized tsunami forecast model (**Figures 5.a.1, 5.b.3, and 5.c.3**). Each set consists of three levels of telescoped grids with increasing resolution. The regional grids cover the major Hawaiian Islands, and the coastal grids cover Maui, Lanai, Kaho'olawe, and East Molokai. Runup and inundation simulations are on the coastline in the nearshore grids. In **Figure 7**, the solid red boxes indicate boundaries of the nested reference model grids, while the dashed red boxes represent the corresponding boundaries of the forecast model. Grid details and input parameters at each level are summarized in **Table 4**. In the forecast nearshore grid (2" resolution), the water depth of the closest wet node to the Kahului tide station (203.531296°E 20.894629°N) is approximately 2 m.

To reduce numerical instability for certain worst-case scenarios, a large Manning coefficient may be required. The friction coefficient does not change the offshore results. Its effect on model inundation will be discussed in section 4.1.2. For a simulation of a 4-hr event, the optimized forecast model takes less than 10 min of CPU time on a Linux system using a single 3.6 GHz Xeon processor, while the reference model takes about 41 hr.

The bathymetry and topography used in the development of this forecast model was considered by the authors a good representation of the local topography/bathymetry. As new digital elevation models become available, forecast models will be updated and report updates will be posted at http://nctr.pmel.noaa.gov/forecast_reports/.

Table 4: MOST setup of the reference and forecast models for Kahului, Hawaii.

Grid	Region	Reference Model				Forecast Model			
		Coverage	Cell Size	nx	Time Step	Coverage	Cell Size	nx	Time Step
		Lat. [$^{\circ}$ N]	\times	ny	[sec]	Lat. [$^{\circ}$ N]	\times	ny	[sec]
A	Hawaii	18–23 199–205.98	36 × 36	699 × 500	1.6	18.0317–22.9983 199–205.9667	120 × 120	210 × 150	12
B	Maui Complex	20.4–21.3933 202.5717–204.098	6 × 6	917 × 597	0.4	20.4017–21.255 202.8967–204.0967	12 × 12	361 × 257	1.5
C	Kahului	20.8364–20.975 203.4681–203.71	1/3 × 1/3	2613 × 1498	0.2	20.8674–20.9507 203.4869–203.6319	2 × 2	262 × 151	1.5
Minimum offshore depth [m]		1				1			
Water depth for dry land [m]		0.1				0.1			
Manning coefficient, n		0.01, 0.025, 0.032				0.01, 0.025			
CPU time for a 4-hr simulation		~41 hr				<10 min			

Computations were performed on a single Intel Xeon processor at 3.6 GHz, Dell PowerEdge 1850.

4. Results and Discussion

4.1 Sensitivity study of model output to model setup

How sensitive are the model outputs, including time series and inundation, to changes in the grid resolution, computational domains, accuracy of bathymetry/topography, and other parameters? This issue is central to the forecast model development, since inappropriate model setup or inaccurate bathymetry/topography can produce poor results.

4.1.1 Sensitivity of modeled time series to grid resolutions and computational domains

Figure 8 and **Table 5** show how the changes of grid setup affect the model accuracy and speed at Kahului for the May 2006 Tonga tsunami. The grids for setups 1, 2, and 3 in **Table 5** were derived from the same DEMs developed in 2005. Setups 1 and 2 are the first and revised Kahului forecast model. Setup 3 was the first Kahului reference inundation model. Prior to the 3 May 2006 Tonga tsunami, the forecast model setup 1 was tested with six past tsunamis: 2003 Rat Island, 2003 Hokkaido, 1996 Andreanov, 1994 Kuril Islands, 1964 Alaska, and 1957 Andreanov, producing good comparisons to observations at Kahului tide station. The 2006 Tonga event provided the first empirical test of the model with a wave propagating from the southwest. The incoming waves traveled through the shallow channels among the Maui Complex and exposed substantial deficiencies in the resolution and computational domain in the intermediate grid of setup 1. This illustrates the importance of testing tsunamis propagating from all directions, especially for the Hawaiian Islands, which are exposed to the Pacific Ocean. In 2007, nearshore topography/bathymetry SHOALS airborne LIDAR with 1–5-m horizontal resolution from the Joint Airborne Lidar Bathymetry Technical Center of Expertise became available for Maui. Then, the digital elevation models were updated and Kahului forecast and reference models were also redeveloped using the newest data source (**Figures 5 and 7**).

Forecast inundation models are developed to balance computational speed and result accuracy. The highest-resolution grid and largest possible computational domain are retained while satisfying the computational time constraint necessary for operational forecasts.

4.1.2 Sensitivity of modeled inundation to friction coefficients

Accurate simulation of tsunami runup and inundation requires high-resolution bathymetry and topography data in the runup area and good tsunami source parameters. Titov *et al.* (2005) have shown that, under these conditions, the MOST runup and inundation agree quite well with the stereo aerial photo data

Table 5: Model speed and accuracy for different setups in Fig. 8 for Kahului for the May 2006 Tonga tsunami.

Setup	Grid resolution (arc sec)	Grid sizes	¹ Computational time for a 4-hr simulation	Max. computed wave height, H (cm)	Error $ (H - H_{\text{obs}})/H_{\text{obs}} $ (%)
1	108, 24, 3	153 × 130, 129 × 103, 291 × 121	8 min	25	49
2	120, 12, 3	196 × 150, 361 × 257, 200 × 167	10 min	40	18
3	36, 6, 1	650 × 500, 601 × 421, 872 × 371	8 hour	52	6
Maximum observed wave height, H_{obs} (cm).					49

¹The computations were performed on a single 3.6 GHz Intel Xeon processor in a DELL PowerEdge 1850.

and filed survey data on Okushiri Island by the 12 July 1993 Hokkaido-Nansei-Oki Mw 7.8 earthquake.

At present, one major difficulty in inundation forecasting is the lack of high-quality inundation/runup measurements to verify the accuracy of topography and to calibrate the friction coefficient. In this section, we focus on the sensitivity of inundation computed by the Kahului forecast model to the friction coefficient.

Runup data is available for Kahului for the 1946, 1957, 1960, and 1964 tsunamis (Pararas-Carayannis, 1969; Walker, 2004). The 1946 Alaskan tsunami has the most runup data, with nine points in the study area, so it is selected as the test case. The runup survey points, after conversion from an assumed original Old Hawaiian Datum to the WGS84 horizontal datum that the topography and shorelines are referenced to, are plotted in **Figure 9**. The quality of the measurements is ambiguous, as some points fall within the ocean. **Figure 9a** shows inundation in the Kahului nearshore grid computed from three Manning coefficients, $n = 0.01, 0.025$, and 0.032 . The coefficients generate similar inundation lines for most of the coastline where the slope is relatively steep. However, a small Manning coefficient of 0.01 produces further inundation at several flat areas, such as the southeast area adjacent to the Kahului harbor, including the Maui Mall, the Kanaha Ponds, and Lower Paia. The waterfront to the southeast of Kahului harbor has a near-flat slope of 0.0019 from 2-m contour to the shoreline. **Figure 9b** shows the inundation computed with $n = 0.025$ and 0.032 for the magnitude 9.3 Kamchatka scenario (No. 2). Though there are some minor differences at several local areas, the inundation limit agrees well for this test case.

In all, a smaller Manning coefficient can produce further inundation at some flat areas for certain test cases. However, the model can become unstable with a small Manning coefficient for large tsunami waves, such as $n = 0.01$ for the magnitude 9.3 Kamchatka scenario, from which the maximum elevation exceeds 9 m at Kahului tide station. Therefore, for the forecast operational purpose, we suggest $n = 0.01$ to $n = 0.025$. Additionally, we recommend considering the waterfront area to the southeast of the Kahului Harbor, including the Maui Mall, the Kanaha Ponds, and Lower Paia, as areas of inundation uncertainty due to lack of measurements to calibrate the Manning coefficient. The computed time series of tsunami elevation at Kahului gauge is insensitive to changes of the Manning coefficients.

4.2 Validation, verification, and testing of the forecast model

4.2.1 Validation

Both the reference and the forecast models for Kahului were tested with the 17 past tsunamis summarized in **Table 1**. **Figures 10, 1–17** show the comparison of observed and modeled time series by the models at Kahului tide station. **Figures 11, 1–17** show the corresponding wavelet-derived amplitude spectra, the description of which can be found in Tang *et al.* (2008b). Tide gauge data of the recent tsunamis, Nos. 1 to 12 on **Table 2**, are from the NOAA National Water Level Observation Network (NWLON) (Allen *et al.*, 2008), while others were digitized from Shepard *et al.* (1950), Zerbe (1953), Salsman (1959), Berkman and Symons (1964), and Spaeth and Berkman (1967). In this section, we evaluate the model performance through comparison of tsunami amplitude time series, period/frequency components via wavelet-derived spectra, and error estimation.

The most recently tested event is the 11 March 2011 Japan tsunami, which was generated by a Mw 9.1 mega-thrust earthquake that occurred along the oceanic subduction zone located 130 km east of Sendai, Japan. Data from station 21418 showed a 1.64 m first amplitude (3.0 m wave height), the largest tsunami wave ever recorded in the deep ocean. The tsunami source inverted in real time from the two closest DART stations, 21418 and 21401, produced accurate forecasts of tsunami amplitude time series and coastal flooding at Kahului. The forecast and observed maximum wave heights were 4.01 and 4.15 m respectively, a 96% accuracy (**Figure 10.1**). The forecasts were available 6 hr before the tsunami waves arrived at Kahului.

The 27 February 2010 Chile tsunami was generated by a Mw 8.8 earthquake NNE of Concepcion, Chile. In approximately 3 hr, the tsunami was recorded at DART station 32412. The real-time data was combined with the propagation database to produce a tsunami source. **Figure 10.2** shows the comparison of observations and model time series. The observed maximum wave height is 1.96 m, while the model shows 2.2 m. The model time series was shifted 9 min behind in the plot.

The 29 September 2009 Samoa tsunami was generated by a Mw 8.1 earthquake that occurred near the northern end of the Tonga Trench. Data recorded at DART stations 51425 and 51426 were inverted to produce a tsunami source. The observed maximum wave height is 0.74 m, while the forecast showed 1.09 m (**Figure 10.3**). The model accurately forecasted the maximum wave, which arrived 1 hr after the first wave arrival.

A detailed description of the real-time experimental forecast for the 15 August 2007 Peru tsunami can be found at Wei *et al.* (2008). At Kahului tide gauge, the observed maximum wave height is 0.56 m, while the forecast is 0.55 m (**Figure 10.4**). A 12-min adjustment was applied to the modeled time series. The modulated amplitude spectrum in **Figure 11.4.b** indicates that two groups of oscillations with peak periods near 32 and 16 min exist prior to the arrival of the tsunami. The 13 January 2007 Kuril Islands earthquake occurred as nor-

mal faulting (USGS, 2007). The magnitude 7.9 was inverted from the first waves recorded at three DARTs closest to the epicenter: 21414, 46413, and 21413. This tsunami source overestimates the wave heights at Kahului (**Figure 10.5**).

The 15 November 2006 Kuril Islands tsunami provided ample tsunami data and the first test of the new experimental tsunami forecast system. At the Kahului tide station, the largest wave is the eighth wave, arriving about 2 hr after the first wave, the latest arrival of the maximum wave among the historical tsunamis studied in this report. The modeled first waves agree well with the observations, while the maximum wave height is underestimated (**Figure 11.6.a**).

The 3 May 2006 Tonga earthquake generated a tsunami that was detected about 6 hr later by two offshore DARTs located south of the Hawaiian Islands, the Dart II (station 51407) and a DART ETD that was under testing. This data was combined with the model propagation database to produce the tsunami source by inversion (Tang *et al.*, 2008b). **Figure 11.7.a** compares the observations at Kahului tide station with model results up to 24 hr after the earthquake. Very good agreement is obtained for the amplitudes, arrival times, and wave periods of the first six waves. In addition, the Kahului forecast model correctly reproduced tsunami waves reflected off of the west coast of North America and those scattered by the East Pacific Rise, which reached the Hawaiian Islands 16 hr and 18.5 hr, respectively, after the earthquake.

The 17 November 2003 Rat Island tsunami provided the first genuine test of PMEL's forecast methodology (Titov *et al.*, 2005). This tsunami was detected by three DARTs located along the Aleutian Trench. The real-time data was combined with the propagation database to produce the earthquake source by inversion. Titov *et al.* (2005) showed excellent agreement between the model prediction and observed data at Hilo tide gauge. The same source was applied here and results are plotted in **Figure 11.8**. Both the reference and forecast models correctly produced amplitudes, arrival time, and periods for the first several waves.

The 25 September 2003 Hokkaido earthquake generated tsunami waves of very long periods. Kahului tide station recorded the first waves with peak periods near 34 min. The wave amplitude decreased slowly and steadily (**Figure 11.9**).

DART station 51406, located midway between South America and Hawaii at $8^{\circ}29'S$ $125^{\circ}1'W$, was not deployed until one month after the 23 June 2001 Peru tsunami. Therefore, the source for this event was derived based on an inversion of Kahului tide station records using the Kahului forecast model. Six tsunami source functions, AB 15 to 17 along the South American Subduction Zone near the epicenter, were involved. The linear least square inversion estimates a magnitude of 8.2. Results agreed well with data of the first waves arriving at the Honolulu and Hilo tide stations. **Figure 11.10.a** shows that the wave amplitude remains fairly constant even 14 hr after the first arrival. The underestimation of the model wave heights for waves near $t = 20$ hr is due to the lack of long-period components (**Figures 11.10.b to d**).

Deep-ocean BPR data are also available for two additional tsunamis. The inversion of the 4 October 1994 Kuril Island data was done using five BPR recordings, while only one was used for the 10 June 1996 Andreanov data (Titov *et al.*, 2005). Model results agree well with Kahului tide station records for the

first several waves (**Figures 11.11 and 11.12**), especially regarding the 1994 West Kuril Islands tsunami. Though the models missed the second wave, they accurately described the large third-sixth waves (**Figure 11.12.a**).

The limited number of DART records does not include any of the destructive tsunamis described in section 3.2. Previous studies of seismic, geodetic, and water-level data have estimated source parameters for some of the events (Green, 1946; Kanamori and Ciper, 1974; Johnson *et al.*, 1994; 1996; Johnson and Satake, 1999; López and Okal, 2006). However, those sources are subject to debate and adjustment. Most of the source estimates that have been done are based on low-resolution tsunami propagation models. The forecast models that have been developed at NCTR provide a unique chance to reinvestigate the historical sources by inversion of the water level data with the high-resolution quality inundation and propagation models. Preliminary results are available for the 1964, 1957, 1952, and 1946 tsunamis. The fault parameters of the 22 May 1960 Chile tsunami are taken from Kanamori and Ciper (1974). Model results are plotted in **Figures 11, 13–17**.

Error estimates of the maximum wave height computed by the Kahului forecast model for eleven past tsunamis are presented as in **Figures 12.a**. When the observed maximum wave height is between 0.3 to 1.0 m, the error is within 50%. The low signal-to-noise ratio of the observations and the low ratio of signal-to-uncertainty from the model setup are major contributors to this error. When the maximum wave height is greater than 1.0 m, the error reduces to within 20% and can be attributed to uncertainties from the tsunami source, model setup, and bathymetry. First arrivals in general agree well with the observations, with errors less than 3% of the travel time. So far, the largest discrepancy between the modeled and observed first arrival time is –12 min for the 15 August 2007 (200708) Peru tsunami. However, the arrival of the 23 June 2001 (200106) Peru tsunami has only –3 min discrepancy with an earthquake epicenter 460 km northwest of the 200708 Peru tsunami, and the 12-min arrival discrepancy is currently under investigation.

To further explore the tsunami frequency responses at Kahului, **Figure 12b** compares the 11 observed and modeled peak wave periods from the amplitude spectra in **Figure 11**. The observed peak wave periods fall into one of the three groups of 16-, 24-, or 34-min periods (± 2 min). This indicates that the peak wave period is usually one of the local resonant frequencies. An interesting question is, for a particular tsunami, which local frequency can be excited as the peak frequency? **Figure 12b** indicates that it can be related to the geographic locations of the earthquakes. Tsunamis originating from nearby subduction zone earthquakes excite similar peak frequency at Kahului. For example, the 15 November 2006 (200611) and 13 January 2007 (200701) Central Kuril Islands tsunamis have peak periods near 16 min (group 1), while the 4 October 1994 (199410) West Kuril Islands tsunami and the nearby 25 September 2003 (200309) Hokkaido tsunami present the same peak period near 32 min (group 3). The remaining seven tsunamis have similar peak wave periods near 24 min (group 2). The Kahului forecast model correctly reproduced the peak wave periods within groups 2 and 3. Although the modeled group 1 period does show up in the amplitude spectra for the 200611 and 200701 Central Kuril Islands tsunamis, it is not the observed peak period (**Figures 11.5 and 11.6**).

The deep-ocean tsunami observations at DARTs for these two events show that high-frequency components appear in the later wave chains, which were not well resolved in the propagation models. This may cause the peak period computed by the Kahului forecast model to shift from group 1 to group 2.

4.2.2 Verification

The computed maximum water elevation above MHW and maximum current of 17 past tsunamis are plotted in **Figure 13**. Both the reference and forecast models produced similar patterns and values. The maximum water elevation exhibits two typical patterns: (1) gradually increasing elevation toward Kahului harbor, such as the 2003 Hokkaido tsunami (**Figure 13.9**); and (2) large waves along the coastline, such as the 1946 Unimak tsunami (**Figure 13.17**). These patterns relate to the tsunami wave periods. For pattern two, the tsunami wave amplitude increases dramatically due to shoaling when the tsunami waves enter a nearshore area shallower than 20 m and even more so because of local shelf and harbor resonances and other coastal effects. This emphasizes the importance of using high-resolution inundation models, which resolve the local coast and harbor geometries, in order to achieve accurate tsunami amplitude forecasts for coastal communities.

4.2.3 Robustness and stability tests

Recorded historical tsunamis provide only a limited number of events, from limited locations. More comprehensive test cases of destructive tsunamis with different directionalities are needed to check the stability and robustness of the forecast model. The same set of 18 synthetic magnitude 9.3 tsunamis as in Tang *et al.* (2008a; 2009a) was selected here for further examination. Results computed by the forecast model are compared with those from the high-resolution reference model in **Figures 14 and 15**. Both models were numerically stable for all scenarios. Waveforms computed by the forecast model agree well with those from the reference model (**Figure 14**). Both models compute similar maximum water elevation and inundation in the study area (**Figure 15**). These results indicate that the forecast model is capable of providing robust and stable predictions of long duration for Pacific-wide tsunamis. Tsunami waves in the study area vary significantly for the 18 magnitude 9.3 scenarios. These results show the complexity and high nonlinearity of tsunami waves nearshore, which again demonstrate the value of the forecast model for providing accurate site-specific forecast details. The No. 2 scenario (as shown in **Figure 14**) at Kamchatka subduction generates severe inundation in Kahului. The computed maximum water elevation reaches nearly 10 m at the tide station.

4.3 Tsunami hazard assessment from simulated magnitudes 7.5, 8.2, 8.7, and 9.3 tsunamis

Located in the middle of Pacific Ocean, Kahului is vulnerable to a variety of Pacific-wide tsunamis. At what magnitude from which location on a subduc-

Table 6: Simulated tsunamis for hazard assessment study for Kahului.

T_{Mw}	Numbers of TSFs	Tsunami source coef.	Lines	Numbers of tests	Range of η_{\max}		Ratio max/min
					min	max	
¹ 7.5	1	1	BA	804	0.005 cm	1.90 cm	380
² 7.5	1	1	BA	804	0.05 cm	28.5 cm	570
³ 8.2	1	10	B	405	0.01 m	1.55 m	155
⁴ 8.7	6 (3 pairs)	12	BA	381	0.06 m	2.88 m	48
⁵ 9.3	20 (10 pairs)	29	BA	294	0.56 m	9.26 m	17

1: at water depth 4951 m offshore Kahului from the precomputed propagation database; 2 to 5: at Kahului tide station computed by the Kahului forecast model (at approximately 2 m water depth).

tion zone can a tsunami have devastating impact on the community? Assessment of the potential impact can provide useful and important information in advance of a real event. The validated Kahului forecast model, which was optimized for speed and accuracy, along with the forecast propagation database, provide powerful tools to address this question.

Even the construction of tsunamis of the same magnitude can be an enormous task, with various numbers of tsunami source functions and coefficients. For simplicity, we apply a uniform coefficient to tsunamis of the same magnitude. Four different magnitudes, 7.5, 8.2, 8.7, and 9.3, were tested. The details of the synthetic tsunami sources and results are summarized in **Table 6** and **Figure 16**. The maximum water elevation, η_{\max} , at Kahului tide station from magnitude 7.5 tsunamis computed by the forecast model, is plotted in **Figure 16b**. Color represents the first arrival at the station, which is the time at which the water level reaches 20% of the height of the first significant peak or trough. **Figure 16a** indicates the maximum elevation at deep water offshore Kahului from the same sources, which are from the propagation database. **Figures 16c, d, and e** show η_{\max} at Kahului tide station from magnitude 8.2, 8.7, and 9.3 tsunamis, respectively. The color represents the difference in time between the arrival of the maximum elevation, t_{\max} , and first arrival, t_1 .

Tsunami waves in the study area generated by the same magnitude tsunamis from the major subduction zones in the Pacific can vary significantly. Test results in **Table 6** show that the ratio of maximum to minimum η_{\max} at the station from the same magnitude tsunamis varies from 570 to 17, with magnitude ranging from 7.5 to 9.3. These results show an impressive local variability of tsunami amplitudes even for far-field tsunamis, which illustrate the complexity of forecasting tsunami amplitudes at coastal locations. Tang *et al.* (2009b) have shown that the location of the most effective source for a given location also differs from site to site. Therefore, a moment magnitude alone is inadequate to provide warning guidance for coastal communities. The forecast models contain local bathymetric and topographic information and use the dynamic boundary conditions from the propagation database. They are designed to provide accurate forecasting for site-specific coastal communities and to avoid false alarms resulting from incomplete information.

To further investigate the transformations of tsunami amplitudes from offshore to the tide gauges, we have looked at the ratios of these amplitudes. The

ratio of the offshore and nearshore η_{\max} for all computed scenarios are plotted and the linear regression analyses performed in **Figure 17**. To better illustrate the data trends, both the logarithmic and Cartesian coordinates were plotted with the same datasets. The logarithmic scales give a full picture of the wide range of values, while the Cartesian coordinates better illustrate the actual spread and trends of the data. In **Figure 17b**, the solid black lines are the best fit to the data and the dashed black lines are prediction bounds based on a 95% confidence level. The results show:

1. The relationship between tide-gauge maximum amplitude and offshore maximum amplitude appears to be complex and non-linear in nature.
2. Larger amplitudes offshore do not necessarily produce larger amplitudes at tide gauges, and larger tsunami magnitudes may not produce larger waves either offshore, or at tide gauges.
3. The simple relationships obtained through regression analysis (**Figure 17a**) are insufficient to provide warning guidance during an event. The 95% confidence interval is too wide to provide any certainty for the forecast accuracy.

Tang *et al.* (2009b) also show that the trends of offshore/tide gauge amplitudes are site-specific. Different sites show different regression analysis curves. These results indicate that high-resolution tsunami models are essential for providing useful accuracy for coastal amplitude forecast. If high-resolution tsunami nearshore dynamics are not included in the forecast procedures, the accuracy and the uncertainty of the amplitude forecast appear to be too high for practical guidance.

5. Summary and Conclusions

A tsunami forecast model was developed for the coastal community of Kahului, Hawaii. The computational grids for this forecast model were derived from the best available bathymetric and topographic data sources. Sensitivity studies of tsunami wave characteristics nearshore and inundations were conducted for ranges of model grid setups, resolutions, and parameters. The forecast model is optimally constructed at a resolution of 2 arc sec (~ 60 m) to enable a 4-hr inundation simulation within 10 min of computational time. A reference inundation model of higher resolution 1/3 arc sec (~ 10 m) was also developed in parallel to provide modeling references for the forecast model. Both models were tested for 17 past tsunamis and a set of 18 synthetic magnitude 9.3 tsunamis.

Based on 14 historical tsunami water level records at Kahului tide station, the error of the maximum wave height computed by the forecast model is within 20% when the observation is greater than 1.0 m; when the observation is below 1.0 m, the error is less than 50%. The error of the modeled first arrivals is within 3% of the travel time. Wavelet analysis of the observed time-series tsunami amplitude at Kahului indicates that the peak wave period mainly falls into one of the three local resonant periods: 16, 24, or 34 min (± 2 min), and can be relevant to the geographic location of the tsunami sources. The optimized forecast model can accurately provide a 4-hr site-specified forecast of first wave arrival, amplitudes, and reasonable inundation limit within minutes of receiving tsunami source information constrained by deep-ocean DART measurements. It is also capable of reproducing later tsunami waves reflected or scattered by far-field bathymetry that may arrive hours after the first wave arrival.

A tsunami could strike Kahului with large waves from the Kamchatka, Alaska-Aleutian, Canada, Cascadia, and South America subduction zones. At 4.25 hr, the Aleutian tsunami has the shortest first arrival at the Kahului gauge. Special attention must also be paid to locations from which the main offshore wave energy propagates toward the Hawaiian Islands, including the East Philippines and Marianas subduction zones to the east and Vanuatu to the southeast. In addition to Kahului Harbor, larger tsunami waves may be expected at Waiehu Point and Sprecklesville when the peak period is 16 min or less. The study suggests considering the waterfront area to the southeast of Kahului harbor, including the Maui Mall, the Kanaha Ponds, and Lower Paia, an area of inundation uncertainty due to the lack of measurements to calibrate the friction coefficient for the forecast model. The developed forecast model was further applied to hazard assessment from 1,884 scenarios of synthetic magnitude 7.5, 8.2, 8.7, and 9.3 tsunamis based on subduction zone earthquakes in the Pacific. The results demonstrate the nonlinearity between offshore and nearshore maximum wave amplitudes and indicate that the use of a seismic magnitude alone for a tsunami source assessment is inadequate for tsunami forecasts. The forecast models apply local bathymetric and topographic information and use

dynamic boundary conditions from the tsunami source function database to provide site- and event-specific coastal predictions.

6. Acknowledgments

Special thanks to Elena Tolkova's extensive assistance in pre-processing model input, MOST versioning, and post-processing data. We thank Mick Spillane for providing information on Kahului offshore; Harold Mofjeld, Marie Eble, Lindsey Wright, Nazila Merati, Clyde Kakazu, and Allison Allen for assistance with tide gauge data; Robert Weiss, Diego Arcas, Yong Wei, and Burak Uslu for discussion; Edison Gica and Jean Newman for assistance with the propagation database; and Katherine Burgess, Ryan Layne Whitney, and Sandra Bigley for comments and editing.

This research is funded by the NOAA Center for Tsunami Research (NCTR). This publication is partially funded by the Joint Institute for the Study of the Atmosphere and Ocean (JISAO) under NOAA Cooperative Agreement No. NA17RJ1232, JISAO Contribution No. 1773. This is PMEL Contribution No. 3352.

7. References

- Allen, A.L., N.A. Donoho, S.A. Duncan, S.K. Gill, C.R. McGrath, R.S. Meyer, and M.R. Samant (2008): NOAA's National Ocean Service supports tsunami detection and warning through operation of coastal tide stations. In *Solutions to Coastal Disasters 2008/Tsunamis: Proceedings of Sessions of the Conference*, American Society of Civil Engineers, Turtle Bay, Oahu, Hawaii, 13–16 April.
- Berkman, S.C., and J.M. Symons (1964): The tsunami of May 22, 1960 as recorded at tide stations. Coastal and Geodetic Survey, U.S. Department of Commerce, 79 pp.
- Bernard, E.N., H.O. Mofjeld, V.V. Titov, C.E. Synolakis, and F.I. González (2006): Tsunami: Scientific frontiers, mitigation, forecasting, and policy implications. *Proc. Roy. Soc. Lond. A*, 364(1845), 1989–2007, doi: 10.1098/rsta.2006.1809.
- Bernard, E.N., and V.V. Titov (2007): Improving tsunami forecast skill using deep ocean observations. *Mar. Technol. Soc. J.*, 40(4), 23–26.
- Fraser, G.D., P.J. Eaton, and C.K. Wentworth (1959): The tsunami of March 9, 1957, on the Island of Hawaii. *Bull. Seismol. Soc. Am.*, 49(1), 79–90.
- Gica, E., M.C. Spillane, V.V. Titov, C.D. Chamberlin, and J.C. Newman (2008): Development of the forecast propagation database for NOAA's Short-term Inundation Forecast for Tsunamis (SIFT). NOAA Tech. Memo. OAR PMEL-139, NTIS: PB2008-109391, NOAA/Pacific Marine Environmental Laboratory, Seattle, WA, 89 pp.
- González, F.I., E.N. Bernard, C. Meinig, M. Eble, H.O. Mofjeld, and S. Stalin (2005): The NTHMP tsunami network. *Nat. Hazards*, 35(1), 25–39, Special Issue, U.S. National Tsunami Hazard Mitigation Program.
- Green, C.K. (1946): Seismic sea wave of April 1, 1946, as recorded on tide gages. *Eos Trans. AGU*, 27, 489–500.
- Gusiakov, V.K. (1978): Static displacement on the surface of an elastic space. Ill-posed problems of mathematical physics and interpretation of geophysical data. *VC SOAN SSSR*, 23–51, Novosibirsk (in Russian).
- Johnson, J.M., and K. Satake (1999): Asperity distribution of the 1952 Great Kamchatka earthquake and its relation to future earthquake potential in Kamchatka. *Pure Appl. Geophys.*, 154(3–4), 541–553.
- Johnson, J.M., K. Satake, S.R. Holdahl, and J. Sauber (1996): The 1964 Prince William earthquake: Joint inversion of tsunami and geodetic data. *J. Geophys. Res.*, 101(B1), 523–532.

- Johnson, J.M., Y. Tanioka, L.J. Ruff, K. Satake, H. Kanamori, and L.R. Sykes (1994): The 1957 Great Aleutian Earthquake. *Pure Appl. Geophys.*, 142(1), 3–28.
- Kanamori, H., and J.J. Ciper (1974): Focal process of the great Chilean earthquake, May 22, 1960. *Phys. Earth Planet. In.*, 9, 128–136.
- Liu, P.L.-F. (2009): Tsunami modeling—Propagation. In *The Sea*, E. Bernard, and A. Robinson (eds.), Vol. 15, Chapter 9, Harvard University Press, Cambridge, MA, 295–319.
- López, A.M., and E.A. Okal (2006): A seismological reassessment of the source of the 1946 Aleutian “tsunami” earthquake. *Geophys. J. Int.*, 165(3), 835–849, doi: 10.1111/j.1365-246x.2006.02899.x.
- National Center for Tsunami Research (2010): <http://nctr.pmel.noaa.gov/database-devel.html>.
- NOAA/NOS (1991): Next Generation Water Level Measurement System (NG-WLMS) Site Design, Preparation, and Installation Manual. NOAA/NOS, January 1991.
- Okada, Y. (1985): Surface deformation due to shear and tensile faults in a half-space. *Bull. Seismol. Soc. Am.*, 75, 1135–1154.
- Pararas-Carayannis, G. (1969): Catalog of Tsunamis in The Hawaii Islands. World Data Center A Tsunami, ESSA Coast and Geodetic Survey, 94 pp.
- Salsman, G.G. (1959): The tsunami of March 9, 1957, as recorded at tide stations. U.S. Coast and Geodetic Survey, 18 pp.
- Satake, K., Y. Hasegawa, Y. Nishimae, and Y. Igarashi (2008): Recent tsunamis that affected the Japanese coasts and evaluation of JMA’s tsunami warnings. OS42B-03, AGU Fall Meeting, San Francisco.
- Shepard, F.P., G.A. Macdonald, and D.C. Cox (1950): The tsunami of April 1, 1946. *Bull. Scripps Inst. Oceanogr. Univ. Calif.*, 5, 391–528.
- Spaeth, M.G., and S.C. Berkman (1967): The tsunami of March 28, 1964, as recorded at tide stations. ESSA Technical Report Coast and Geodetic Survey Technical Bulletin No. 33, U.S. Dept. of Commerce, Coast and Geodetic Survey, Rockville, MD, 86 pp.
- Synolakis, C.E., E.N. Bernard, V.V. Titov, U. Kânoğlu, and F.I. González (2008): Validation and verification of tsunami numerical models. *Pure Appl. Geophys.*, 165(11–12), 2197–2228.
- Tang, L., C. Chamberlin, E. Tolkova, M. Spillane, V.V. Titov, E.N. Bernard, and H.O. Mofjeld (2006): Assessment of potential tsunami impact for Pearl Harbor, Hawaii. NOAA Tech. Memo. OAR PMEL-131, NTIS: PB2007-100617, NOAA/Pacific Marine Environmental Laboratory, Seattle, WA, 36 pp.

- Tang, L., C.D. Chamberlin, and V.V. Titov (2008a): Developing tsunami forecast inundation models for Hawaii: Procedures and testing. NOAA Tech. Memo. OAR PMEL-141, NTIS: PB2009-100620, NOAA/Pacific Marine Environmental Laboratory, Seattle, WA, 46 pp.
- Tang, L., V.V. Titov, and C. Chamberlin (2009a): A tsunami forecast model for Hilo, Hawaii, PMEL Tsunami Forecast Series: Vol. 1. NOAA OAR Special Report, NOAA/Pacific Marine Environmental Laboratory, Seattle, WA, 44 pp.
- Tang, L., V.V. Titov, and C.D. Chamberlin (2009b): Development, testing, and applications of site-specific tsunami inundation models for real-time forecasting. *J. Geophys. Res.*, 114, C12025, doi: 10.1029/2009JC005476.
- Tang, L., V.V. Titov, Y. Wei, H.O. Mofjeld, M. Spillane, D. Arcas, E.N. Bernard, C. Chamberlin, E. Gica, and J. Newman (2008b): Tsunami forecast analysis for the May 2006 Tonga tsunami. *J. Geophys. Res.*, 113, C12015, doi: 10.1029/2008JC004922.
- Titov, V.V. (2009): Tsunami forecasting. In *The Sea*, Vol. 15, Chapter 12, Harvard University Press, Cambridge, MA, and London, England, 371–400.
- Titov, V.V., and F.I. González (1997): Implementation and testing of the Method of Splitting Tsunami (MOST) model. NOAA Tech. Memo. ERL PMEL-112 (PB98-122773), NOAA/Pacific Marine Environmental Laboratory, Seattle, WA, 11 pp.
- Titov, V.V., F.I. González, E.N. Bernard, M.C. Eble, H.O. Mofjeld, J.C. Newman, and A.J. Venturato (2005): Real-time tsunami forecasting: Challenges and solutions. *Nat. Hazards*, 35(1), Special Issue, U.S. National Tsunami Hazard Mitigation Program, 41–58.
- Titov, V.V., H.O. Mofjeld, F.I. González, and J.C. Newman (1999): Offshore forecasting of Alaska-Aleutian Subduction Zone tsunamis in Hawaii. NOAA Tech. Memo. ERL PMEL-114, NTIS PB2002-101567, NOAA/Pacific Marine Environmental Laboratory, Seattle, WA, 22 pp.
- Titov, V.V., H.O. Mofjeld, F.I. González, and J.C. Newman (2001): Offshore forecasting of Alaska tsunamis in Hawaii. In *Tsunami Research at the End of a Critical Decade*, G.T. Hebenstreit (ed.), Kluwer Academic Publishers, 75–90.
- Titov, V.V., and C.E. Synolakis (1998): Numerical modeling of tidal wave runup. *J. Waterw. Port Coast. Ocean Eng.*, 124(4), 157–171.
- USGS (2007): M 8.1 Kuril Islands earthquake of 13 January 2007. Earthquake Summary Map XXX, U.S. Geological Survey.
- Walker, D.A. (2004): Regional tsunami evacuations for the state of Hawaii: A feasibility study on historical runup data. *Sci. Tsunami Haz.*, 22(1), 3–22.
- Wei, Y., E. Bernard, L. Tang, R. Weiss, V. Titov, C. Moore, M. Spillane, M. Hopkins, and U. Kânoğlu (2008): Real-time experimental forecast of the Peruvian tsunami of August 2007 for U.S. coastlines. *Geophys. Res. Lett.*, 35, L04609, doi: 10.1029/2007GL032250.

Whitmore, P.M. (2003): Tsunami amplitude prediction during events: A test based on previous tsunamis. *Sci. Tsunami Haz.*, 21, 135–143.

Zerbe, W.B. (1953): The tsunami of November 4, 1952, as recorded at tide stations. C&GS Special Publication #300, U.S. Dept. of Commerce, C&GS, 62 pp.

FIGURES

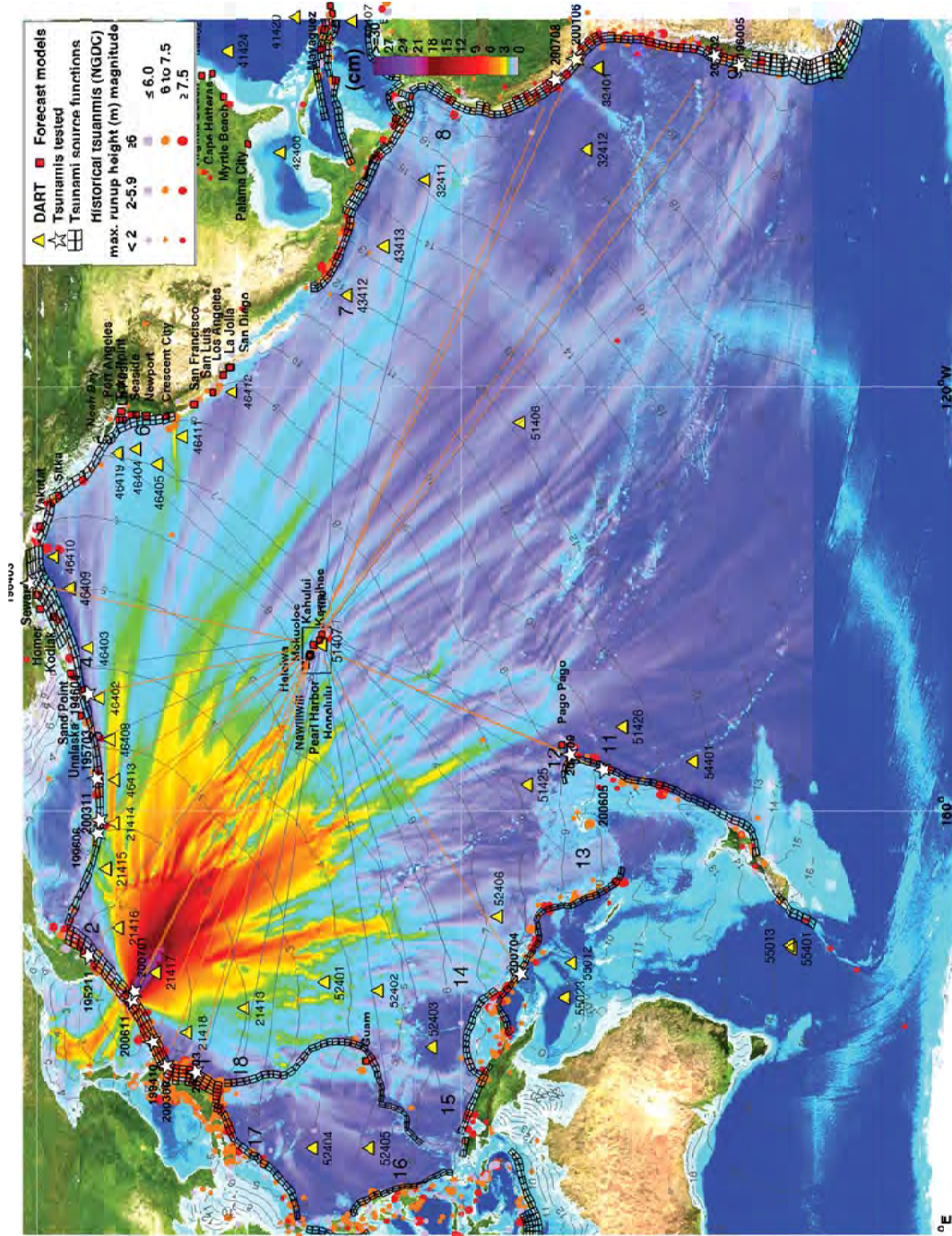


Figure 1: Overview of the Tsunami Forecast System. System components include DART system (yellow triangles), pre-computed tsunami source function (unfilled black rectangles) and high-resolution forecast models (red squares). Colors show the offshore forecast of the computed maximum tsunami amplitude in cm for the 13 January 2007 Kuril Islands tsunami in the Pacific. Contours indicate the travel time in hours. —, 17 past tsunamis and —, 18 synthetic tsunamis tested in this study.

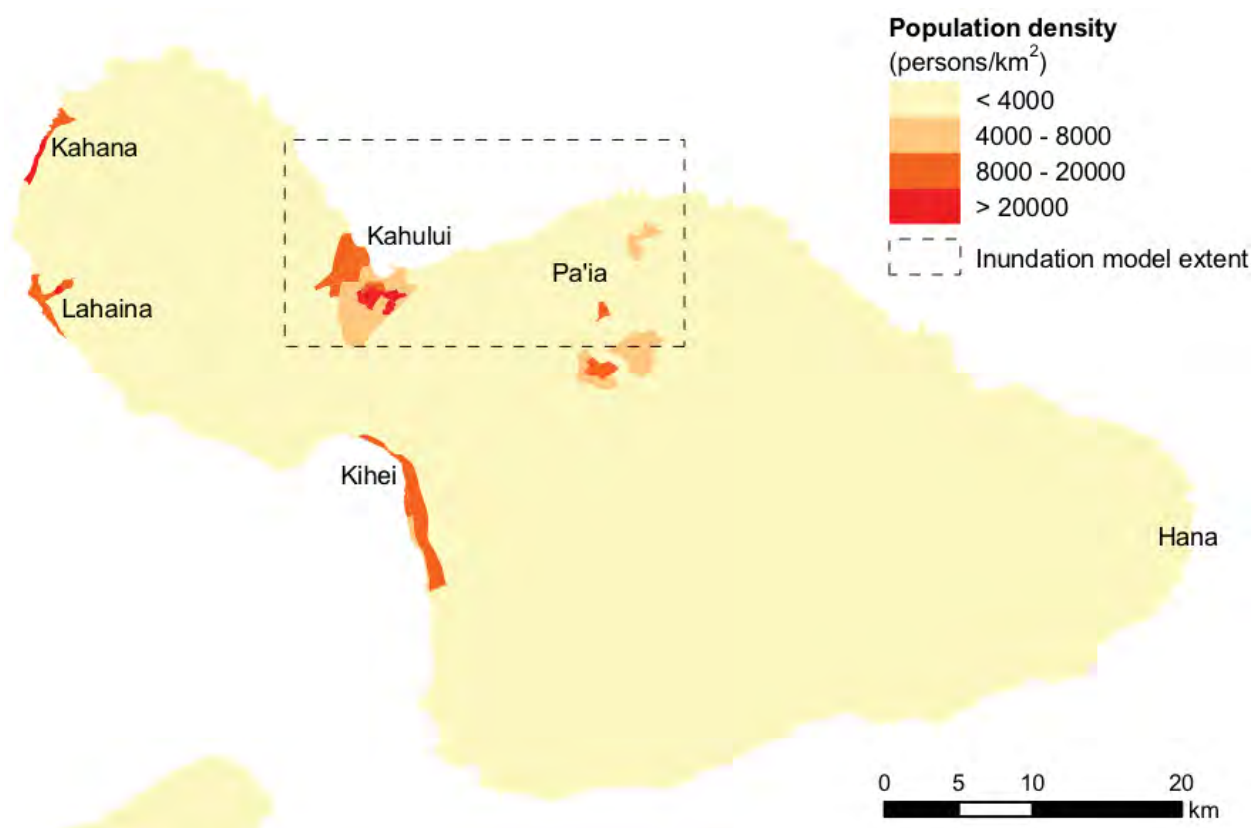


Figure 2: Population density, Maui. (Source: 2000 Census)

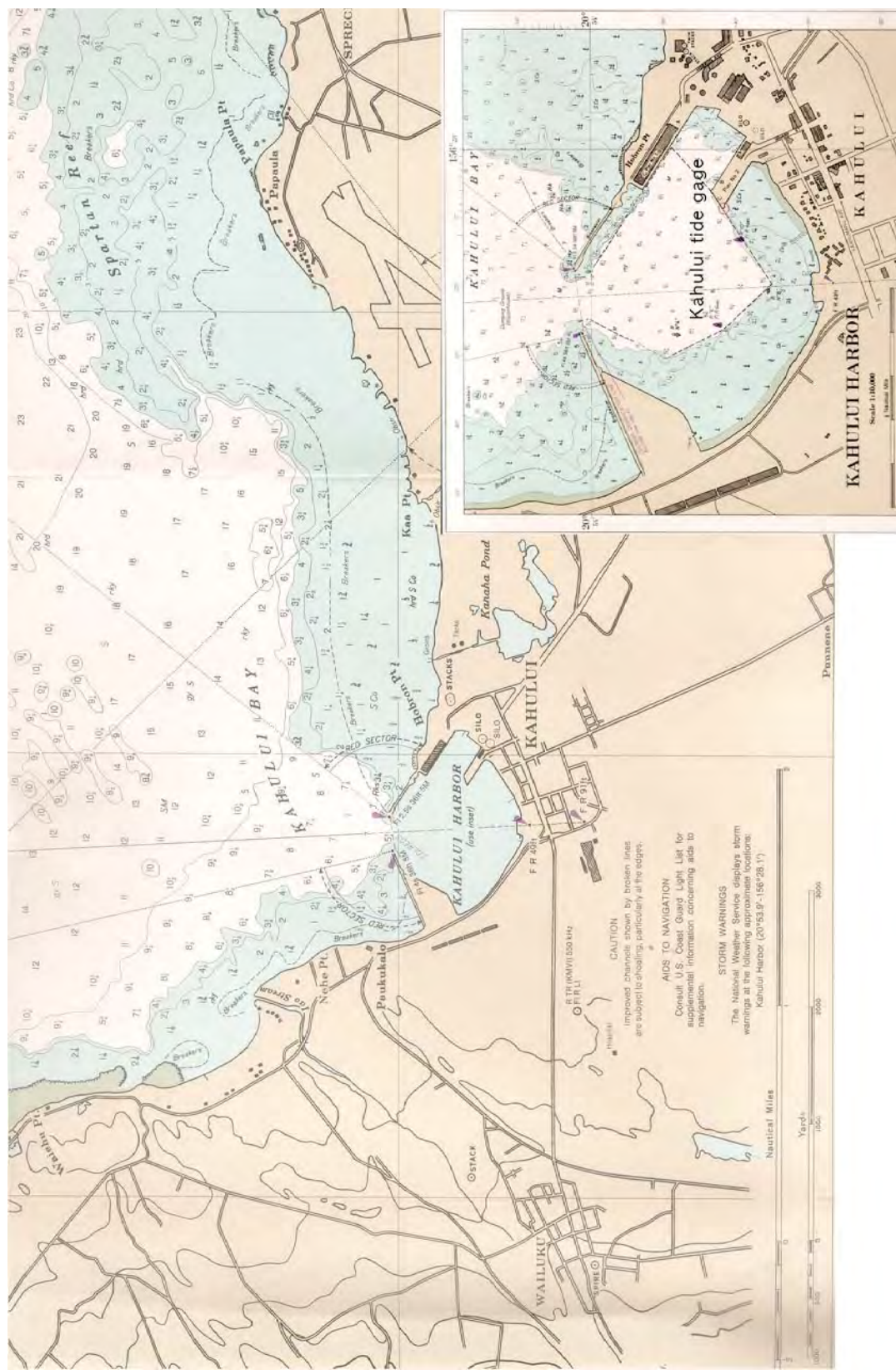


Figure 3: A chart of Kahului. Red circle, Kahului tide gauge (the warning point).



Figure 4: An aerial photo of Kahului. (Image courtesy of <http://www.soest.hawaii.edu/coasts/>.)

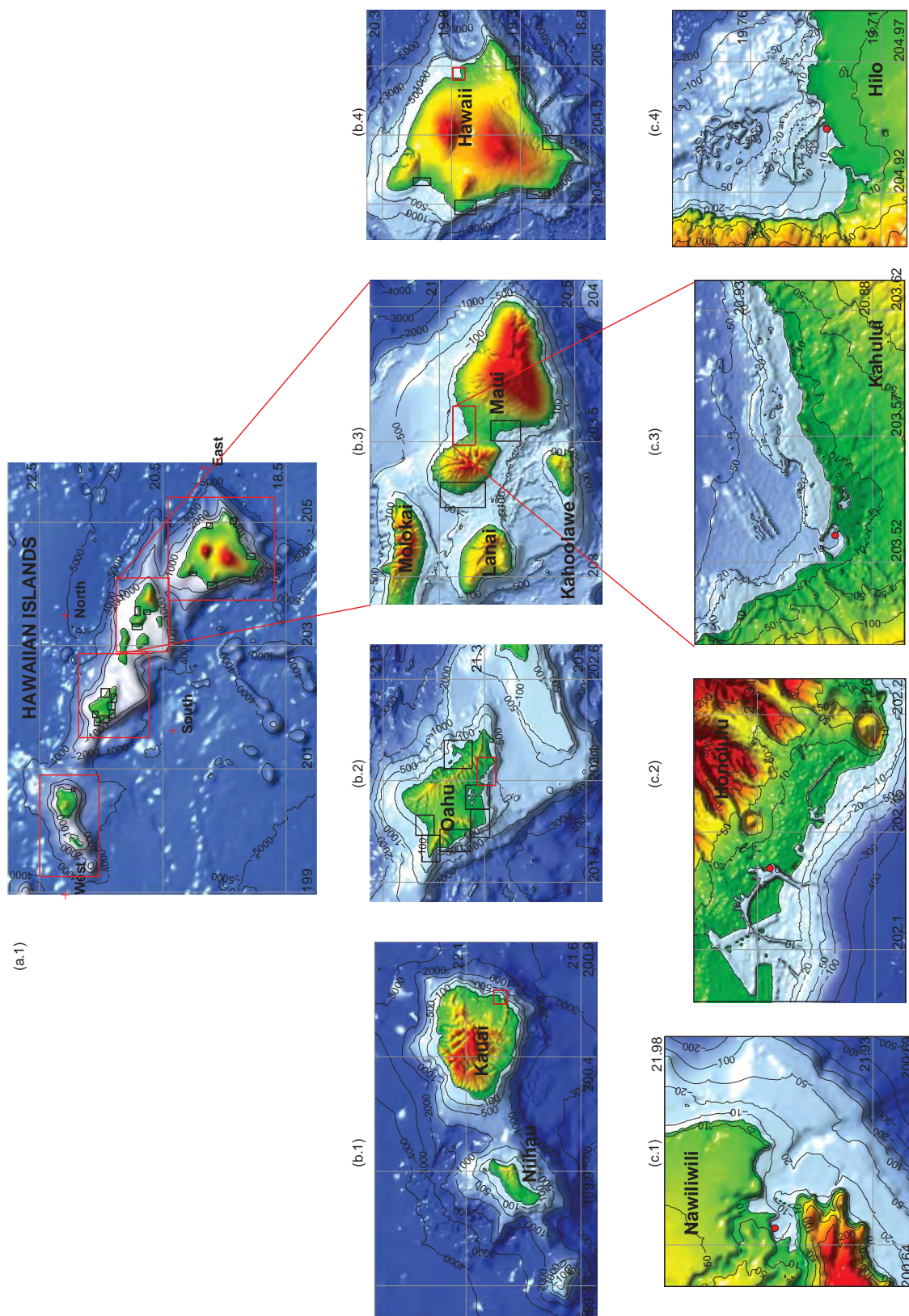


Figure 5: Forecast model setups in Hawaii: (a) 2-arc-min (~3600 m) regional, (b) 12–18-arc-sec (~360–540 m) intermediate and (c) 2-arc-sec (~60 m) nearshore grids for Nawiliwili, Honolulu, Kahului, and Hilo. Red dots, coastal tide stations; red pluses, offshore locations.

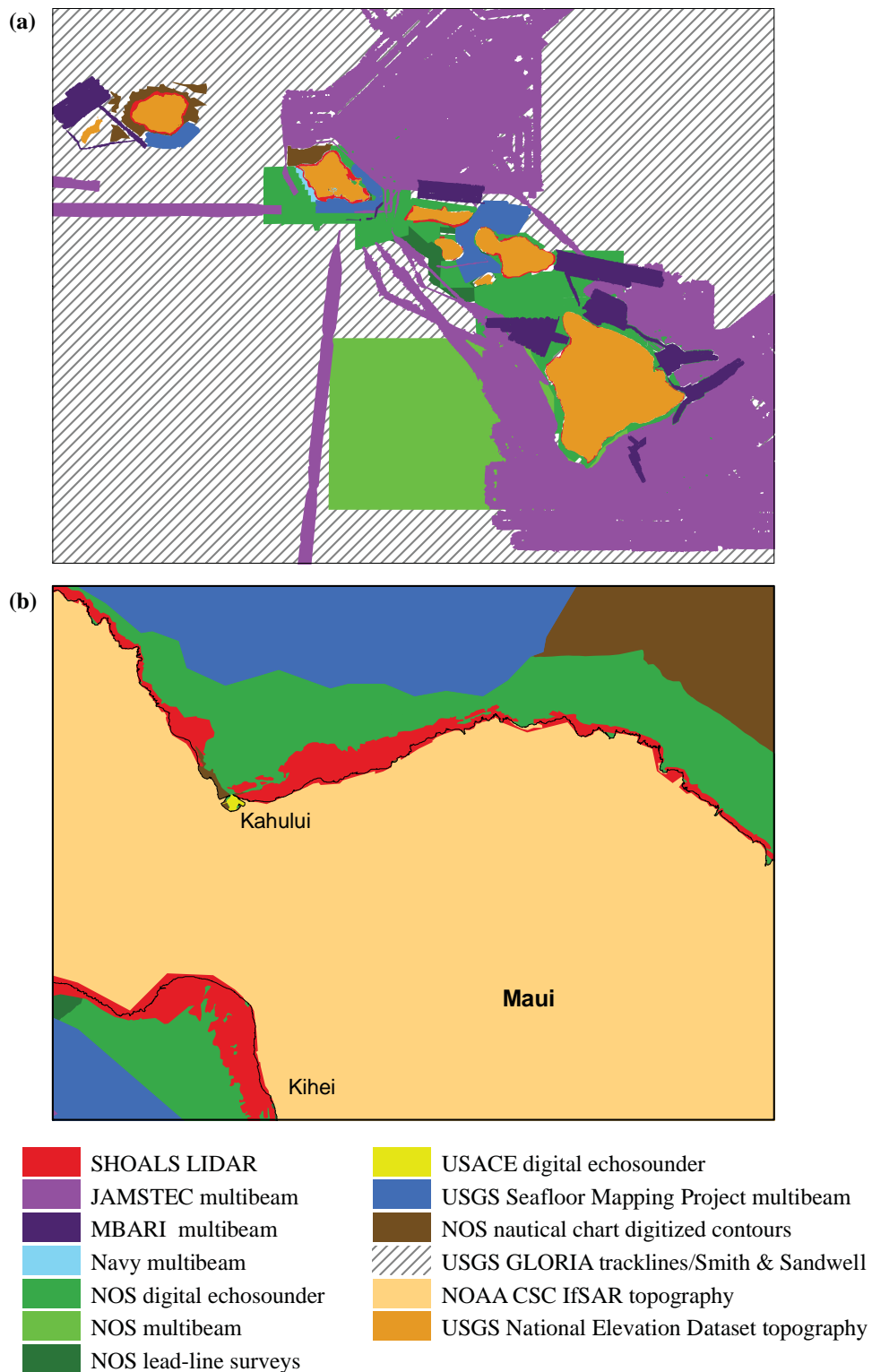


Figure 6: Bathymetric and topographic data source overview. (a) Hawaiian Islands with 6-arc-sec (~180 m) resolution; (b) Maui with 1/3-arc-sec (~10 m) resolution.

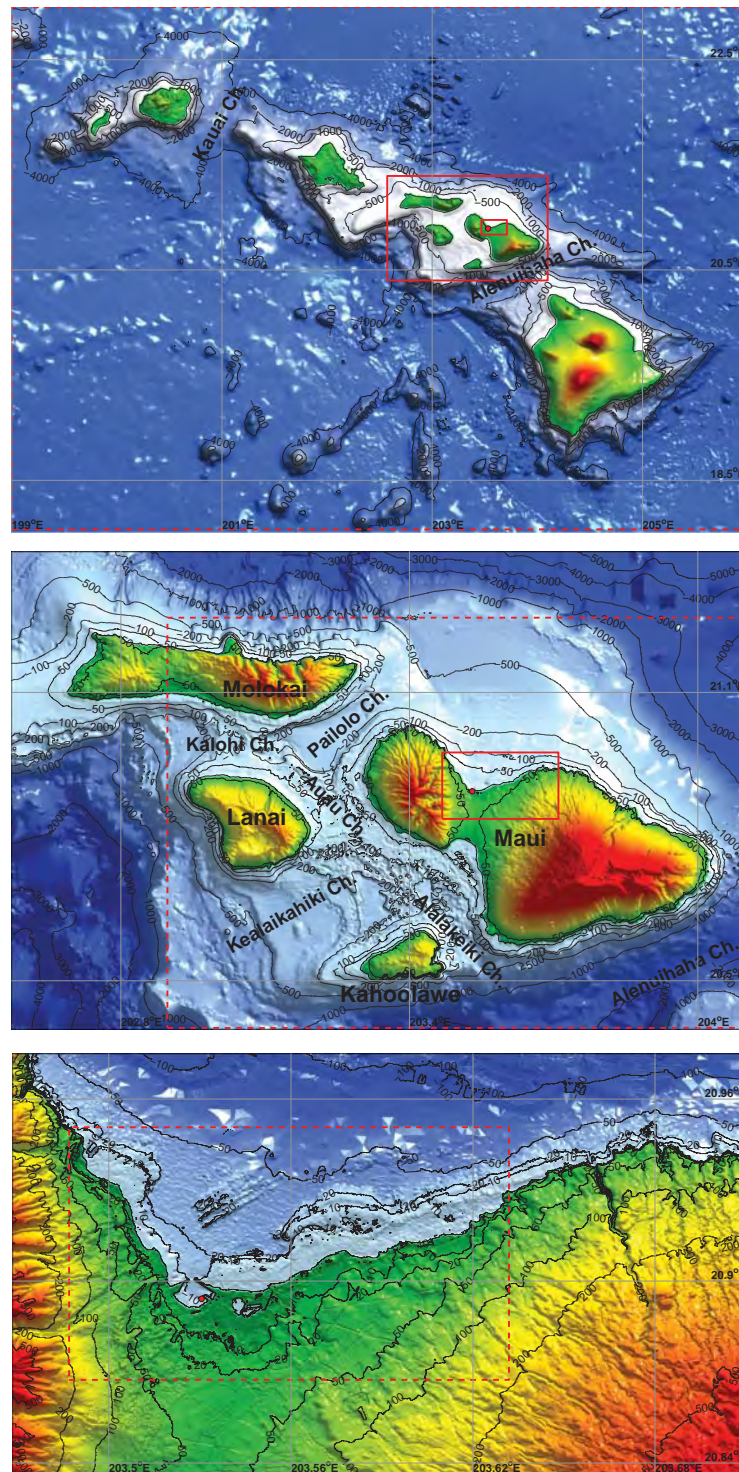


Figure 7: Grid setup of the reference inundation model for Kahului with resolution of (a) $36''$ (~ 1080 m), (b) $6''$ (~ 18 m) and (c) $1/3''$ (~ 10 m). Solid red lines represent the telescoping grids. Dashed red lines indicate the corresponding boundaries of the Kahului forecast model as in **Figure 2**.

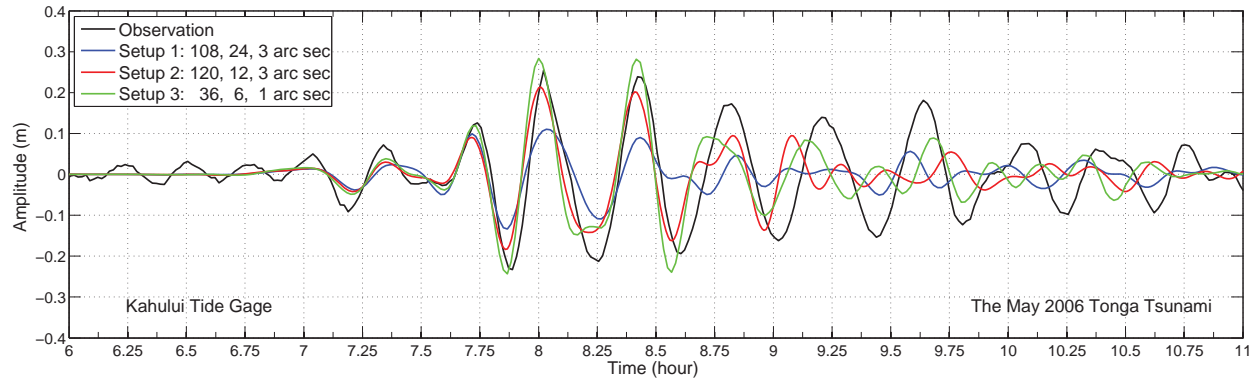


Figure 8: Tsunami time series computed from different grid setups at Kahului tide gauge for the 3 May 2006 Tonga tsunami.

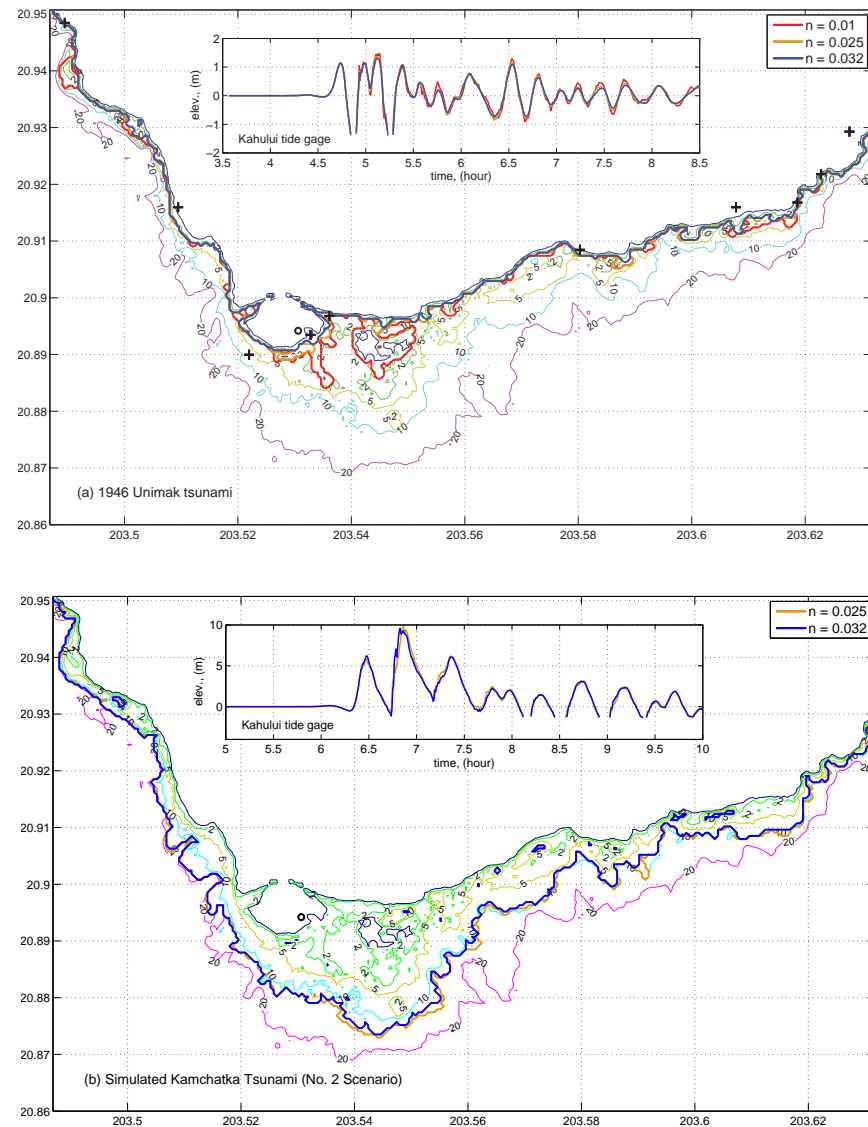


Figure 9: Sensitivity of inundation and time series of tsunami amplitudes computed by the Kahului forecast model to Manning coefficients for (a) the 1946 Unimak tsunami, and (b) the synthetic magnitude 9.3 Kamchatka tsunami (the No. 2 scenario).

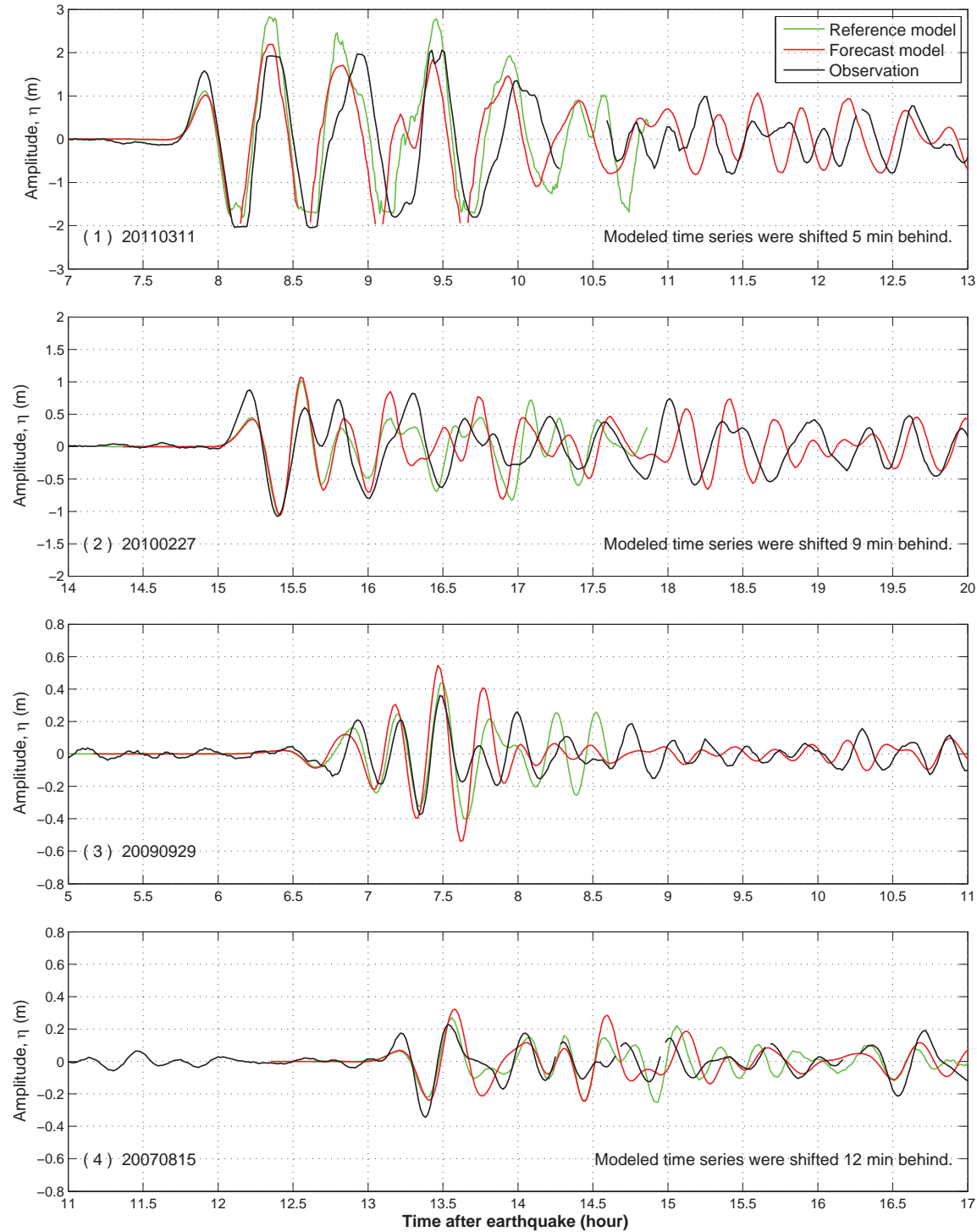


Figure 10: Observed and modeled time series of wave amplitudes at Kahului tide gauge for 17 past tsunamis. Observations were not available for the 1946, 1952, and 1960 tsunamis.

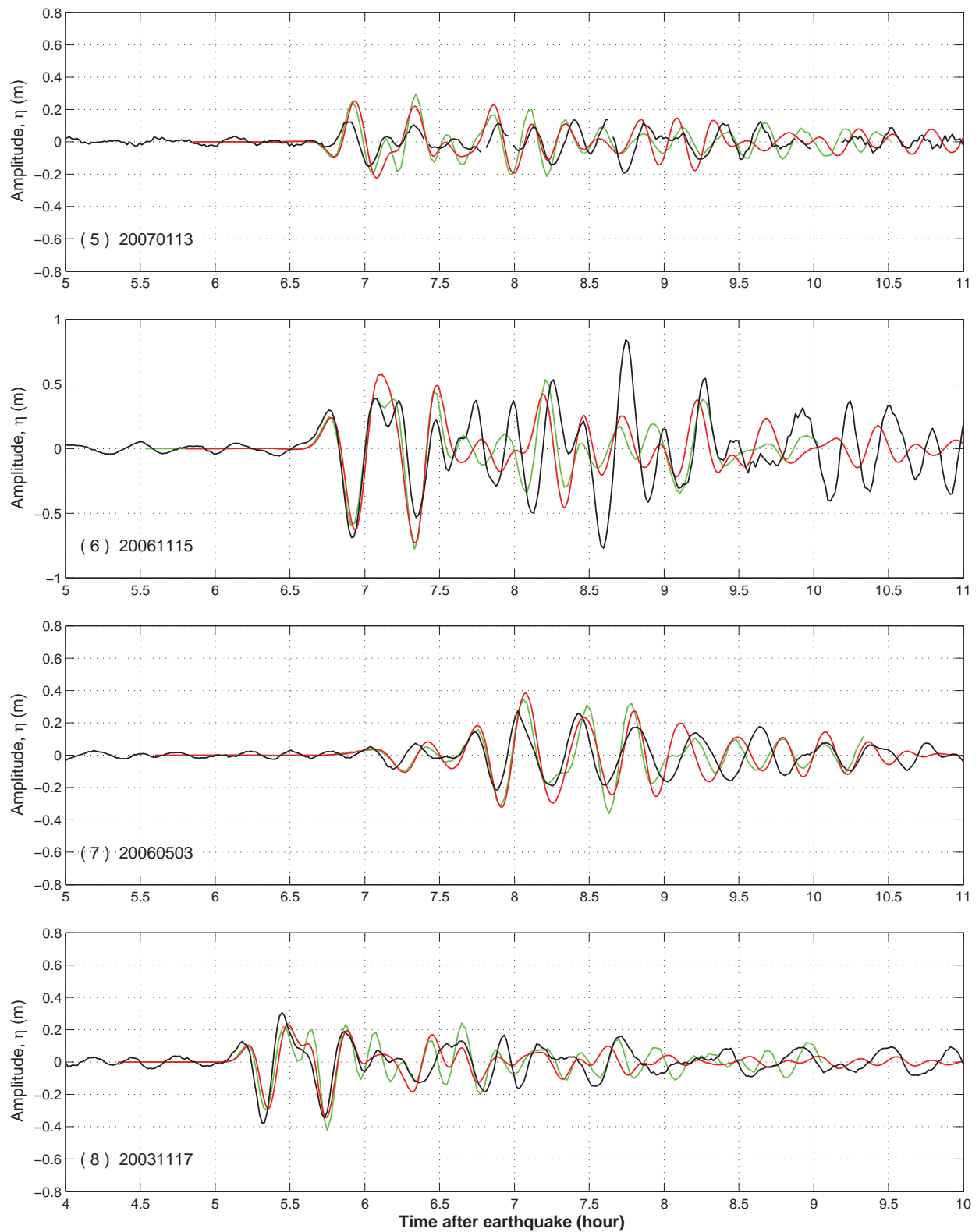
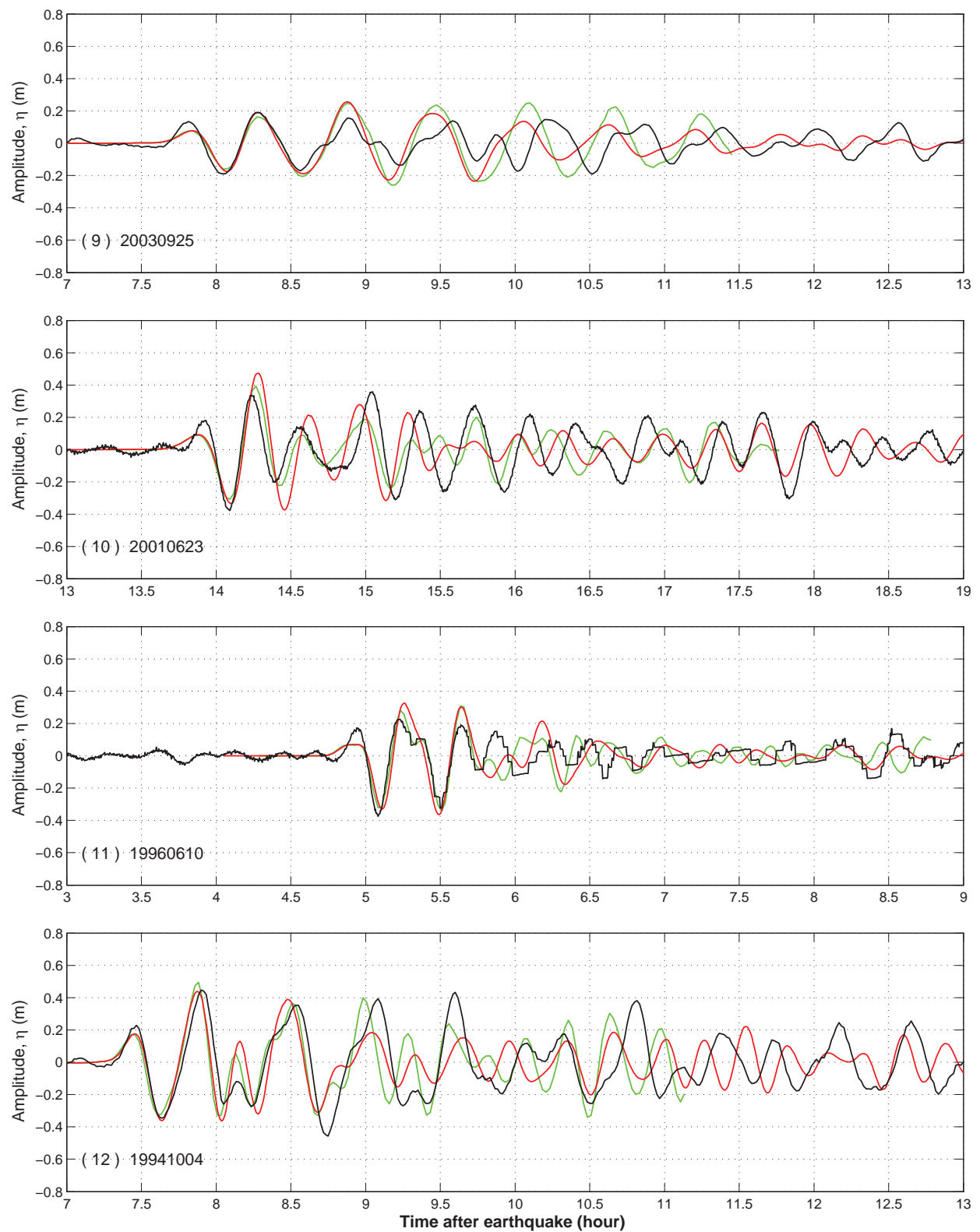


Figure 10: Continued.

**Figure 10:** Continued.

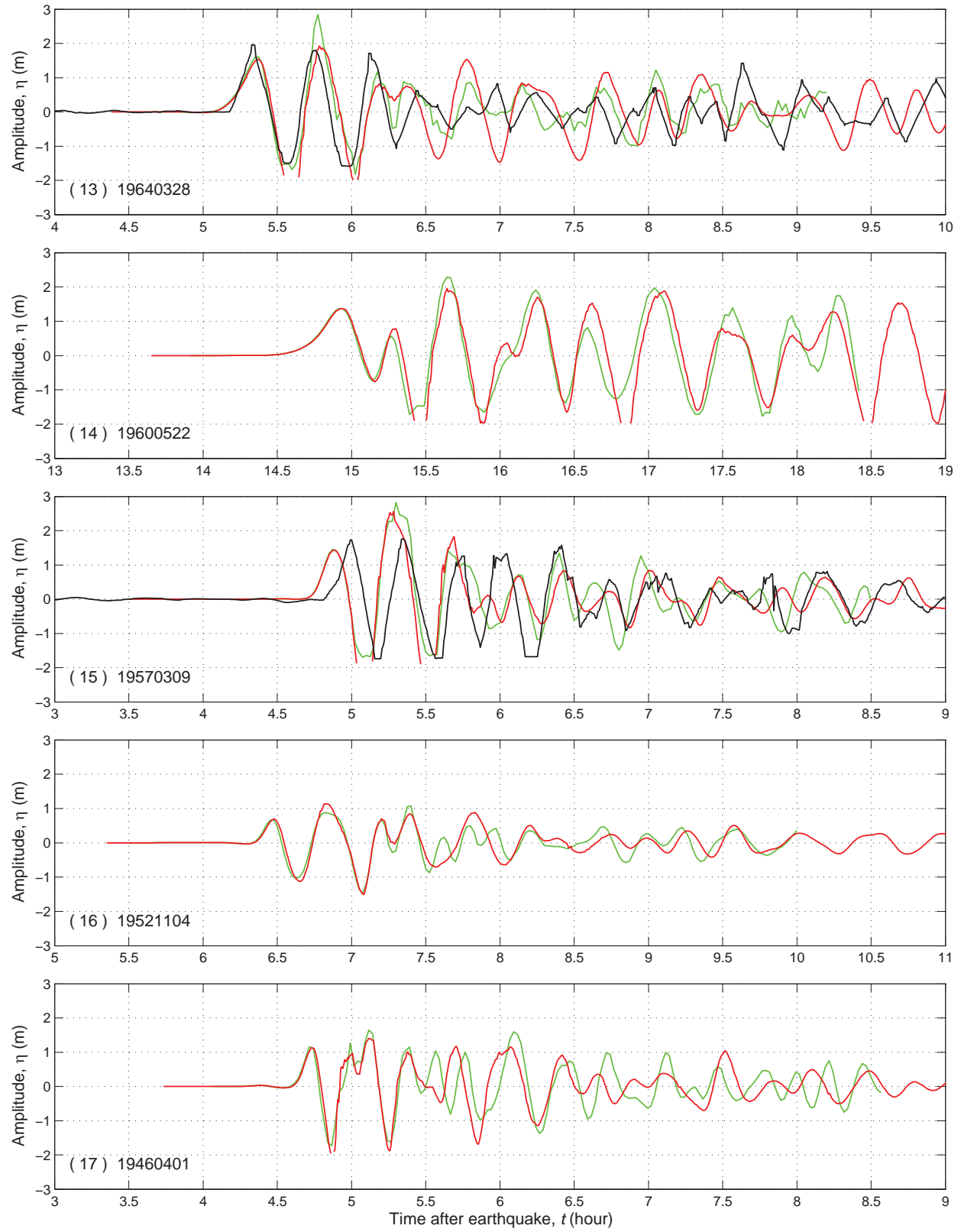


Figure 10: Continued.

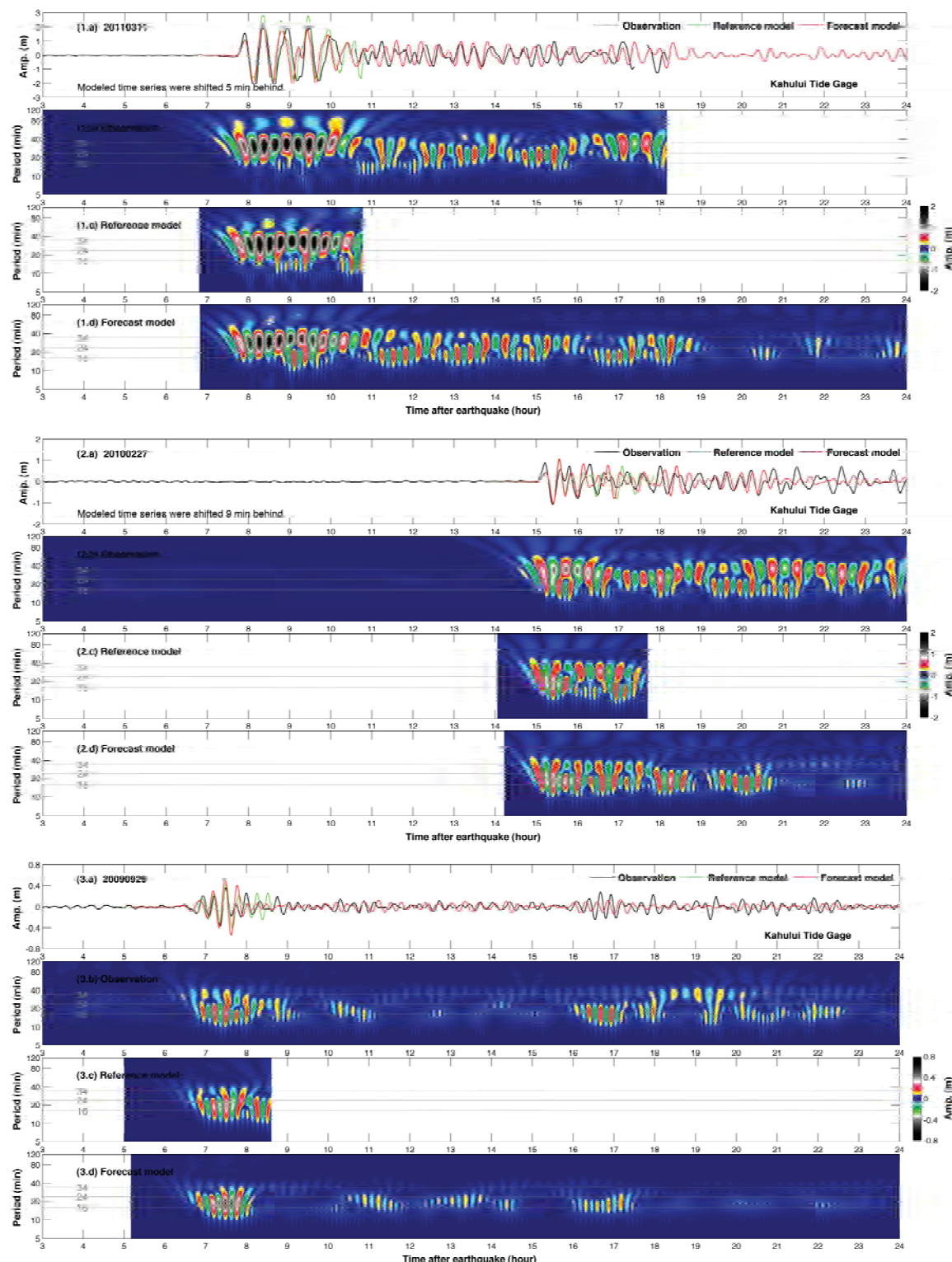


Figure 11: Observed and modeled time series of (a) wave amplitudes and (b, c, and d) wavelet-derived amplitude spectra at Kahului tide gauge up to 24 hr since tsunami generation for 17 past tsunamis.

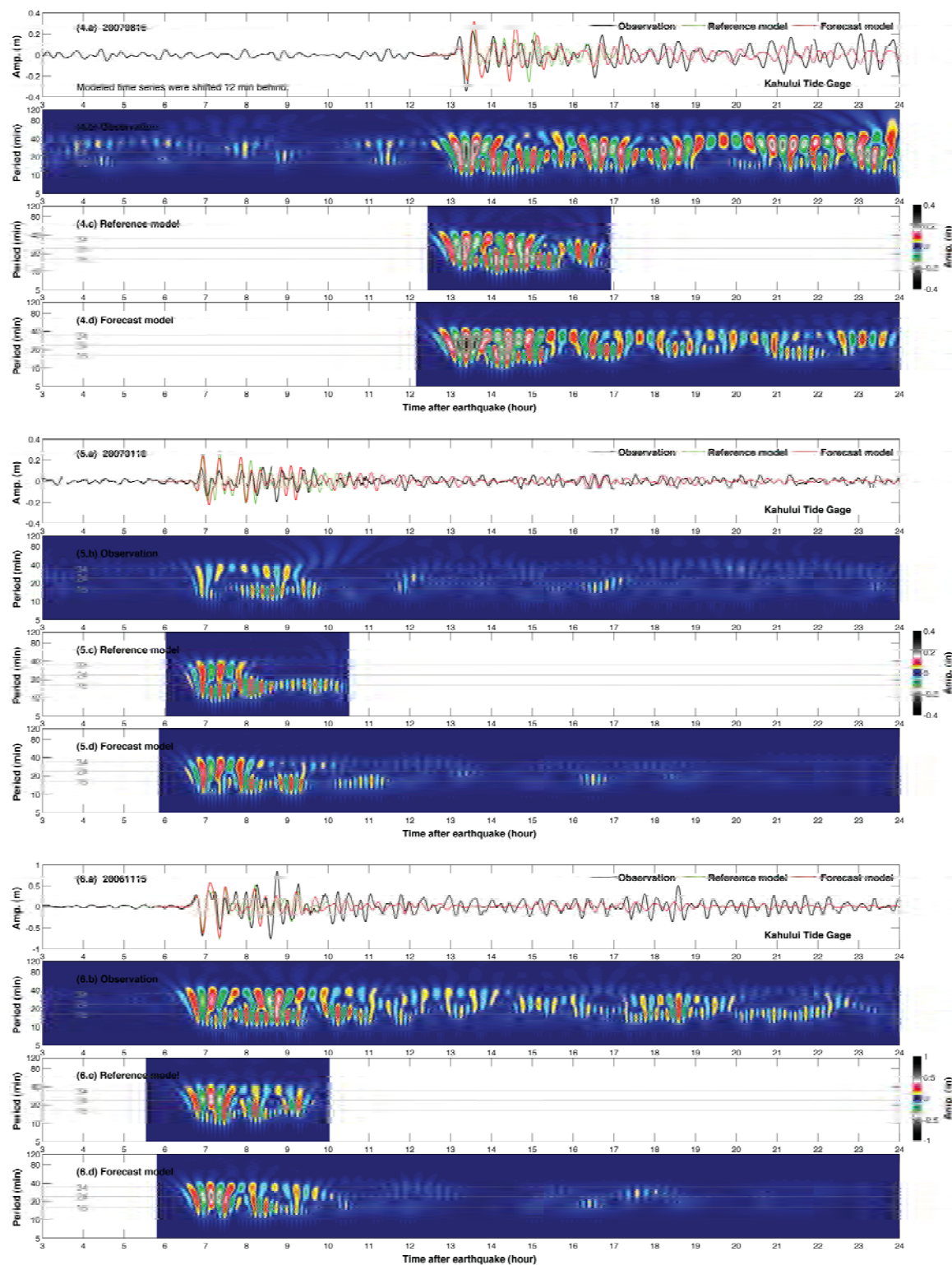


Figure 11: Continued.

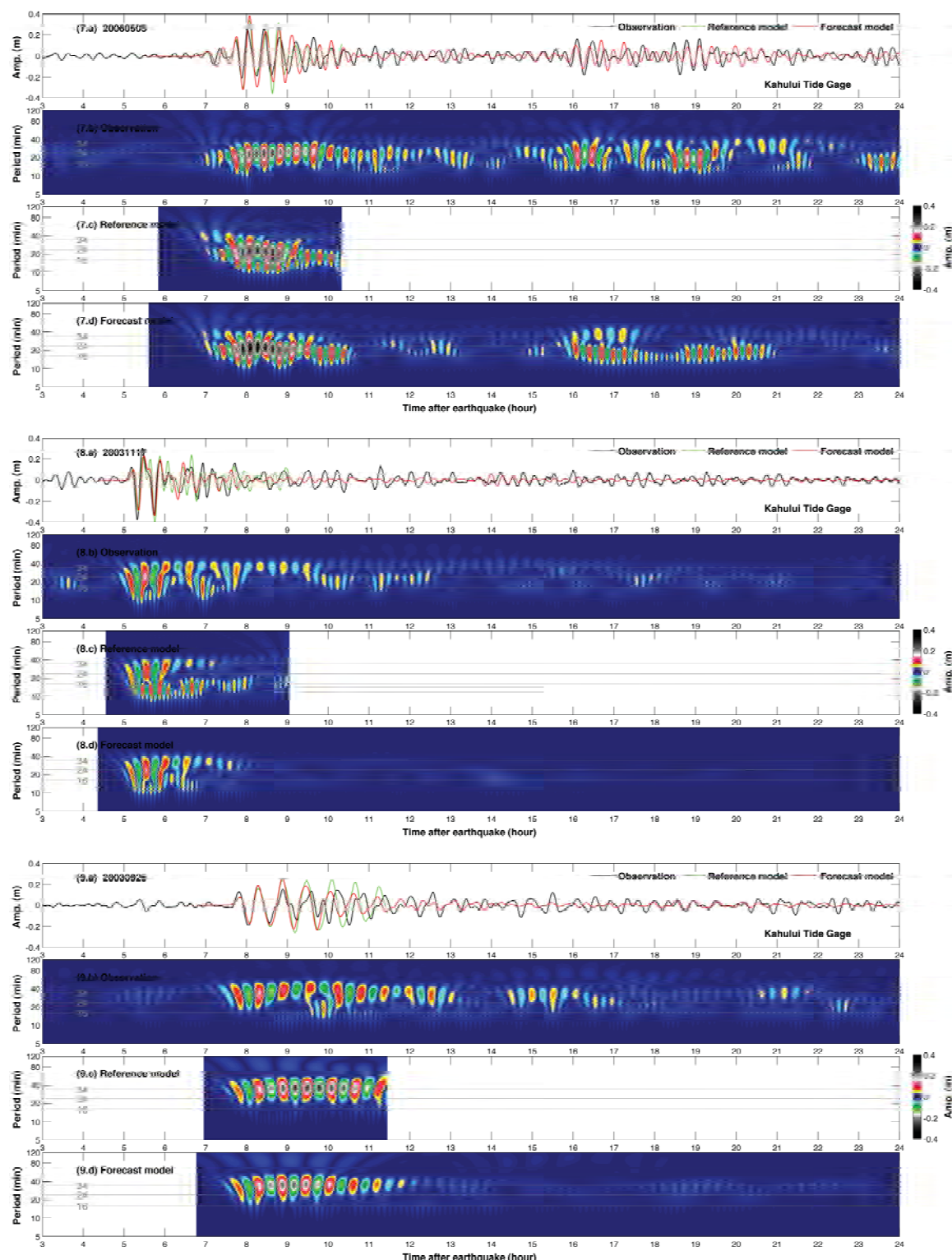


Figure 11: Continued.

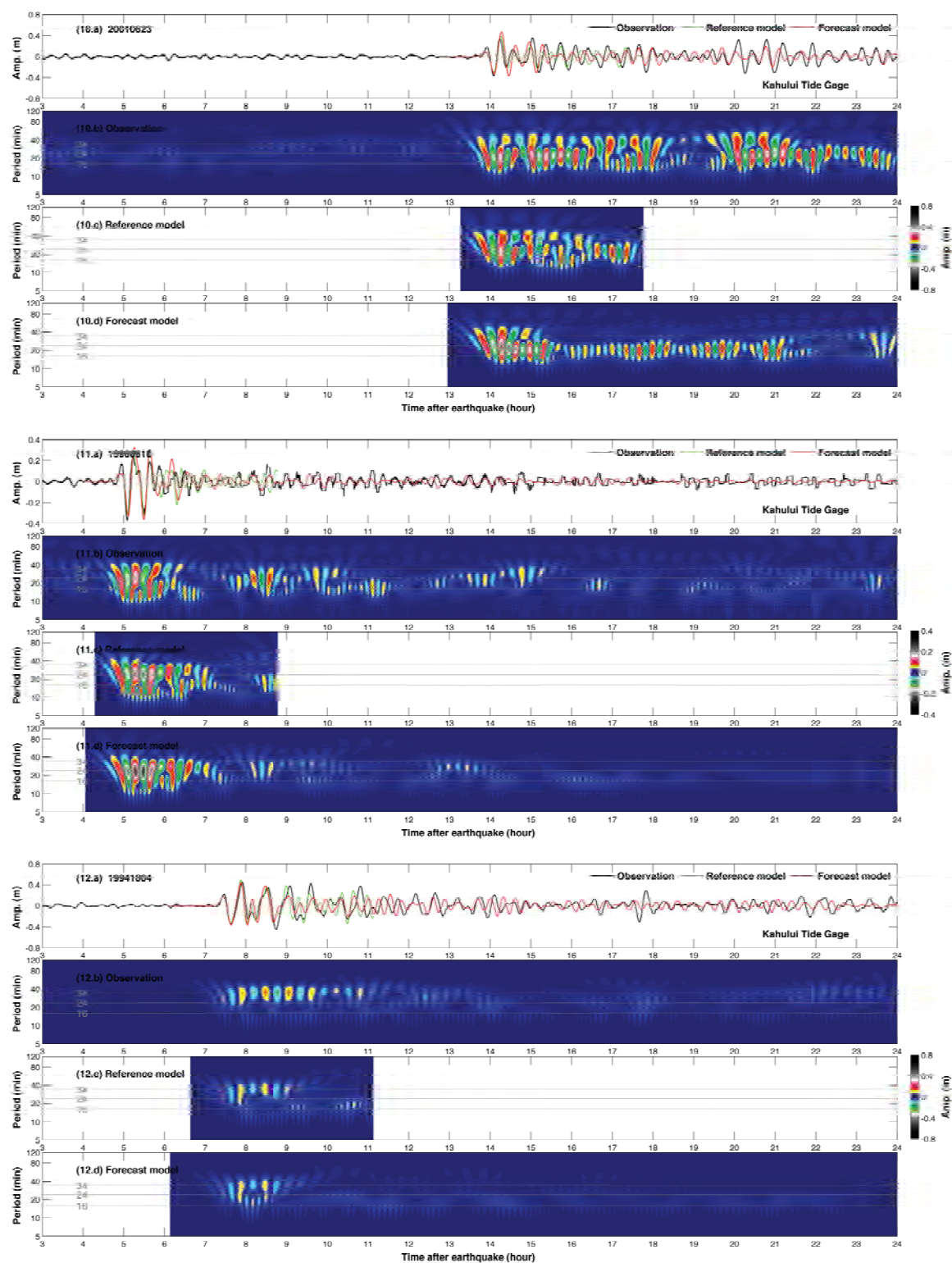


Figure 11: Continued.

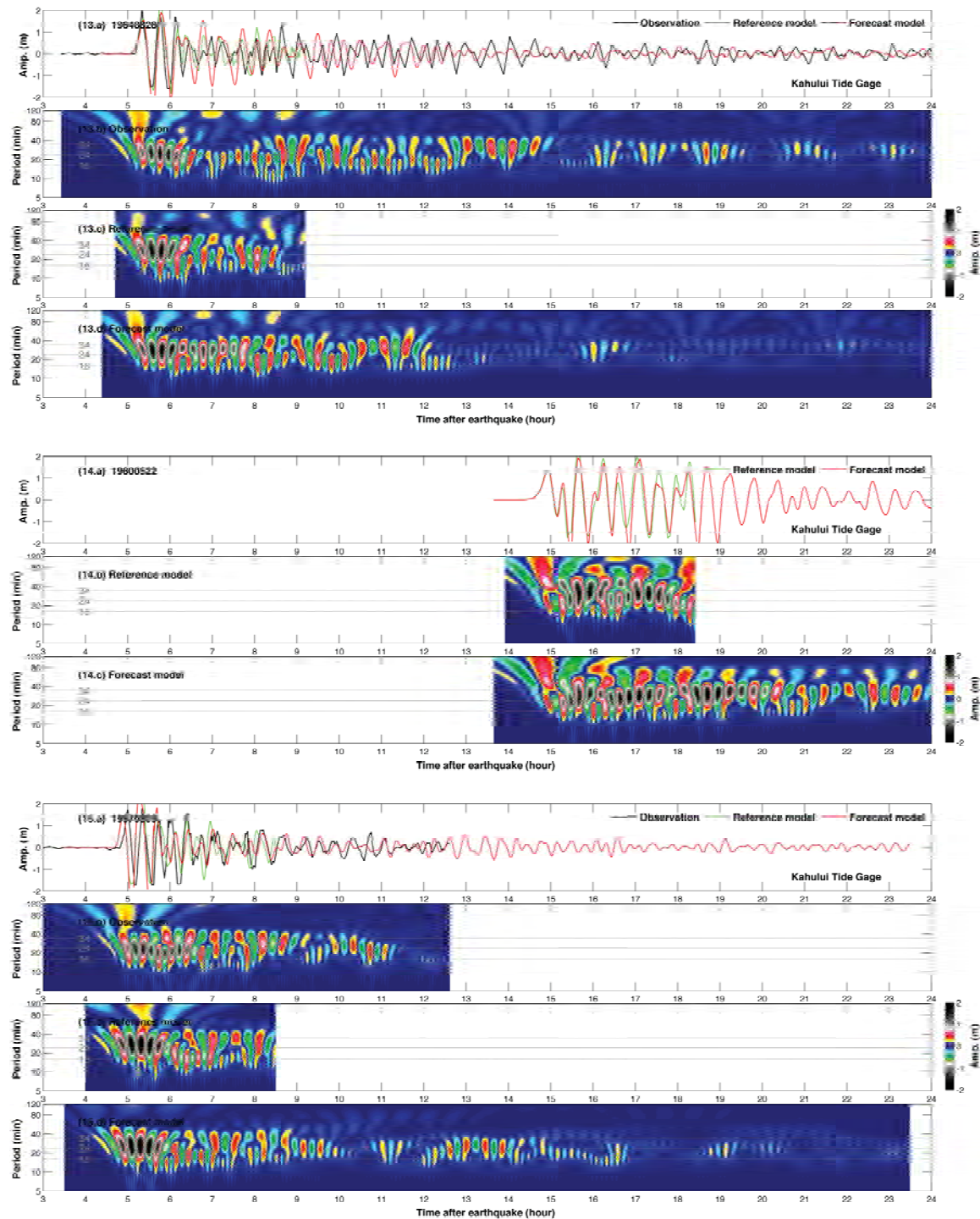


Figure 11: Continued.

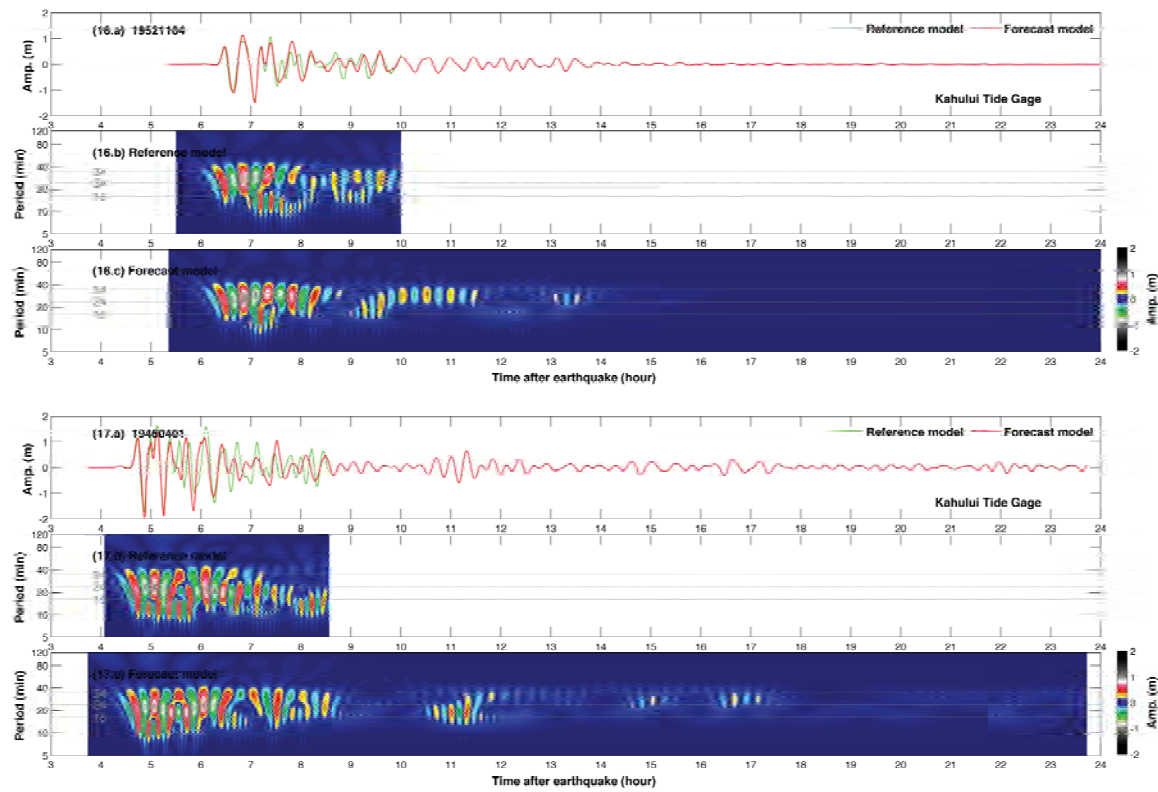


Figure 11: Continued.

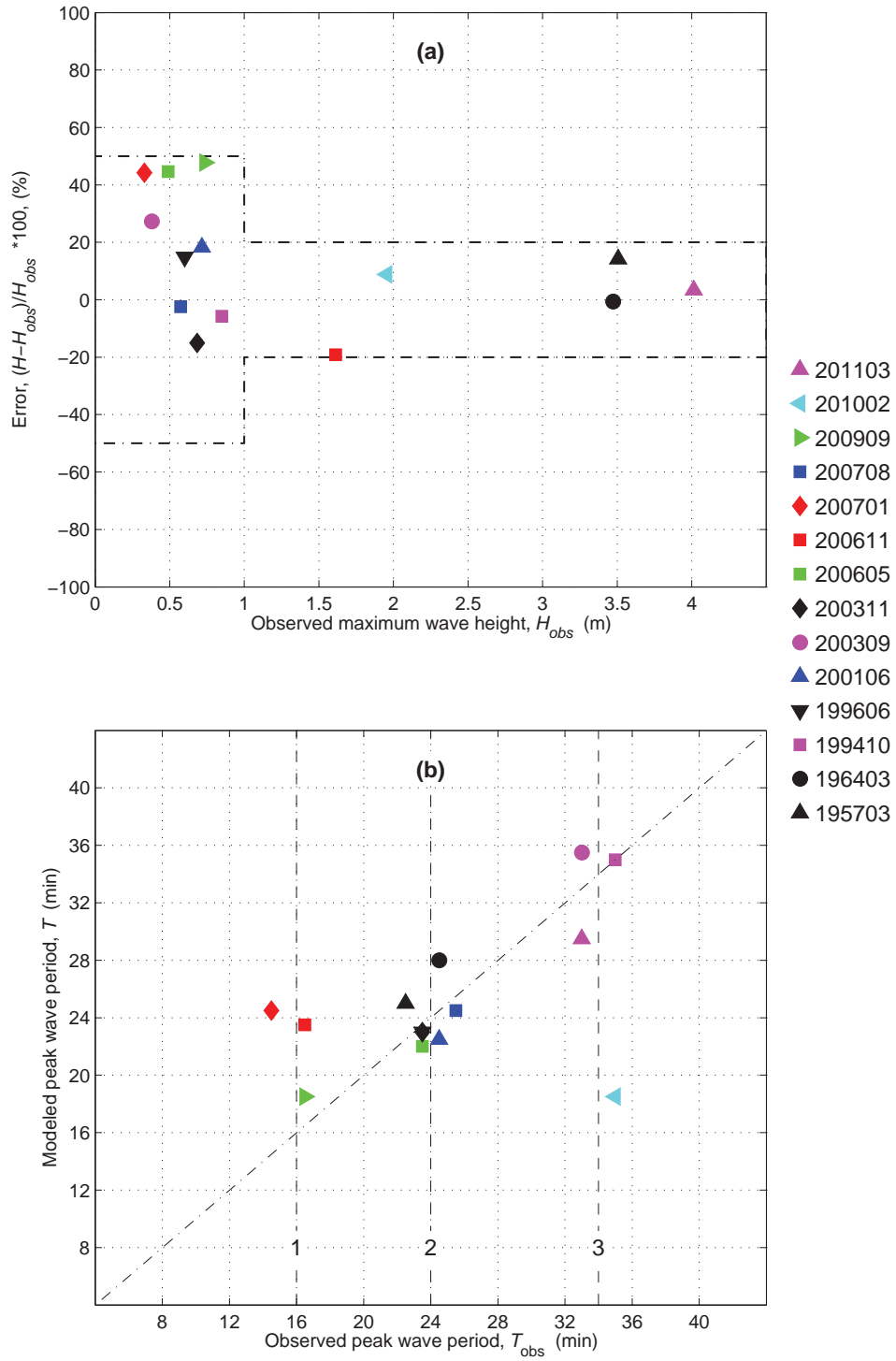


Figure 12: (a) Error of the maximum wave height, and (b) peak wave period from observations and results computed by the Kahului forecast model. Error = $(H - H_{obs})/H_{obs}$, where H is the modeled maximum wave height and H_{obs} is the observation. Colors represent subduction zones of the earthquakes. Red, central Kuril and Kamchatka; magenta, Hokkaido and west Kuril; black, Aleutian and Alaska; green, Tonga; blue, Peru; cyan, Chile.

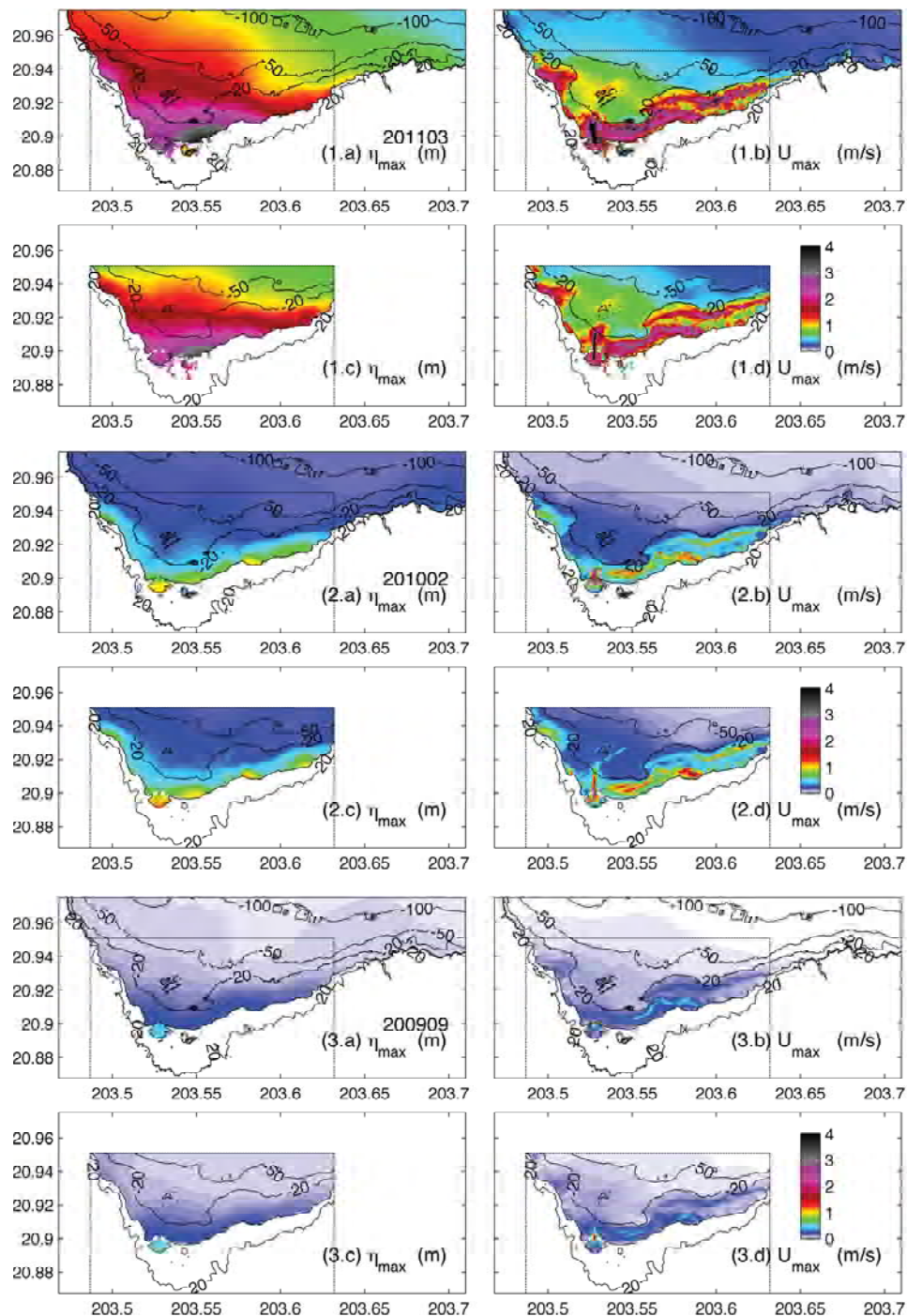


Figure 13: Computed maximum amplitude and current by the Kahului (a and b) reference model and (c and d) forecast model for 17 past tsunamis.

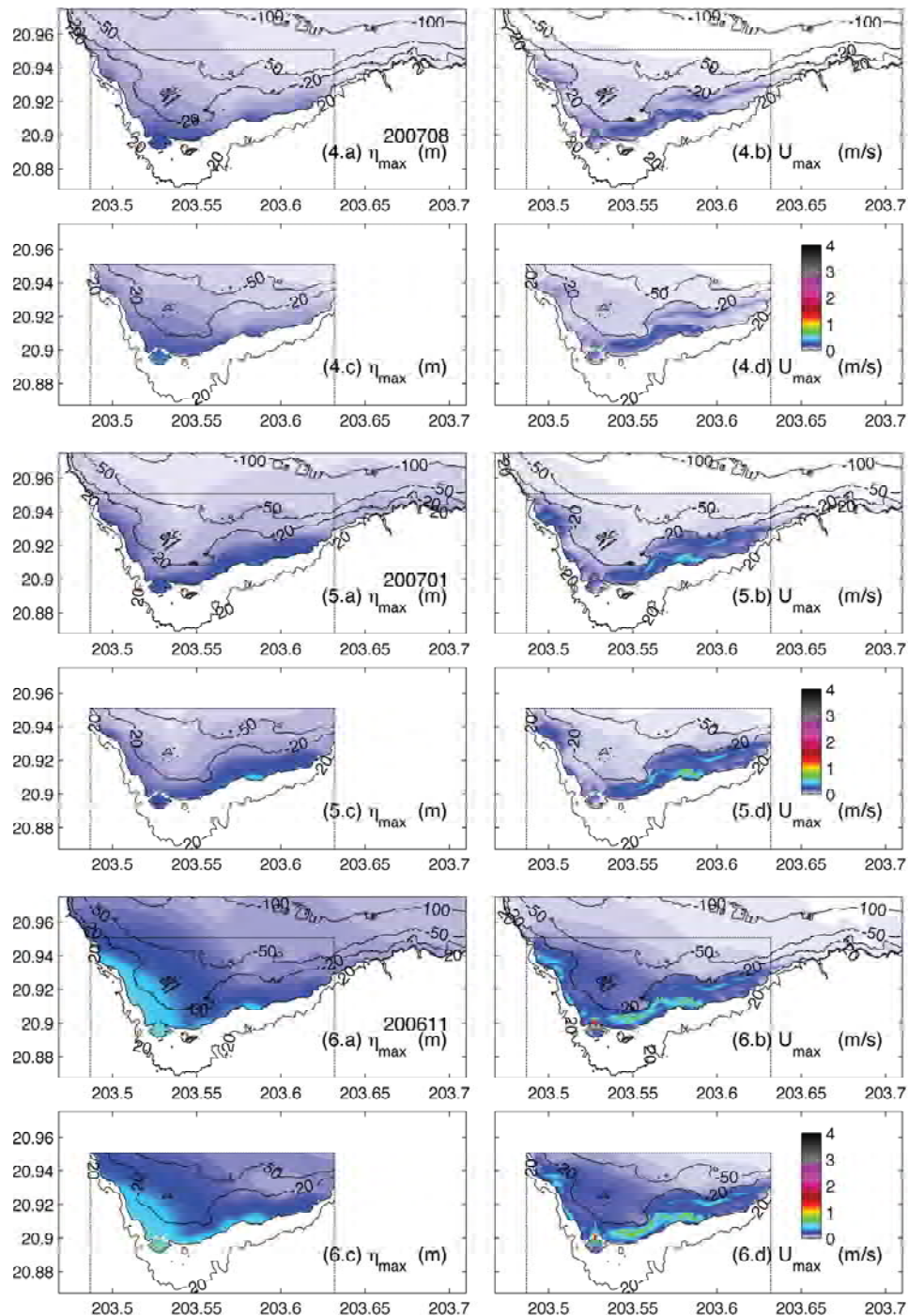


Figure 13: Continued.

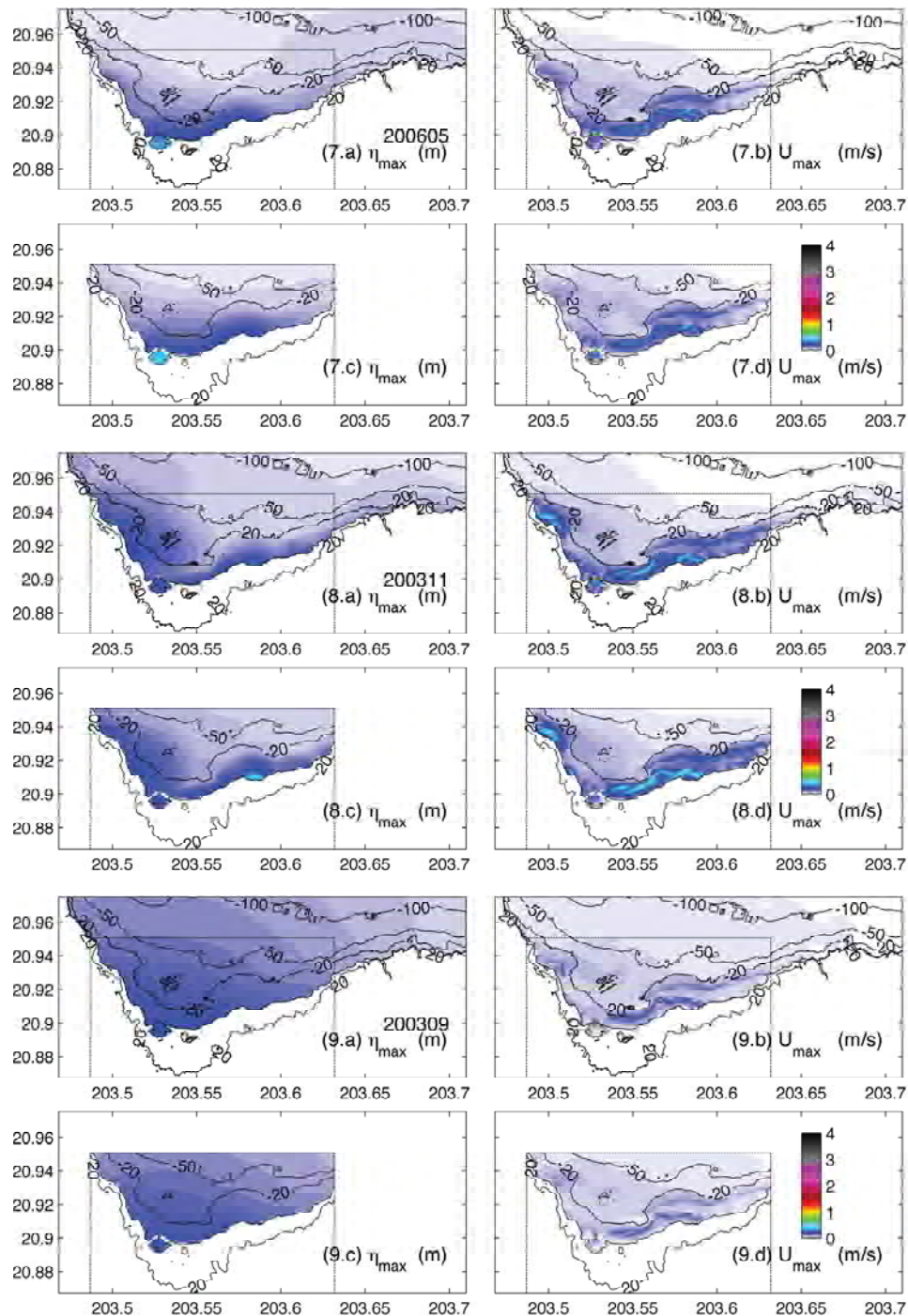


Figure 13: Continued.

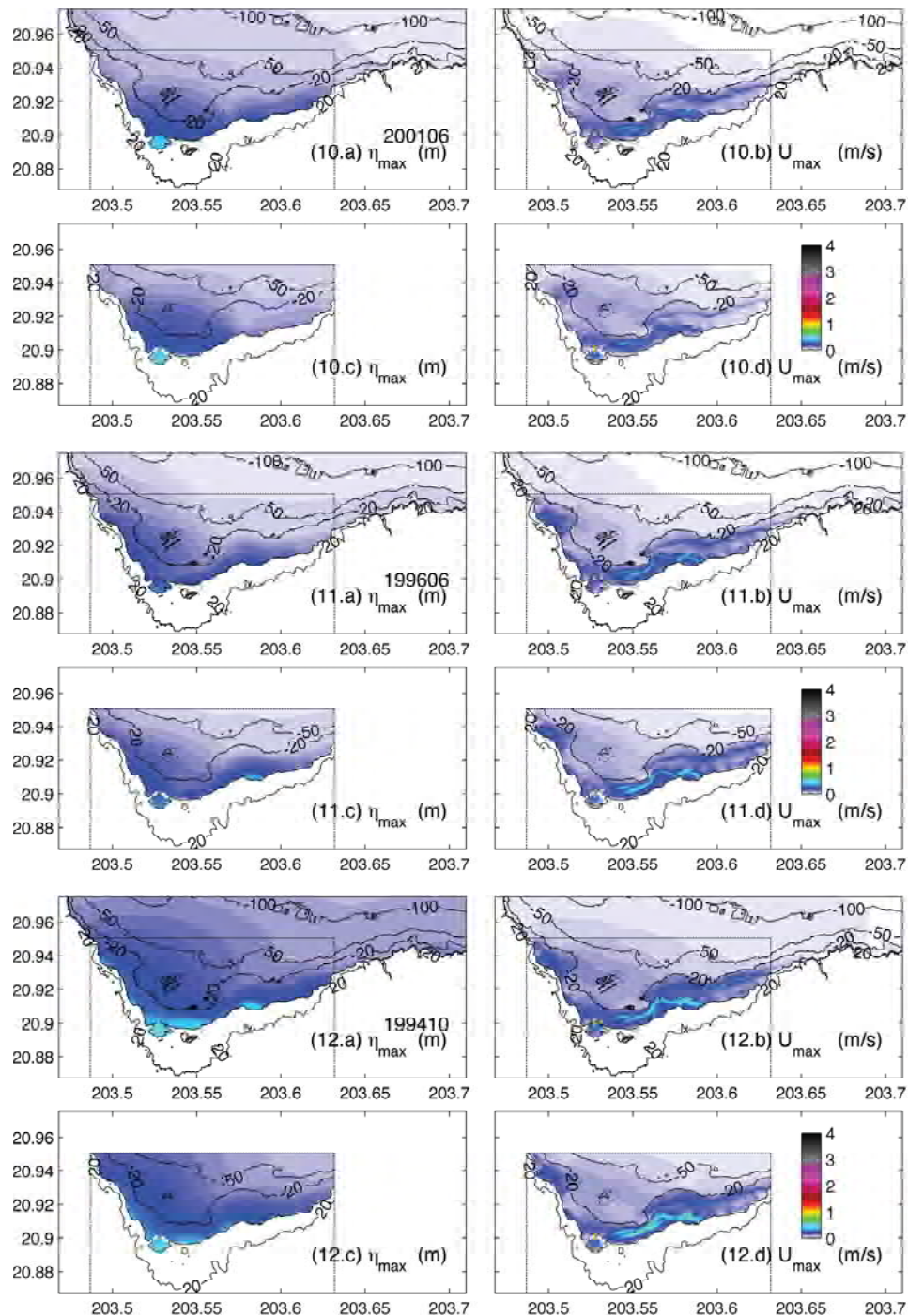


Figure 13: Continued.

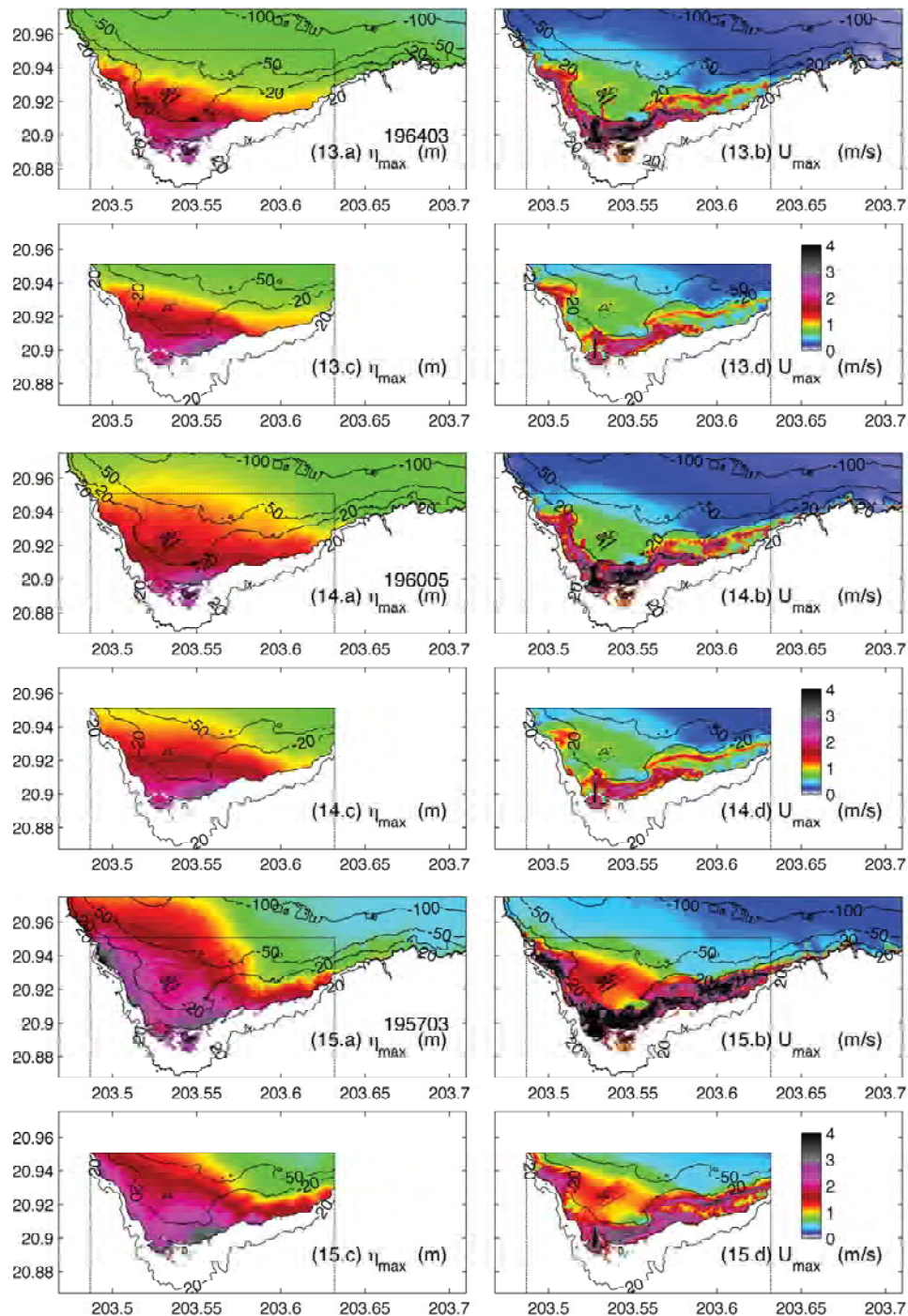


Figure 13: Continued.

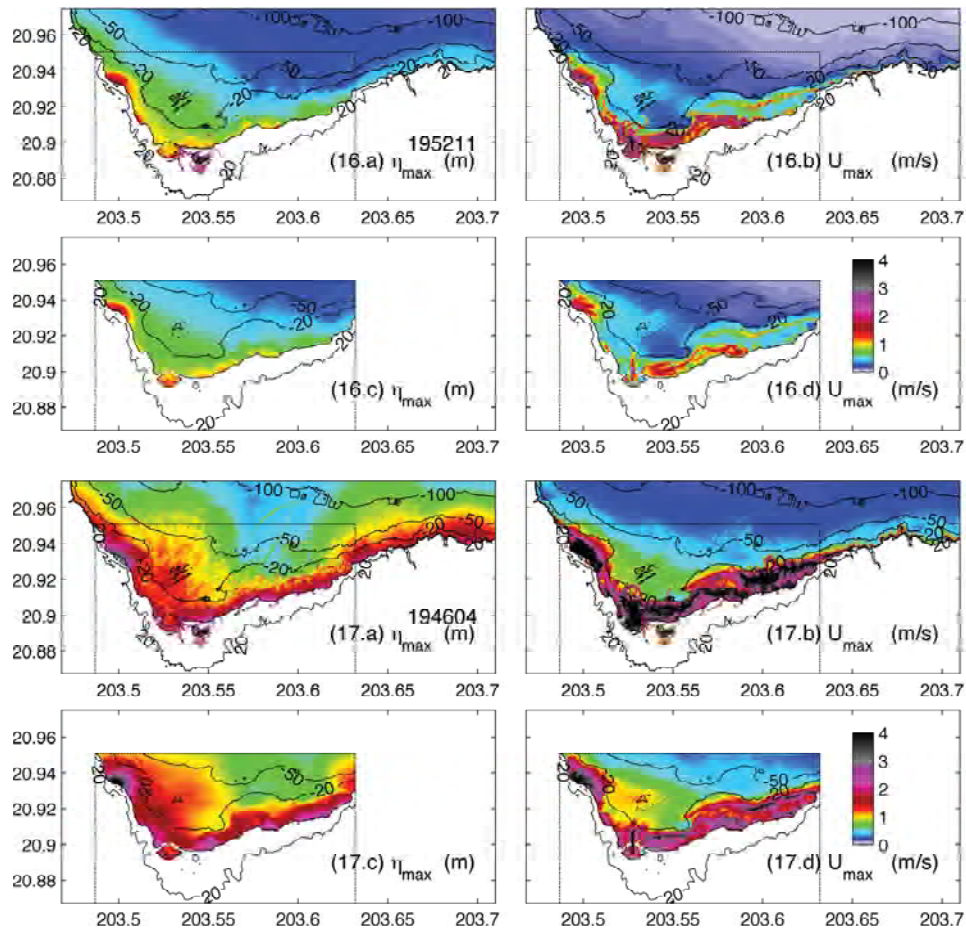


Figure 13: Continued.

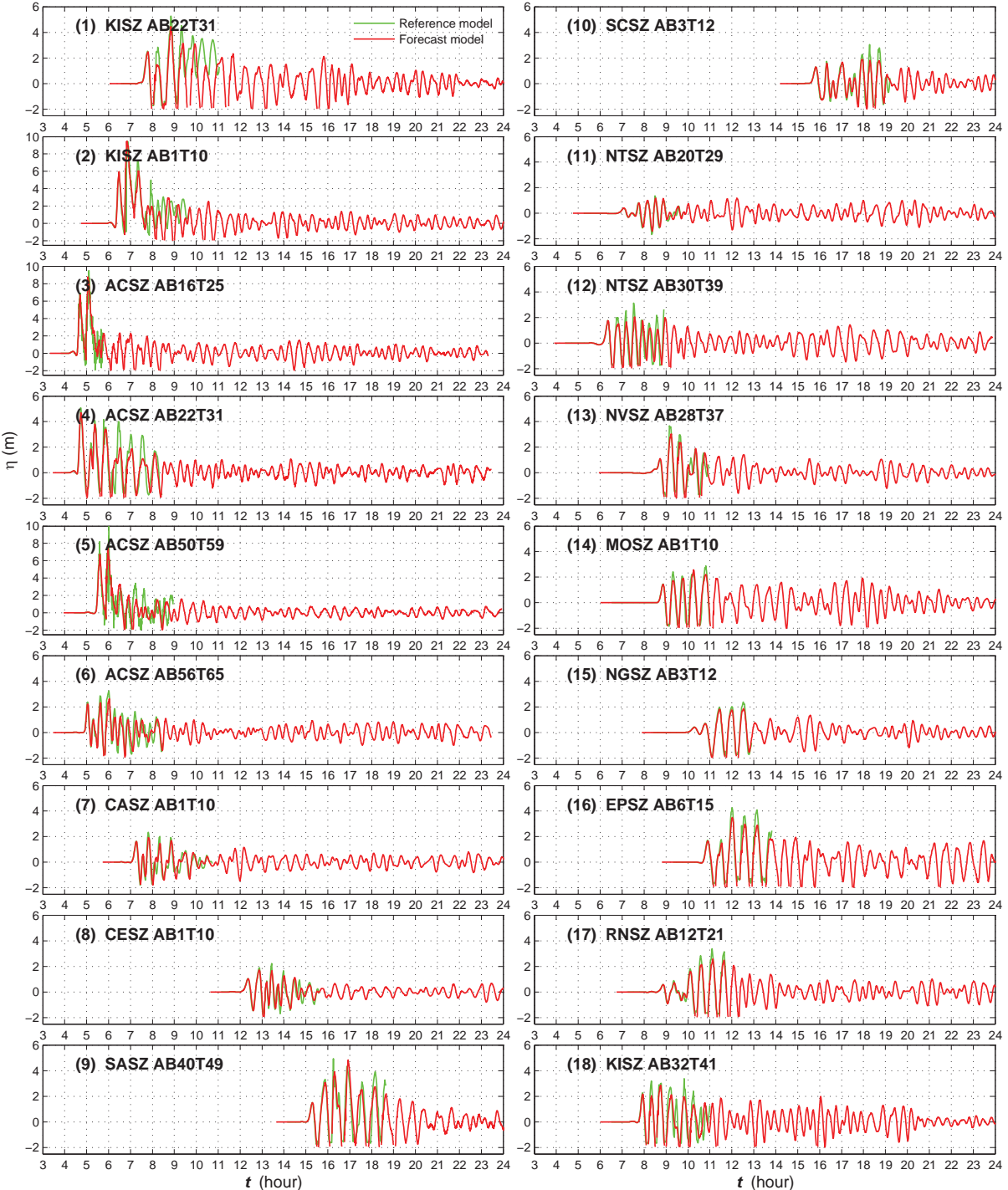


Figure 14: Modeled tsunami time series by the Kahului reference and forecast models for 18 synthetic magnitude 9.3 tsunamis. Locations of the tsunamis can be found in **Figure 1**.

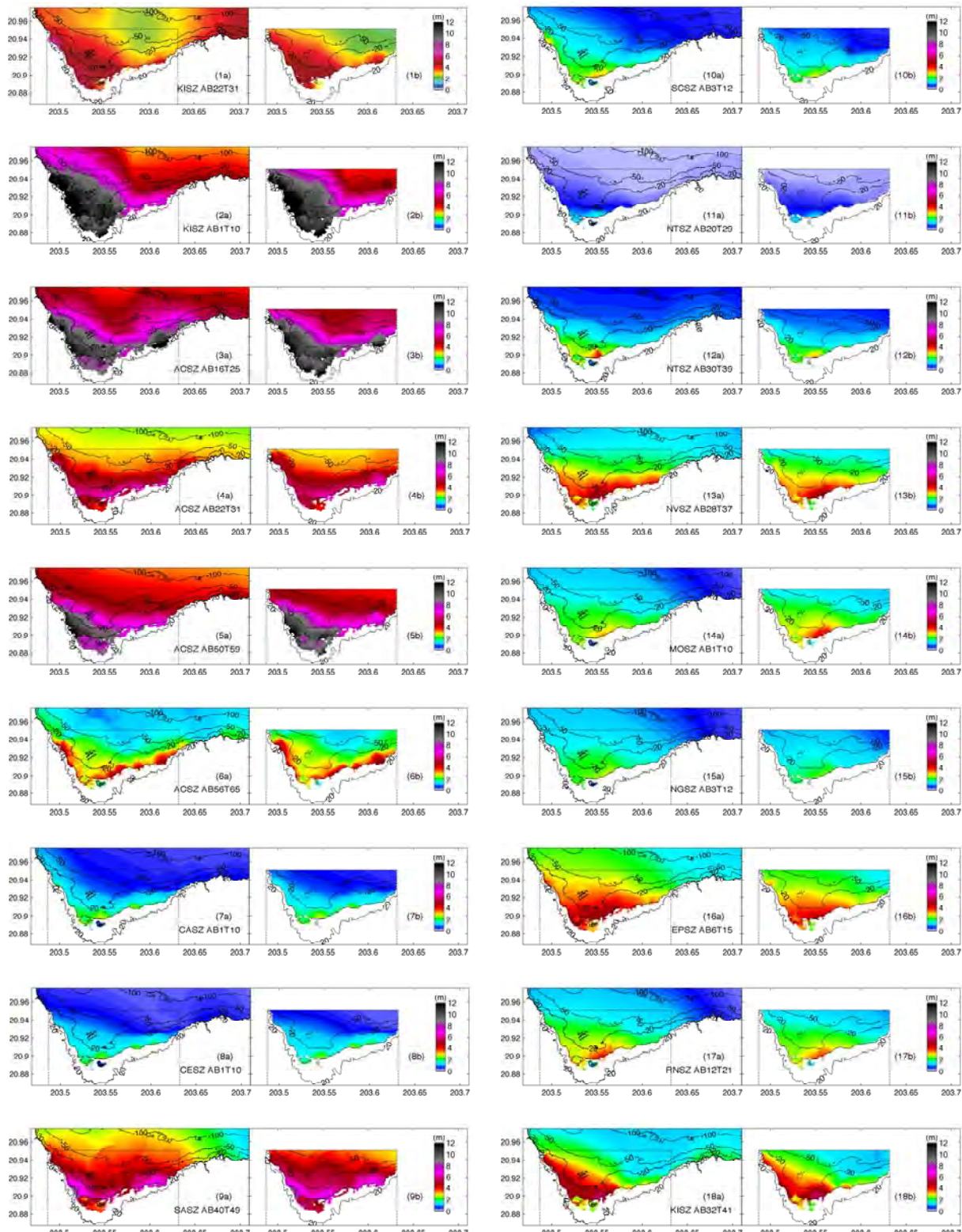


Figure 15: Maximum water elevation computed by the Kahului (a) reference model and (b) forecast model for 18 synthetic magnitude 9.3 tsunamis. Locations of the tsunamis can be found in **Figure 1**.

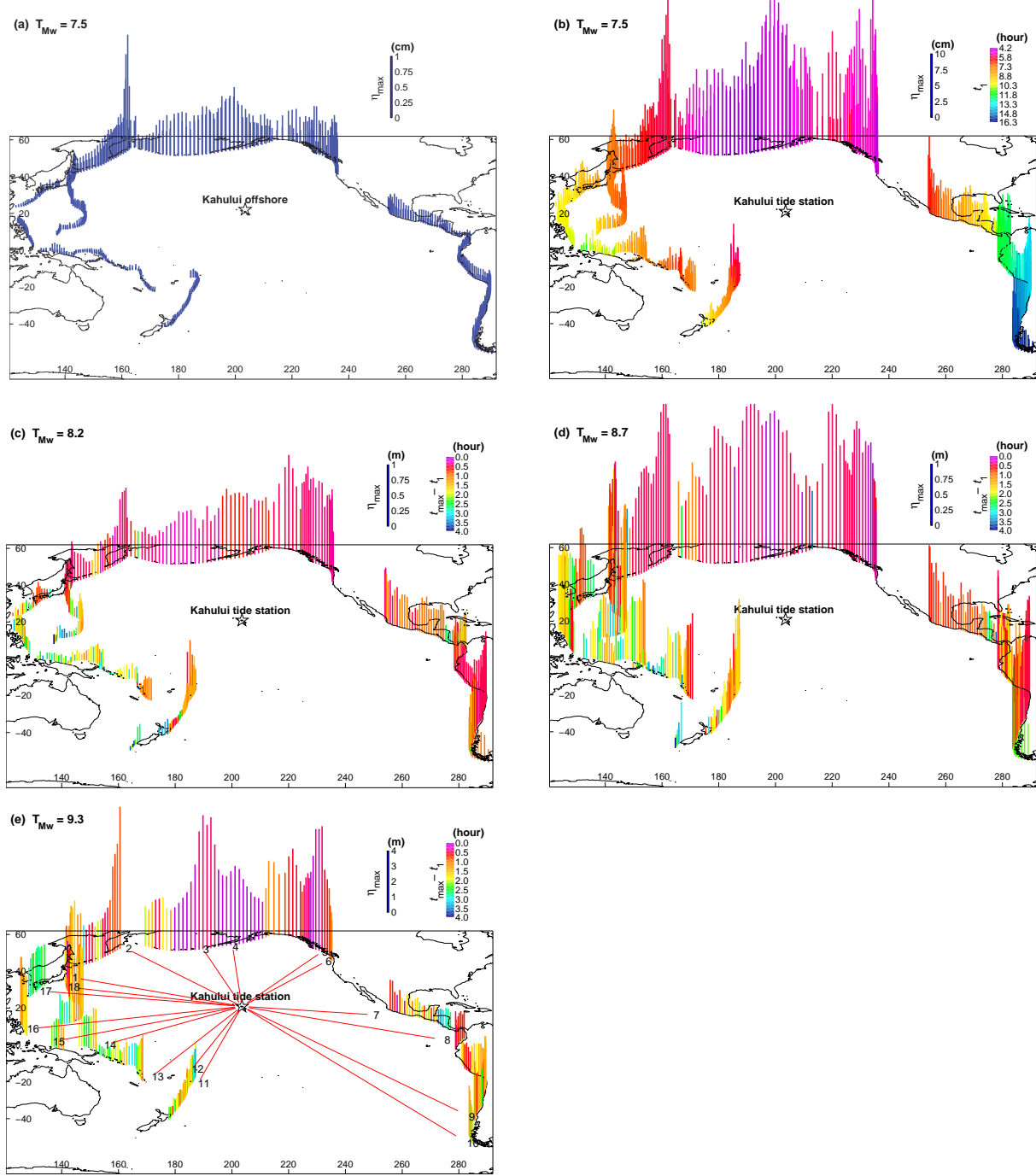


Figure 16: Maximum water elevation at (a) 4951-m water depth offshore Kahului from the propagation database (magnitude 7.5) and (b), (c), (d), and (e) at Kahului tide station computed by the forecast model at approximately 2 m water depth for synthetic magnitude 7.5, 8.2, 8.7, and 9.3 tsunamis. Colors in (b) represent the first arrival at the station. Colors in (c), (d), and (e) represent the difference in time between the arrival of the maximum elevation and the first arrival.

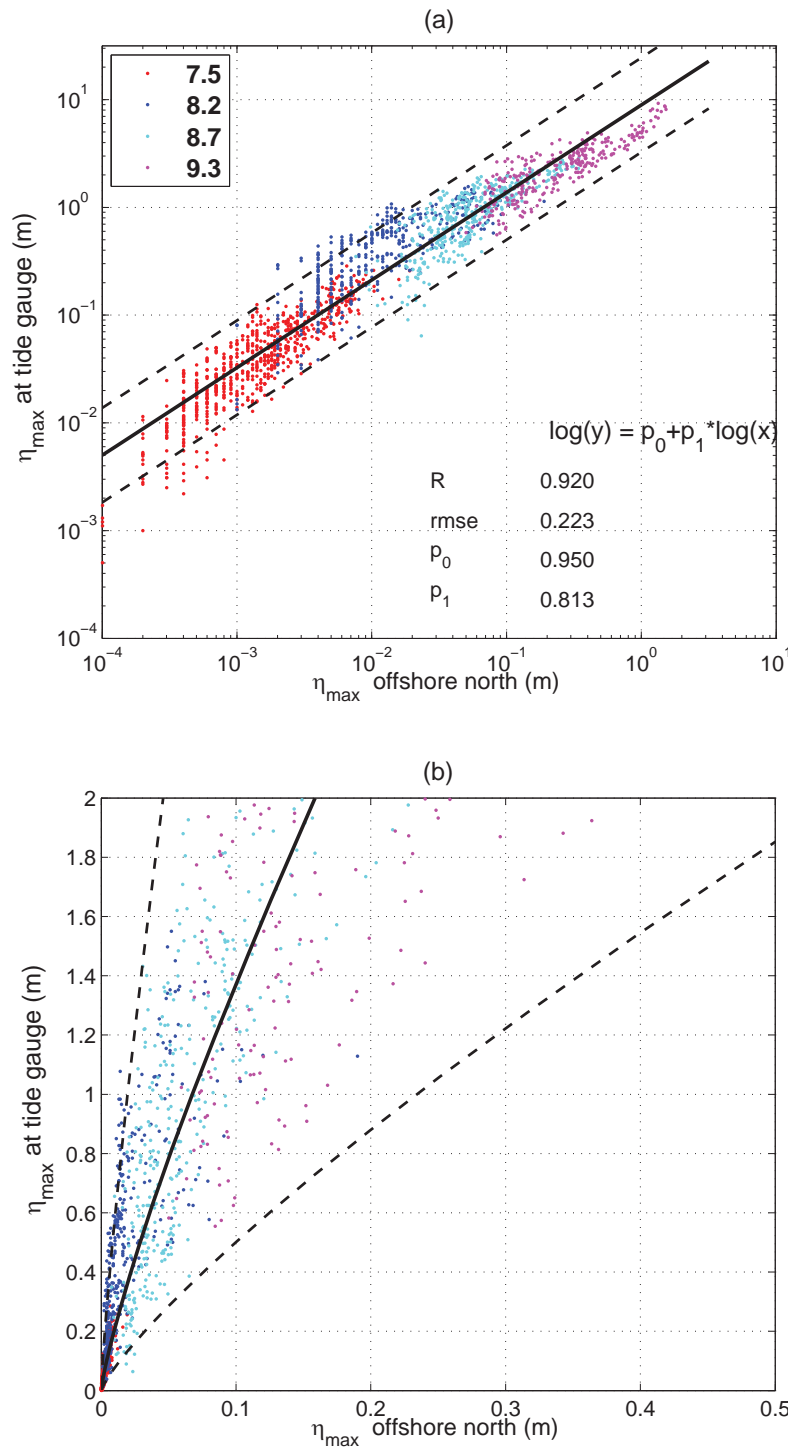


Figure 17: Computed maximum water elevation at offshore deep water (4951 m) and Kahului tide station (~ 2 m) in (a) logarithmic and (b) Cartesian coordinates. Colors represent tsunami moment magnitudes. Solid line is the fit by regression analysis in logarithmic scale. Dashed lines are the prediction bounds based on 95% confident level. R, square of the correlation; rmse, root mean squared error; p_0 and p_1 , parameters.

Appendix A.

Since the initial development of the forecast model for Kahului, Hawaii, the parameters for the input file for running the forecast and reference models have been changed to reflect changes to the MOST model code. The following appendix lists the new input files for Kahului.

A1. Reference model *.in file for Kahului, Hawaii—updated for 2009

```
0.0001 Minimum amplitude of input offshore wave (m):  
1 Input minimum depth for offshore (m)  
0.1 Input "dry land" depth for inundation (m)  
0.000625 Input friction coefficient (n**2)  
1 runup flag for grids A and B (1=yes,0=no)  
300.0 blowup limit  
0.2 Input time step (sec)  
72000 Input amount of steps  
8 Compute "A" arrays every n-th time step, n=  
2 Compute "B" arrays every n-th time step, n=  
150 Input number of steps between snapshots  
1 ...Starting from  
1 ...Saving grid every n-th node, n=
```

A2. Forecast model *.in file for Kahului, Hawaii—updated for 2009

```
0.0001 Minimum amplitude of input offshore wave (m):  
1 Input minimum depth for offshore (m)  
0.1 Input "dry land" depth for inundation (m)  
0.000625 Input friction coefficient (n**2)  
1 runup flag for grids A and B (1 = yes, 0 = no)  
300.0 blowup limit  
1.5 Input time step (sec)  
9600 Input amount of steps  
8 Compute "A" arrays every n-th time step, n=  
1 Compute "B" arrays every n-th time step, n=  
20 Input number of steps between snapshots  
1 ...Starting from  
1 ...Saving grid every n-th node, n=
```


Appendix B. Propagation Database: Pacific Ocean Unit Sources

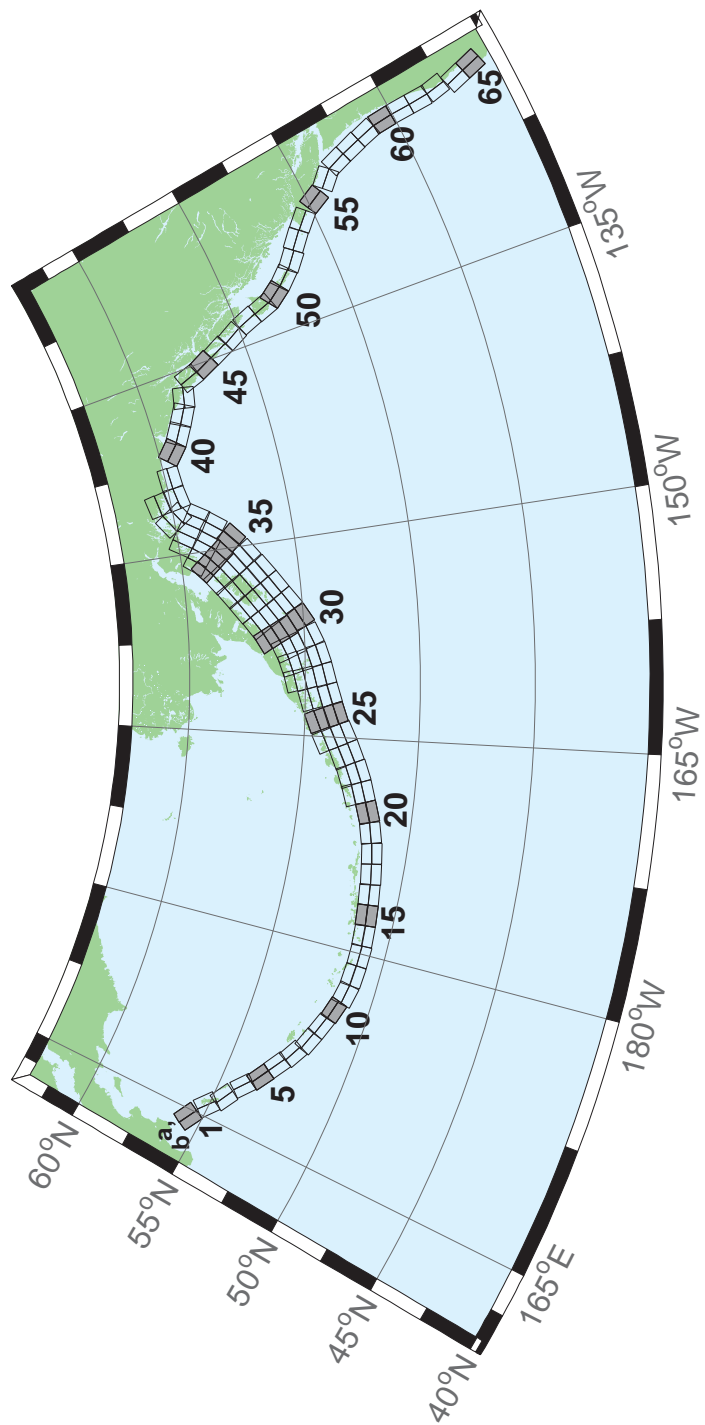


Figure B1: Aleutian-Alaska-Cascadia Subduction Zone unit sources.

Table B1: Earthquake parameters for Aleutian-Alaska-Cascadia Subduction Zone unit sources.

Segment	Description	Longitude (°E)	Latitude (°N)	Strike (°)	Dip (°)	Depth (km)
acsz-1a	Aleutian-Alaska-Cascadia	164.7994	55.9606	299	17	19.61
acsz-1b	Aleutian-Alaska-Cascadia	164.4310	55.5849	299	17	5
acsz-2a	Aleutian-Alaska-Cascadia	166.3418	55.4016	310.2	17	19.61
acsz-2b	Aleutian-Alaska-Cascadia	165.8578	55.0734	310.2	17	5
acsz-3a	Aleutian-Alaska-Cascadia	167.2939	54.8919	300.2	23.36	24.82
acsz-3b	Aleutian-Alaska-Cascadia	166.9362	54.5356	300.2	23.36	5
acsz-4a	Aleutian-Alaska-Cascadia	168.7131	54.2852	310.2	38.51	25.33
acsz-4b	Aleutian-Alaska-Cascadia	168.3269	54.0168	310.2	24	5
acsz-5a	Aleutian-Alaska-Cascadia	169.7447	53.7808	302.8	37.02	23.54
acsz-5b	Aleutian-Alaska-Cascadia	169.4185	53.4793	302.8	21.77	5
acsz-6a	Aleutian-Alaska-Cascadia	171.0144	53.3054	303.2	35.31	22.92
acsz-6b	Aleutian-Alaska-Cascadia	170.6813	52.9986	303.2	21	5
acsz-7a	Aleutian-Alaska-Cascadia	172.1500	52.8528	298.2	35.56	20.16
acsz-7b	Aleutian-Alaska-Cascadia	171.8665	52.5307	298.2	17.65	5
acsz-8a	Aleutian-Alaska-Cascadia	173.2726	52.4579	290.8	37.92	20.35
acsz-8b	Aleutian-Alaska-Cascadia	173.0681	52.1266	290.8	17.88	5
acsz-9a	Aleutian-Alaska-Cascadia	174.5866	52.1434	289	39.09	21.05
acsz-9b	Aleutian-Alaska-Cascadia	174.4027	51.8138	289	18.73	5
acsz-10a	Aleutian-Alaska-Cascadia	175.8784	51.8526	286.1	40.51	20.87
acsz-10b	Aleutian-Alaska-Cascadia	175.7265	51.5245	286.1	18.51	5
acsz-11a	Aleutian-Alaska-Cascadia	177.1140	51.6488	280	15	17.94
acsz-11b	Aleutian-Alaska-Cascadia	176.9937	51.2215	280	15	5
acsz-12a	Aleutian-Alaska-Cascadia	178.4500	51.5690	273	15	17.94
acsz-12b	Aleutian-Alaska-Cascadia	178.4130	51.1200	273	15	5
acsz-13a	Aleutian-Alaska-Cascadia	179.8550	51.5340	271	15	17.94
acsz-13b	Aleutian-Alaska-Cascadia	179.8420	51.0850	271	15	5
acsz-14a	Aleutian-Alaska-Cascadia	181.2340	51.5780	267	15	17.94
acsz-14b	Aleutian-Alaska-Cascadia	181.2720	51.1290	267	15	5
acsz-15a	Aleutian-Alaska-Cascadia	182.6380	51.6470	265	15	17.94
acsz-15b	Aleutian-Alaska-Cascadia	182.7000	51.2000	265	15	5
acsz-16a	Aleutian-Alaska-Cascadia	184.0550	51.7250	264	15	17.94
acsz-16b	Aleutian-Alaska-Cascadia	184.1280	51.2780	264	15	5
acsz-17a	Aleutian-Alaska-Cascadia	185.4560	51.8170	262	15	17.94
acsz-17b	Aleutian-Alaska-Cascadia	185.5560	51.3720	262	15	5
acsz-18a	Aleutian-Alaska-Cascadia	186.8680	51.9410	261	15	17.94
acsz-18b	Aleutian-Alaska-Cascadia	186.9810	51.4970	261	15	5
acsz-19a	Aleutian-Alaska-Cascadia	188.2430	52.1280	257	15	17.94
acsz-19b	Aleutian-Alaska-Cascadia	188.4060	51.6900	257	15	5
acsz-20a	Aleutian-Alaska-Cascadia	189.5810	52.3550	251	15	17.94
acsz-20b	Aleutian-Alaska-Cascadia	189.8180	51.9300	251	15	5
acsz-21a	Aleutian-Alaska-Cascadia	190.9570	52.6470	251	15	17.94
acsz-21b	Aleutian-Alaska-Cascadia	191.1960	52.2220	251	15	5
acsz-21z	Aleutian-Alaska-Cascadia	190.7399	53.0443	250.8	15	30.88
acsz-22a	Aleutian-Alaska-Cascadia	192.2940	52.9430	247	15	17.94
acsz-22b	Aleutian-Alaska-Cascadia	192.5820	52.5300	247	15	5
acsz-22z	Aleutian-Alaska-Cascadia	192.0074	53.3347	247.8	15	30.88
acsz-23a	Aleutian-Alaska-Cascadia	193.6270	53.3070	245	15	17.94
acsz-23b	Aleutian-Alaska-Cascadia	193.9410	52.9000	245	15	5
acsz-23z	Aleutian-Alaska-Cascadia	193.2991	53.6768	244.6	15	30.88
acsz-24a	Aleutian-Alaska-Cascadia	194.9740	53.6870	245	15	17.94
acsz-24b	Aleutian-Alaska-Cascadia	195.2910	53.2800	245	15	5
acsz-24y	Aleutian-Alaska-Cascadia	194.3645	54.4604	244.4	15	43.82
acsz-24z	Aleutian-Alaska-Cascadia	194.6793	54.0674	244.6	15	30.88
acsz-25a	Aleutian-Alaska-Cascadia	196.4340	54.0760	250	15	17.94
acsz-25b	Aleutian-Alaska-Cascadia	196.6930	53.6543	250	15	5

(continued on next page)

Table B1: (continued)

Segment	Description	Longitude (°E)	Latitude (°N)	Strike (°)	Dip (°)	Depth (km)
acsz-25y	Aleutian-Alaska-Cascadia	195.9009	54.8572	247.9	15	43.82
acsz-25z	Aleutian-Alaska-Cascadia	196.1761	54.4536	248.1	15	30.88
acsz-26a	Aleutian-Alaska-Cascadia	197.8970	54.3600	253	15	17.94
acsz-26b	Aleutian-Alaska-Cascadia	198.1200	53.9300	253	15	5
acsz-26y	Aleutian-Alaska-Cascadia	197.5498	55.1934	253.1	15	43.82
acsz-26z	Aleutian-Alaska-Cascadia	197.7620	54.7770	253.3	15	30.88
acsz-27a	Aleutian-Alaska-Cascadia	199.4340	54.5960	256	15	17.94
acsz-27b	Aleutian-Alaska-Cascadia	199.6200	54.1600	256	15	5
acsz-27x	Aleutian-Alaska-Cascadia	198.9736	55.8631	256.5	15	56.24
acsz-27y	Aleutian-Alaska-Cascadia	199.1454	55.4401	256.6	15	43.82
acsz-27z	Aleutian-Alaska-Cascadia	199.3135	55.0170	256.8	15	30.88
acsz-28a	Aleutian-Alaska-Cascadia	200.8820	54.8300	253	15	17.94
acsz-28b	Aleutian-Alaska-Cascadia	201.1080	54.4000	253	15	5
acsz-28x	Aleutian-Alaska-Cascadia	200.1929	56.0559	252.5	15	56.24
acsz-28y	Aleutian-Alaska-Cascadia	200.4167	55.6406	252.7	15	43.82
acsz-28z	Aleutian-Alaska-Cascadia	200.6360	55.2249	252.9	15	30.88
acsz-29a	Aleutian-Alaska-Cascadia	202.2610	55.1330	247	15	17.94
acsz-29b	Aleutian-Alaska-Cascadia	202.5650	54.7200	247	15	5
acsz-29x	Aleutian-Alaska-Cascadia	201.2606	56.2861	245.7	15	56.24
acsz-29y	Aleutian-Alaska-Cascadia	201.5733	55.8888	246	15	43.82
acsz-29z	Aleutian-Alaska-Cascadia	201.8797	55.4908	246.2	15	30.88
acsz-30a	Aleutian-Alaska-Cascadia	203.6040	55.5090	240	15	17.94
acsz-30b	Aleutian-Alaska-Cascadia	203.9970	55.1200	240	15	5
acsz-30w	Aleutian-Alaska-Cascadia	201.9901	56.9855	239.5	15	69.12
acsz-30x	Aleutian-Alaska-Cascadia	202.3851	56.6094	239.8	15	56.24
acsz-30y	Aleutian-Alaska-Cascadia	202.7724	56.2320	240.2	15	43.82
acsz-30z	Aleutian-Alaska-Cascadia	203.1521	55.8534	240.5	15	30.88
acsz-31a	Aleutian-Alaska-Cascadia	204.8950	55.9700	236	15	17.94
acsz-31b	Aleutian-Alaska-Cascadia	205.3400	55.5980	236	15	5
acsz-31w	Aleutian-Alaska-Cascadia	203.0825	57.3740	234.5	15	69.12
acsz-31x	Aleutian-Alaska-Cascadia	203.5408	57.0182	234.9	15	56.24
acsz-31y	Aleutian-Alaska-Cascadia	203.9904	56.6607	235.3	15	43.82
acsz-31z	Aleutian-Alaska-Cascadia	204.4315	56.3016	235.7	15	30.88
acsz-32a	Aleutian-Alaska-Cascadia	206.2080	56.4730	236	15	17.94
acsz-32b	Aleutian-Alaska-Cascadia	206.6580	56.1000	236	15	5
acsz-32w	Aleutian-Alaska-Cascadia	204.4129	57.8908	234.3	15	69.12
acsz-32x	Aleutian-Alaska-Cascadia	204.8802	57.5358	234.7	15	56.24
acsz-32y	Aleutian-Alaska-Cascadia	205.3385	57.1792	235.1	15	43.82
acsz-32z	Aleutian-Alaska-Cascadia	205.7880	56.8210	235.5	15	30.88
acsz-33a	Aleutian-Alaska-Cascadia	207.5370	56.9750	236	15	17.94
acsz-33b	Aleutian-Alaska-Cascadia	207.9930	56.6030	236	15	5
acsz-33w	Aleutian-Alaska-Cascadia	205.7126	58.3917	234.2	15	69.12
acsz-33x	Aleutian-Alaska-Cascadia	206.1873	58.0371	234.6	15	56.24
acsz-33y	Aleutian-Alaska-Cascadia	206.6527	57.6808	235	15	43.82
acsz-33z	Aleutian-Alaska-Cascadia	207.1091	57.3227	235.4	15	30.88
acsz-34a	Aleutian-Alaska-Cascadia	208.9371	57.5124	236	15	17.94
acsz-34b	Aleutian-Alaska-Cascadia	209.4000	57.1400	236	15	5
acsz-34w	Aleutian-Alaska-Cascadia	206.9772	58.8804	233.5	15	69.12
acsz-34x	Aleutian-Alaska-Cascadia	207.4677	58.5291	233.9	15	56.24
acsz-34y	Aleutian-Alaska-Cascadia	207.9485	58.1760	234.3	15	43.82
acsz-34z	Aleutian-Alaska-Cascadia	208.4198	57.8213	234.7	15	30.88
acsz-35a	Aleutian-Alaska-Cascadia	210.2597	58.0441	230	15	17.94
acsz-35b	Aleutian-Alaska-Cascadia	210.8000	57.7000	230	15	5
acsz-35w	Aleutian-Alaska-Cascadia	208.0204	59.3199	228.8	15	69.12
acsz-35x	Aleutian-Alaska-Cascadia	208.5715	58.9906	229.3	15	56.24

(continued on next page)

Table B1: (continued)

Segment	Description	Longitude (°E)	Latitude (°N)	Strike (°)	Dip (°)	Depth (km)
acsz-35y	Aleutian-Alaska-Cascadia	209.1122	58.6590	229.7	15	43.82
acsz-35z	Aleutian-Alaska-Cascadia	209.6425	58.3252	230.2	15	30.88
acsz-36a	Aleutian-Alaska-Cascadia	211.3249	58.6565	218	15	17.94
acsz-36b	Aleutian-Alaska-Cascadia	212.0000	58.3800	218	15	5
acsz-36w	Aleutian-Alaska-Cascadia	208.5003	59.5894	215.6	15	69.12
acsz-36x	Aleutian-Alaska-Cascadia	209.1909	59.3342	216.2	15	56.24
acsz-36y	Aleutian-Alaska-Cascadia	209.8711	59.0753	216.8	15	43.82
acsz-36z	Aleutian-Alaska-Cascadia	210.5412	58.8129	217.3	15	30.88
acsz-37a	Aleutian-Alaska-Cascadia	212.2505	59.2720	213.7	15	17.94
acsz-37b	Aleutian-Alaska-Cascadia	212.9519	59.0312	213.7	15	5
acsz-37x	Aleutian-Alaska-Cascadia	210.1726	60.0644	213	15	56.24
acsz-37y	Aleutian-Alaska-Cascadia	210.8955	59.8251	213.7	15	43.82
acsz-37z	Aleutian-Alaska-Cascadia	211.6079	59.5820	214.3	15	30.88
acsz-38a	Aleutian-Alaska-Cascadia	214.6555	60.1351	260.1	0	15
acsz-38b	Aleutian-Alaska-Cascadia	214.8088	59.6927	260.1	0	15
acsz-38y	Aleutian-Alaska-Cascadia	214.3737	60.9838	259	0	15
acsz-38z	Aleutian-Alaska-Cascadia	214.5362	60.5429	259	0	15
acsz-39a	Aleutian-Alaska-Cascadia	216.5607	60.2480	267	0	15
acsz-39b	Aleutian-Alaska-Cascadia	216.6068	59.7994	267	0	15
acsz-40a	Aleutian-Alaska-Cascadia	219.3069	59.7574	310.9	0	15
acsz-40b	Aleutian-Alaska-Cascadia	218.7288	59.4180	310.9	0	15
acsz-41a	Aleutian-Alaska-Cascadia	220.4832	59.3390	300.7	0	15
acsz-41b	Aleutian-Alaska-Cascadia	220.0382	58.9529	300.7	0	15
acsz-42a	Aleutian-Alaska-Cascadia	221.8835	58.9310	298.9	0	15
acsz-42b	Aleutian-Alaska-Cascadia	221.4671	58.5379	298.9	0	15
acsz-43a	Aleutian-Alaska-Cascadia	222.9711	58.6934	282.3	0	15
acsz-43b	Aleutian-Alaska-Cascadia	222.7887	58.2546	282.3	0	15
acsz-44a	Aleutian-Alaska-Cascadia	224.9379	57.9054	340.9	12	11.09
acsz-44b	Aleutian-Alaska-Cascadia	224.1596	57.7617	340.9	7	5
acsz-45a	Aleutian-Alaska-Cascadia	225.4994	57.1634	334.1	12	11.09
acsz-45b	Aleutian-Alaska-Cascadia	224.7740	56.9718	334.1	7	5
acsz-46a	Aleutian-Alaska-Cascadia	226.1459	56.3552	334.1	12	11.09
acsz-46b	Aleutian-Alaska-Cascadia	225.4358	56.1636	334.1	7	5
acsz-47a	Aleutian-Alaska-Cascadia	226.7731	55.5830	332.3	12	11.09
acsz-47b	Aleutian-Alaska-Cascadia	226.0887	55.3785	332.3	7	5
acsz-48a	Aleutian-Alaska-Cascadia	227.4799	54.6763	339.4	12	11.09
acsz-48b	Aleutian-Alaska-Cascadia	226.7713	54.5217	339.4	7	5
acsz-49a	Aleutian-Alaska-Cascadia	227.9482	53.8155	341.2	12	11.09
acsz-49b	Aleutian-Alaska-Cascadia	227.2462	53.6737	341.2	7	5
acsz-50a	Aleutian-Alaska-Cascadia	228.3970	53.2509	324.5	12	11.09
acsz-50b	Aleutian-Alaska-Cascadia	227.8027	52.9958	324.5	7	5
acsz-51a	Aleutian-Alaska-Cascadia	229.1844	52.6297	318.4	12	11.09
acsz-51b	Aleutian-Alaska-Cascadia	228.6470	52.3378	318.4	7	5
acsz-52a	Aleutian-Alaska-Cascadia	230.0306	52.0768	310.9	12	11.09
acsz-52b	Aleutian-Alaska-Cascadia	229.5665	51.7445	310.9	7	5
acsz-53a	Aleutian-Alaska-Cascadia	231.1735	51.5258	310.9	12	11.09
acsz-53b	Aleutian-Alaska-Cascadia	230.7150	51.1935	310.9	7	5
acsz-54a	Aleutian-Alaska-Cascadia	232.2453	50.8809	314.1	12	11.09
acsz-54b	Aleutian-Alaska-Cascadia	231.7639	50.5655	314.1	7	5
acsz-55a	Aleutian-Alaska-Cascadia	233.3066	49.9032	333.7	12	11.09
acsz-55b	Aleutian-Alaska-Cascadia	232.6975	49.7086	333.7	7	5
acsz-56a	Aleutian-Alaska-Cascadia	234.0588	49.1702	315	11	12.82
acsz-56b	Aleutian-Alaska-Cascadia	233.5849	48.8584	315	9	5
acsz-57a	Aleutian-Alaska-Cascadia	234.9041	48.2596	341	11	12.82
acsz-57b	Aleutian-Alaska-Cascadia	234.2797	48.1161	341	9	5

(continued on next page)

Table B1: (continued)

Segment	Description	Longitude (°E)	Latitude (°N)	Strike (°)	Dip (°)	Depth (km)
acsz-58a	Aleutian-Alaska-Cascadia	235.3021	47.3812	344	11	12.82
acsz-58b	Aleutian-Alaska-Cascadia	234.6776	47.2597	344	9	5
acsz-59a	Aleutian-Alaska-Cascadia	235.6432	46.5082	345	11	12.82
acsz-59b	Aleutian-Alaska-Cascadia	235.0257	46.3941	345	9	5
acsz-60a	Aleutian-Alaska-Cascadia	235.8640	45.5429	356	11	12.82
acsz-60b	Aleutian-Alaska-Cascadia	235.2363	45.5121	356	9	5
acsz-61a	Aleutian-Alaska-Cascadia	235.9106	44.6227	359	11	12.82
acsz-61b	Aleutian-Alaska-Cascadia	235.2913	44.6150	359	9	5
acsz-62a	Aleutian-Alaska-Cascadia	235.9229	43.7245	359	11	12.82
acsz-62b	Aleutian-Alaska-Cascadia	235.3130	43.7168	359	9	5
acsz-63a	Aleutian-Alaska-Cascadia	236.0220	42.9020	350	11	12.82
acsz-63b	Aleutian-Alaska-Cascadia	235.4300	42.8254	350	9	5
acsz-64a	Aleutian-Alaska-Cascadia	235.9638	41.9818	345	11	12.82
acsz-64b	Aleutian-Alaska-Cascadia	235.3919	41.8677	345	9	5
acsz-65a	Aleutian-Alaska-Cascadia	236.2643	41.1141	345	11	12.82
acsz-65b	Aleutian-Alaska-Cascadia	235.7000	41.0000	345	9	5
acsz-238a	Aleutian-Alaska-Cascadia	213.2878	59.8406	236.8	15	17.94
acsz-238y	Aleutian-Alaska-Cascadia	212.3424	60.5664	236.8	15	43.82
acsz-238z	Aleutian-Alaska-Cascadia	212.8119	60.2035	236.8	15	30.88

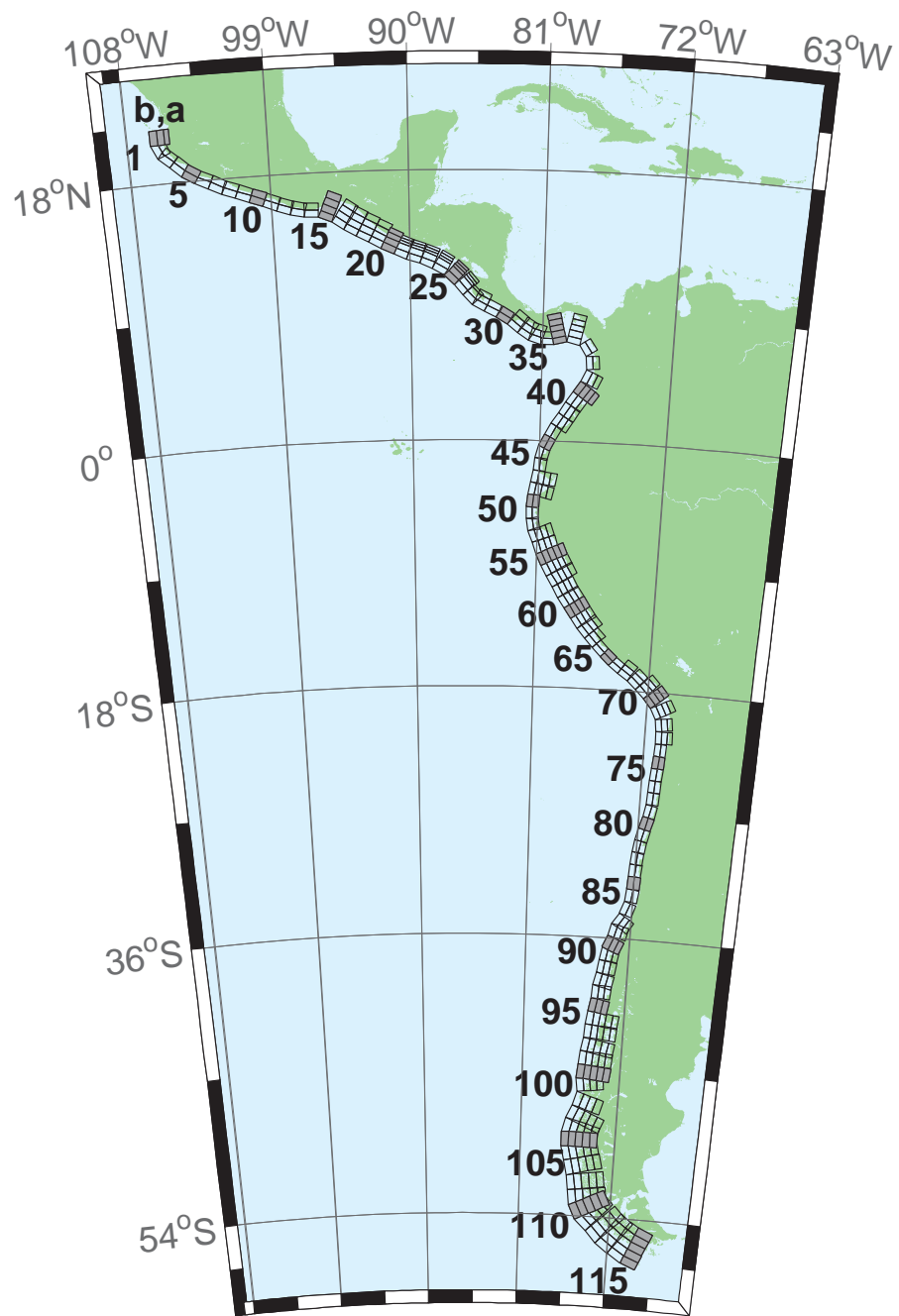


Figure B2: Central and South America Subduction Zone unit sources.

Table B2: Earthquake parameters for Central and South America Subduction Zone unit sources.

Segment	Description	Longitude (°E)	Latitude (°N)	Strike (°)	Dip (°)	Depth (km)
cssz-1a	Central and South America	254.4573	20.8170	359	19	15.4
cssz-1b	Central and South America	254.0035	20.8094	359	12	5
cssz-1z	Central and South America	254.7664	20.8222	359	50	31.67
cssz-2a	Central and South America	254.5765	20.2806	336.8	19	15.4
cssz-2b	Central and South America	254.1607	20.1130	336.8	12	5
cssz-3a	Central and South America	254.8789	19.8923	310.6	18.31	15.27
cssz-3b	Central and South America	254.5841	19.5685	310.6	11.85	5
cssz-4a	Central and South America	255.6167	19.2649	313.4	17.62	15.12
cssz-4b	Central and South America	255.3056	18.9537	313.4	11.68	5
cssz-5a	Central and South America	256.2240	18.8148	302.7	16.92	15
cssz-5b	Central and South America	255.9790	18.4532	302.7	11.54	5
cssz-6a	Central and South America	256.9425	18.4383	295.1	16.23	14.87
cssz-6b	Central and South America	256.7495	18.0479	295.1	11.38	5
cssz-7a	Central and South America	257.8137	18.0339	296.9	15.54	14.74
cssz-7b	Central and South America	257.6079	17.6480	296.9	11.23	5
cssz-8a	Central and South America	258.5779	17.7151	290.4	14.85	14.61
cssz-8b	Central and South America	258.4191	17.3082	290.4	11.08	5
cssz-9a	Central and South America	259.4578	17.4024	290.5	14.15	14.47
cssz-9b	Central and South America	259.2983	16.9944	290.5	10.92	5
cssz-10a	Central and South America	260.3385	17.0861	290.8	13.46	14.34
cssz-10b	Central and South America	260.1768	16.6776	290.8	10.77	5
cssz-11a	Central and South America	261.2255	16.7554	291.8	12.77	14.21
cssz-11b	Central and South America	261.0556	16.3487	291.8	10.62	5
cssz-12a	Central and South America	262.0561	16.4603	288.9	12.08	14.08
cssz-12b	Central and South America	261.9082	16.0447	288.9	10.46	5
cssz-13a	Central and South America	262.8638	16.2381	283.2	11.38	13.95
cssz-13b	Central and South America	262.7593	15.8094	283.2	10.31	5
cssz-14a	Central and South America	263.6066	16.1435	272.1	10.69	13.81
cssz-14b	Central and South America	263.5901	15.7024	272.1	10.15	5
cssz-15a	Central and South America	264.8259	15.8829	293	10	13.68
cssz-15b	Central and South America	264.6462	15.4758	293	10	5
cssz-15y	Central and South America	265.1865	16.6971	293	10	31.05
cssz-15z	Central and South America	265.0060	16.2900	293	10	22.36
cssz-16a	Central and South America	265.7928	15.3507	304.9	15	15.82
cssz-16b	Central and South America	265.5353	14.9951	304.9	12.5	5
cssz-16y	Central and South America	266.3092	16.0619	304.9	15	41.7
cssz-16z	Central and South America	266.0508	15.7063	304.9	15	28.76
cssz-17a	Central and South America	266.4947	14.9019	299.5	20	17.94
cssz-17b	Central and South America	266.2797	14.5346	299.5	15	5
cssz-17y	Central and South America	266.9259	15.6365	299.5	20	52.14
cssz-17z	Central and South America	266.7101	15.2692	299.5	20	35.04
cssz-18a	Central and South America	267.2827	14.4768	298	21.5	17.94
cssz-18b	Central and South America	267.0802	14.1078	298	15	5
cssz-18y	Central and South America	267.6888	15.2148	298	21.5	54.59
cssz-18z	Central and South America	267.4856	14.8458	298	21.5	36.27
cssz-19a	Central and South America	268.0919	14.0560	297.6	23	17.94
cssz-19b	Central and South America	267.8943	13.6897	297.6	15	5
cssz-19y	Central and South America	268.4880	14.7886	297.6	23	57.01
cssz-19z	Central and South America	268.2898	14.4223	297.6	23	37.48
cssz-20a	Central and South America	268.8929	13.6558	296.2	24	17.94
cssz-20b	Central and South America	268.7064	13.2877	296.2	15	5
cssz-20y	Central and South America	269.1796	14.2206	296.2	45.5	73.94
cssz-20z	Central and South America	269.0362	13.9382	296.2	45.5	38.28
cssz-21a	Central and South America	269.6797	13.3031	292.6	25	17.94
cssz-21b	Central and South America	269.5187	12.9274	292.6	15	5

(continued on next page)

Table B2: (continued)

Segment	Description	Longitude (°E)	Latitude (°N)	Strike (°)	Dip (°)	Depth (km)
cssz-21x	Central and South America	269.8797	13.7690	292.6	68	131.8
cssz-21y	Central and South America	269.8130	13.6137	292.6	68	85.43
cssz-21z	Central and South America	269.7463	13.4584	292.6	68	39.07
cssz-22a	Central and South America	270.4823	13.0079	288.6	25	17.94
cssz-22b	Central and South America	270.3492	12.6221	288.6	15	5
cssz-22x	Central and South America	270.6476	13.4864	288.6	68	131.8
cssz-22y	Central and South America	270.5925	13.3269	288.6	68	85.43
cssz-22z	Central and South America	270.5374	13.1674	288.6	68	39.07
cssz-23a	Central and South America	271.3961	12.6734	292.4	25	17.94
cssz-23b	Central and South America	271.2369	12.2972	292.4	15	5
cssz-23x	Central and South America	271.5938	13.1399	292.4	68	131.8
cssz-23y	Central and South America	271.5279	12.9844	292.4	68	85.43
cssz-23z	Central and South America	271.4620	12.8289	292.4	68	39.07
cssz-24a	Central and South America	272.3203	12.2251	300.2	25	17.94
cssz-24b	Central and South America	272.1107	11.8734	300.2	15	5
cssz-24x	Central and South America	272.5917	12.6799	300.2	67	131.1
cssz-24y	Central and South America	272.5012	12.5283	300.2	67	85.1
cssz-24z	Central and South America	272.4107	12.3767	300.2	67	39.07
cssz-25a	Central and South America	273.2075	11.5684	313.8	25	17.94
cssz-25b	Central and South America	272.9200	11.2746	313.8	15	5
cssz-25x	Central and South America	273.5950	11.9641	313.8	66	130.4
cssz-25y	Central and South America	273.4658	11.8322	313.8	66	84.75
cssz-25z	Central and South America	273.3366	11.7003	313.8	66	39.07
cssz-26a	Central and South America	273.8943	10.8402	320.4	25	17.94
cssz-26b	Central and South America	273.5750	10.5808	320.4	15	5
cssz-26x	Central and South America	274.3246	11.1894	320.4	66	130.4
cssz-26y	Central and South America	274.1811	11.0730	320.4	66	84.75
cssz-26z	Central and South America	274.0377	10.9566	320.4	66	39.07
cssz-27a	Central and South America	274.4569	10.2177	316.1	25	17.94
cssz-27b	Central and South America	274.1590	9.9354	316.1	15	5
cssz-27z	Central and South America	274.5907	10.3444	316.1	66	39.07
cssz-28a	Central and South America	274.9586	9.8695	297.1	22	14.54
cssz-28b	Central and South America	274.7661	9.4988	297.1	11	5
cssz-28z	Central and South America	275.1118	10.1643	297.1	42.5	33.27
cssz-29a	Central and South America	275.7686	9.4789	296.6	19	11.09
cssz-29b	Central and South America	275.5759	9.0992	296.6	7	5
cssz-30a	Central and South America	276.6346	8.9973	302.2	19	9.36
cssz-30b	Central and South America	276.4053	8.6381	302.2	5	5
cssz-31a	Central and South America	277.4554	8.4152	309.1	19	7.62
cssz-31b	Central and South America	277.1851	8.0854	309.1	3	5
cssz-31z	Central and South America	277.7260	8.7450	309.1	19	23.9
cssz-32a	Central and South America	278.1112	7.9425	303	18.67	8.49
cssz-32b	Central and South America	277.8775	7.5855	303	4	5
cssz-32z	Central and South America	278.3407	8.2927	303	21.67	24.49
cssz-33a	Central and South America	278.7082	7.6620	287.6	18.33	10.23
cssz-33b	Central and South America	278.5785	7.2555	287.6	6	5
cssz-33z	Central and South America	278.8328	8.0522	287.6	24.33	25.95
cssz-34a	Central and South America	279.3184	7.5592	269.5	18	17.94
cssz-34b	Central and South America	279.3223	7.1320	269.5	15	5
cssz-35a	Central and South America	280.0039	7.6543	255.9	17.67	14.54
cssz-35b	Central and South America	280.1090	7.2392	255.9	11	5
cssz-35x	Central and South America	279.7156	8.7898	255.9	29.67	79.22
cssz-35y	Central and South America	279.8118	8.4113	255.9	29.67	54.47
cssz-35z	Central and South America	279.9079	8.0328	255.9	29.67	29.72
cssz-36a	Central and South America	281.2882	7.6778	282.5	17.33	11.09

(continued on next page)

Table B2: (continued)

Segment	Description	Longitude (°E)	Latitude (°N)	Strike (°)	Dip (°)	Depth (km)
cssz-36b	Central and South America	281.1948	7.2592	282.5	7	5
cssz-36x	Central and South America	281.5368	8.7896	282.5	32.33	79.47
cssz-36y	Central and South America	281.4539	8.4190	282.5	32.33	52.73
cssz-36z	Central and South America	281.3710	8.0484	282.5	32.33	25.99
cssz-37a	Central and South America	282.5252	6.8289	326.9	17	10.23
cssz-37b	Central and South America	282.1629	6.5944	326.9	6	5
cssz-38a	Central and South America	282.9469	5.5973	355.4	17	10.23
cssz-38b	Central and South America	282.5167	5.5626	355.4	6	5
cssz-39a	Central and South America	282.7236	4.3108	24.13	17	10.23
cssz-39b	Central and South America	282.3305	4.4864	24.13	6	5
cssz-39z	Central and South America	283.0603	4.1604	24.13	35	24.85
cssz-40a	Central and South America	282.1940	3.3863	35.28	17	10.23
cssz-40b	Central and South America	281.8427	3.6344	35.28	6	5
cssz-40y	Central and South America	282.7956	2.9613	35.28	35	53.52
cssz-40z	Central and South America	282.4948	3.1738	35.28	35	24.85
cssz-41a	Central and South America	281.6890	2.6611	34.27	17	10.23
cssz-41b	Central and South America	281.3336	2.9030	34.27	6	5
cssz-41z	Central and South America	281.9933	2.4539	34.27	35	24.85
cssz-42a	Central and South America	281.2266	1.9444	31.29	17	10.23
cssz-42b	Central and South America	280.8593	2.1675	31.29	6	5
cssz-42z	Central and South America	281.5411	1.7533	31.29	35	24.85
cssz-43a	Central and South America	280.7297	1.1593	33.3	17	10.23
cssz-43b	Central and South America	280.3706	1.3951	33.3	6	5
cssz-43z	Central and South America	281.0373	0.9573	33.3	35	24.85
cssz-44a	Central and South America	280.3018	0.4491	28.8	17	10.23
cssz-44b	Central and South America	279.9254	0.6560	28.8	6	5
cssz-45a	Central and South America	279.9083	-0.3259	26.91	10	8.49
cssz-45b	Central and South America	279.5139	-0.1257	26.91	4	5
cssz-46a	Central and South America	279.6461	-0.9975	15.76	10	8.49
cssz-46b	Central and South America	279.2203	-0.8774	15.76	4	5
cssz-47a	Central and South America	279.4972	-1.7407	6.9	10	8.49
cssz-47b	Central and South America	279.0579	-1.6876	6.9	4	5
cssz-48a	Central and South America	279.3695	-2.6622	8.96	10	8.49
cssz-48b	Central and South America	278.9321	-2.5933	8.96	4	5
cssz-48y	Central and South America	280.2444	-2.8000	8.96	10	25.85
cssz-48z	Central and South America	279.8070	-2.7311	8.96	10	17.17
cssz-49a	Central and South America	279.1852	-3.6070	13.15	10	8.49
cssz-49b	Central and South America	278.7536	-3.5064	13.15	4	5
cssz-49y	Central and South America	280.0486	-3.8082	13.15	10	25.85
cssz-49z	Central and South America	279.6169	-3.7076	13.15	10	17.17
cssz-50a	Central and South America	279.0652	-4.3635	4.78	10.33	9.64
cssz-50b	Central and South America	278.6235	-4.3267	4.78	5.33	5
cssz-51a	Central and South America	279.0349	-5.1773	359.4	10.67	10.81
cssz-51b	Central and South America	278.5915	-5.1817	359.4	6.67	5
cssz-52a	Central and South America	279.1047	-5.9196	349.8	11	11.96
cssz-52b	Central and South America	278.6685	-5.9981	349.8	8	5
cssz-53a	Central and South America	279.3044	-6.6242	339.2	10.25	11.74
cssz-53b	Central and South America	278.8884	-6.7811	339.2	7.75	5
cssz-53y	Central and South America	280.1024	-6.3232	339.2	19.25	37.12
cssz-53z	Central and South America	279.7035	-6.4737	339.2	19.25	20.64
cssz-54a	Central and South America	279.6256	-7.4907	340.8	9.5	11.53
cssz-54b	Central and South America	279.2036	-7.6365	340.8	7.5	5
cssz-54y	Central and South America	280.4267	-7.2137	340.8	20.5	37.29
cssz-54z	Central and South America	280.0262	-7.3522	340.8	20.5	19.78
cssz-55a	Central and South America	279.9348	-8.2452	335.4	8.75	11.74

(continued on next page)

Table B2: (continued)

Segment	Description	Longitude (°E)	Latitude (°N)	Strike (°)	Dip (°)	Depth (km)
cssz-55b	Central and South America	279.5269	-8.4301	335.4	7.75	5
cssz-55x	Central and South America	281.0837	-7.7238	335.4	21.75	56.4
cssz-55y	Central and South America	280.7009	-7.8976	335.4	21.75	37.88
cssz-55z	Central and South America	280.3180	-8.0714	335.4	21.75	19.35
cssz-56a	Central and South America	280.3172	-8.9958	331.6	8	11.09
cssz-56b	Central and South America	279.9209	-9.2072	331.6	7	5
cssz-56x	Central and South America	281.4212	-8.4063	331.6	23	57.13
cssz-56y	Central and South America	281.0534	-8.6028	331.6	23	37.59
cssz-56z	Central and South America	280.6854	-8.7993	331.6	23	18.05
cssz-57a	Central and South America	280.7492	-9.7356	328.7	8.6	10.75
cssz-57b	Central and South America	280.3640	-9.9663	328.7	6.6	5
cssz-57x	Central and South America	281.8205	-9.0933	328.7	23.4	57.94
cssz-57y	Central and South America	281.4636	-9.3074	328.7	23.4	38.08
cssz-57z	Central and South America	281.1065	-9.5215	328.7	23.4	18.22
cssz-58a	Central and South America	281.2275	-10.5350	330.5	9.2	10.4
cssz-58b	Central and South America	280.8348	-10.7532	330.5	6.2	5
cssz-58y	Central and South America	281.9548	-10.1306	330.5	23.8	38.57
cssz-58z	Central and South America	281.5913	-10.3328	330.5	23.8	18.39
cssz-59a	Central and South America	281.6735	-11.2430	326.2	9.8	10.05
cssz-59b	Central and South America	281.2982	-11.4890	326.2	5.8	5
cssz-59y	Central and South America	282.3675	-10.7876	326.2	24.2	39.06
cssz-59z	Central and South America	282.0206	-11.0153	326.2	24.2	18.56
cssz-60a	Central and South America	282.1864	-11.9946	326.5	10.4	9.71
cssz-60b	Central and South America	281.8096	-12.2384	326.5	5.4	5
cssz-60y	Central and South America	282.8821	-11.5438	326.5	24.6	39.55
cssz-60z	Central and South America	282.5344	-11.7692	326.5	24.6	18.73
cssz-61a	Central and South America	282.6944	-12.7263	325.5	11	9.36
cssz-61b	Central and South America	282.3218	-12.9762	325.5	5	5
cssz-61y	Central and South America	283.3814	-12.2649	325.5	25	40.03
cssz-61z	Central and South America	283.0381	-12.4956	325.5	25	18.9
cssz-62a	Central and South America	283.1980	-13.3556	319	11	9.79
cssz-62b	Central and South America	282.8560	-13.6451	319	5.5	5
cssz-62y	Central and South America	283.8178	-12.8300	319	27	42.03
cssz-62z	Central and South America	283.5081	-13.0928	319	27	19.33
cssz-63a	Central and South America	283.8032	-14.0147	317.9	11	10.23
cssz-63b	Central and South America	283.4661	-14.3106	317.9	6	5
cssz-63z	Central and South America	284.1032	-13.7511	317.9	29	19.77
cssz-64a	Central and South America	284.4144	-14.6482	315.7	13	11.96
cssz-64b	Central and South America	284.0905	-14.9540	315.7	8	5
cssz-65a	Central and South America	285.0493	-15.2554	313.2	15	13.68
cssz-65b	Central and South America	284.7411	-15.5715	313.2	10	5
cssz-66a	Central and South America	285.6954	-15.7816	307.7	14.5	13.68
cssz-66b	Central and South America	285.4190	-16.1258	307.7	10	5
cssz-67a	Central and South America	286.4127	-16.2781	304.3	14	13.68
cssz-67b	Central and South America	286.1566	-16.6381	304.3	10	5
cssz-67z	Central and South America	286.6552	-15.9365	304.3	23	25.78
cssz-68a	Central and South America	287.2481	-16.9016	311.8	14	13.68
cssz-68b	Central and South America	286.9442	-17.2264	311.8	10	5
cssz-68z	Central and South America	287.5291	-16.6007	311.8	26	25.78
cssz-69a	Central and South America	287.9724	-17.5502	314.9	14	13.68
cssz-69b	Central and South America	287.6496	-17.8590	314.9	10	5
cssz-69y	Central and South America	288.5530	-16.9934	314.9	29	50.02
cssz-69z	Central and South America	288.2629	-17.2718	314.9	29	25.78
cssz-70a	Central and South America	288.6731	-18.2747	320.4	14	13.25
cssz-70b	Central and South America	288.3193	-18.5527	320.4	9.5	5

(continued on next page)

Table B2: (continued)

Segment	Description	Longitude (°E)	Latitude (°N)	Strike (°)	Dip (°)	Depth (km)
cssz-70y	Central and South America	289.3032	-17.7785	320.4	30	50.35
cssz-70z	Central and South America	288.9884	-18.0266	320.4	30	25.35
cssz-71a	Central and South America	289.3089	-19.1854	333.2	14	12.82
cssz-71b	Central and South America	288.8968	-19.3820	333.2	9	5
cssz-71y	Central and South America	290.0357	-18.8382	333.2	31	50.67
cssz-71z	Central and South America	289.6725	-19.0118	333.2	31	24.92
cssz-72a	Central and South America	289.6857	-20.3117	352.4	14	12.54
cssz-72b	Central and South America	289.2250	-20.3694	352.4	8.67	5
cssz-72z	Central and South America	290.0882	-20.2613	352.4	32	24.63
cssz-73a	Central and South America	289.7731	-21.3061	358.9	14	12.24
cssz-73b	Central and South America	289.3053	-21.3142	358.9	8.33	5
cssz-73z	Central and South America	290.1768	-21.2991	358.9	33	24.34
cssz-74a	Central and South America	289.7610	-22.2671	3.06	14	11.96
cssz-74b	Central and South America	289.2909	-22.2438	3.06	8	5
cssz-75a	Central and South America	289.6982	-23.1903	4.83	14.09	11.96
cssz-75b	Central and South America	289.2261	-23.1536	4.83	8	5
cssz-76a	Central and South America	289.6237	-24.0831	4.67	14.18	11.96
cssz-76b	Central and South America	289.1484	-24.0476	4.67	8	5
cssz-77a	Central and South America	289.5538	-24.9729	4.3	14.27	11.96
cssz-77b	Central and South America	289.0750	-24.9403	4.3	8	5
cssz-78a	Central and South America	289.4904	-25.8621	3.86	14.36	11.96
cssz-78b	Central and South America	289.0081	-25.8328	3.86	8	5
cssz-79a	Central and South America	289.3491	-26.8644	11.34	14.45	11.96
cssz-79b	Central and South America	288.8712	-26.7789	11.34	8	5
cssz-80a	Central and South America	289.1231	-27.7826	14.16	14.54	11.96
cssz-80b	Central and South America	288.6469	-27.6762	14.16	8	5
cssz-81a	Central and South America	288.8943	-28.6409	13.19	14.63	11.96
cssz-81b	Central and South America	288.4124	-28.5417	13.19	8	5
cssz-82a	Central and South America	288.7113	-29.4680	9.68	14.72	11.96
cssz-82b	Central and South America	288.2196	-29.3950	9.68	8	5
cssz-83a	Central and South America	288.5944	-30.2923	5.36	14.81	11.96
cssz-83b	Central and South America	288.0938	-30.2517	5.36	8	5
cssz-84a	Central and South America	288.5223	-31.1639	3.8	14.9	11.96
cssz-84b	Central and South America	288.0163	-31.1351	3.8	8	5
cssz-85a	Central and South America	288.4748	-32.0416	2.55	15	11.96
cssz-85b	Central and South America	287.9635	-32.0223	2.55	8	5
cssz-86a	Central and South America	288.3901	-33.0041	7.01	15	11.96
cssz-86b	Central and South America	287.8768	-32.9512	7.01	8	5
cssz-87a	Central and South America	288.1050	-34.0583	19.4	15	11.96
cssz-87b	Central and South America	287.6115	-33.9142	19.4	8	5
cssz-88a	Central and South America	287.5309	-35.0437	32.81	15	11.96
cssz-88b	Central and South America	287.0862	-34.8086	32.81	8	5
cssz-88z	Central and South America	287.9308	-35.2545	32.81	30	24.9
cssz-89a	Central and South America	287.2380	-35.5993	14.52	16.67	11.96
cssz-89b	Central and South America	286.7261	-35.4914	14.52	8	5
cssz-89z	Central and South America	287.7014	-35.6968	14.52	30	26.3
cssz-90a	Central and South America	286.8442	-36.5645	22.64	18.33	11.96
cssz-90b	Central and South America	286.3548	-36.4004	22.64	8	5
cssz-90z	Central and South America	287.2916	-36.7142	22.64	30	27.68
cssz-91a	Central and South America	286.5925	-37.2488	10.9	20	11.96
cssz-91b	Central and South America	286.0721	-37.1690	10.9	8	5
cssz-91z	Central and South America	287.0726	-37.3224	10.9	30	29.06
cssz-92a	Central and South America	286.4254	-38.0945	8.23	20	11.96
cssz-92b	Central and South America	285.8948	-38.0341	8.23	8	5
cssz-92z	Central and South America	286.9303	-38.1520	8.23	26.67	29.06

(continued on next page)

Table B2: (continued)

Segment	Description	Longitude (°E)	Latitude (°N)	Strike (°)	Dip (°)	Depth (km)
cssz-93a	Central and South America	286.2047	-39.0535	13.46	20	11.96
cssz-93b	Central and South America	285.6765	-38.9553	13.46	8	5
cssz-93z	Central and South America	286.7216	-39.1495	13.46	23.33	29.06
cssz-94a	Central and South America	286.0772	-39.7883	3.4	20	11.96
cssz-94b	Central and South America	285.5290	-39.7633	3.4	8	5
cssz-94z	Central and South America	286.6255	-39.8133	3.4	20	29.06
cssz-95a	Central and South America	285.9426	-40.7760	9.84	20	11.96
cssz-95b	Central and South America	285.3937	-40.7039	9.84	8	5
cssz-95z	Central and South America	286.4921	-40.8481	9.84	20	29.06
cssz-96a	Central and South America	285.7839	-41.6303	7.6	20	11.96
cssz-96b	Central and South America	285.2245	-41.5745	7.6	8	5
cssz-96x	Central and South America	287.4652	-41.7977	7.6	20	63.26
cssz-96y	Central and South America	286.9043	-41.7419	7.6	20	46.16
cssz-96z	Central and South America	286.3439	-41.6861	7.6	20	29.06
cssz-97a	Central and South America	285.6695	-42.4882	5.3	20	11.96
cssz-97b	Central and South America	285.0998	-42.4492	5.3	8	5
cssz-97x	Central and South America	287.3809	-42.6052	5.3	20	63.26
cssz-97y	Central and South America	286.8101	-42.5662	5.3	20	46.16
cssz-97z	Central and South America	286.2396	-42.5272	5.3	20	29.06
cssz-98a	Central and South America	285.5035	-43.4553	10.53	20	11.96
cssz-98b	Central and South America	284.9322	-43.3782	10.53	8	5
cssz-98x	Central and South America	287.2218	-43.6866	10.53	20	63.26
cssz-98y	Central and South America	286.6483	-43.6095	10.53	20	46.16
cssz-98z	Central and South America	286.0755	-43.5324	10.53	20	29.06
cssz-99a	Central and South America	285.3700	-44.2595	4.86	20	11.96
cssz-99b	Central and South America	284.7830	-44.2237	4.86	8	5
cssz-99x	Central and South America	287.1332	-44.3669	4.86	20	63.26
cssz-99y	Central and South America	286.5451	-44.3311	4.86	20	46.16
cssz-99z	Central and South America	285.9574	-44.2953	4.86	20	29.06
cssz-100a	Central and South America	285.2713	-45.1664	5.68	20	11.96
cssz-100b	Central and South America	284.6758	-45.1246	5.68	8	5
cssz-100x	Central and South America	287.0603	-45.2918	5.68	20	63.26
cssz-100y	Central and South America	286.4635	-45.2500	5.68	20	46.16
cssz-100z	Central and South America	285.8672	-45.2082	5.68	20	29.06
cssz-101a	Central and South America	285.3080	-45.8607	352.6	20	9.36
cssz-101b	Central and South America	284.7067	-45.9152	352.6	5	5
cssz-101y	Central and South America	286.5089	-45.7517	352.6	20	43.56
cssz-101z	Central and South America	285.9088	-45.8062	352.6	20	26.46
cssz-102a	Central and South America	285.2028	-47.1185	17.72	5	9.36
cssz-102b	Central and South America	284.5772	-46.9823	17.72	5	5
cssz-102y	Central and South America	286.4588	-47.3909	17.72	5	18.07
cssz-102z	Central and South America	285.8300	-47.2547	17.72	5	13.72
cssz-103a	Central and South America	284.7075	-48.0396	23.37	7.5	11.53
cssz-103b	Central and South America	284.0972	-47.8630	23.37	7.5	5
cssz-103x	Central and South America	286.5511	-48.5694	23.37	7.5	31.11
cssz-103y	Central and South America	285.9344	-48.3928	23.37	7.5	24.58
cssz-103z	Central and South America	285.3199	-48.2162	23.37	7.5	18.05
cssz-104a	Central and South America	284.3440	-48.7597	14.87	10	13.68
cssz-104b	Central and South America	283.6962	-48.6462	14.87	10	5
cssz-104x	Central and South America	286.2962	-49.1002	14.87	10	39.73
cssz-104y	Central and South America	285.6440	-48.9867	14.87	10	31.05
cssz-104z	Central and South America	284.9933	-48.8732	14.87	10	22.36
cssz-105a	Central and South America	284.2312	-49.4198	0.25	9.67	13.4
cssz-105b	Central and South America	283.5518	-49.4179	0.25	9.67	5
cssz-105x	Central and South America	286.2718	-49.4255	0.25	9.67	38.59

(continued on next page)

Table B2: (continued)

Segment	Description	Longitude (°E)	Latitude (°N)	Strike (°)	Dip (°)	Depth (km)
cssz-105y	Central and South America	285.5908	-49.4236	0.25	9.67	30.2
cssz-105z	Central and South America	284.9114	-49.4217	0.25	9.67	21.8
cssz-106a	Central and South America	284.3730	-50.1117	347.5	9.25	13.04
cssz-106b	Central and South America	283.6974	-50.2077	347.5	9.25	5
cssz-106x	Central and South America	286.3916	-49.8238	347.5	9.25	37.15
cssz-106y	Central and South America	285.7201	-49.9198	347.5	9.25	29.11
cssz-106z	Central and South America	285.0472	-50.0157	347.5	9.25	21.07
cssz-107a	Central and South America	284.7130	-50.9714	346.5	9	12.82
cssz-107b	Central and South America	284.0273	-51.0751	346.5	9	5
cssz-107x	Central and South America	286.7611	-50.6603	346.5	9	36.29
cssz-107y	Central and South America	286.0799	-50.7640	346.5	9	28.47
cssz-107z	Central and South America	285.3972	-50.8677	346.5	9	20.64
cssz-108a	Central and South America	285.0378	-51.9370	352	8.67	12.54
cssz-108b	Central and South America	284.3241	-51.9987	352	8.67	5
cssz-108x	Central and South America	287.1729	-51.7519	352	8.67	35.15
cssz-108y	Central and South America	286.4622	-51.8136	352	8.67	27.61
cssz-108z	Central and South America	285.7505	-51.8753	352	8.67	20.07
cssz-109a	Central and South America	285.2635	-52.8439	353.1	8.33	12.24
cssz-109b	Central and South America	284.5326	-52.8974	353.1	8.33	5
cssz-109x	Central and South America	287.4508	-52.6834	353.1	8.33	33.97
cssz-109y	Central and South America	286.7226	-52.7369	353.1	8.33	26.73
cssz-109z	Central and South America	285.9935	-52.7904	353.1	8.33	19.49
cssz-110a	Central and South America	285.5705	-53.4139	334.2	8	11.96
cssz-110b	Central and South America	284.8972	-53.6076	334.2	8	5
cssz-110x	Central and South America	287.5724	-52.8328	334.2	8	32.83
cssz-110y	Central and South America	286.9081	-53.0265	334.2	8	25.88
cssz-110z	Central and South America	286.2408	-53.2202	334.2	8	18.92
cssz-111a	Central and South America	286.1627	-53.8749	313.8	8	11.96
cssz-111b	Central and South America	285.6382	-54.1958	313.8	8	5
cssz-111x	Central and South America	287.7124	-52.9122	313.8	8	32.83
cssz-111y	Central and South America	287.1997	-53.2331	313.8	8	25.88
cssz-111z	Central and South America	286.6832	-53.5540	313.8	8	18.92
cssz-112a	Central and South America	287.3287	-54.5394	316.4	8	11.96
cssz-112b	Central and South America	286.7715	-54.8462	316.4	8	5
cssz-112x	Central and South America	288.9756	-53.6190	316.4	8	32.83
cssz-112y	Central and South America	288.4307	-53.9258	316.4	8	25.88
cssz-112z	Central and South America	287.8817	-54.2326	316.4	8	18.92
cssz-113a	Central and South America	288.3409	-55.0480	307.6	8	11.96
cssz-113b	Central and South America	287.8647	-55.4002	307.6	8	5
cssz-113x	Central and South America	289.7450	-53.9914	307.6	8	32.83
cssz-113y	Central and South America	289.2810	-54.3436	307.6	8	25.88
cssz-113z	Central and South America	288.8130	-54.6958	307.6	8	18.92
cssz-114a	Central and South America	289.5342	-55.5026	301.5	8	11.96
cssz-114b	Central and South America	289.1221	-55.8819	301.5	8	5
cssz-114x	Central and South America	290.7472	-54.3647	301.5	8	32.83
cssz-114y	Central and South America	290.3467	-54.7440	301.5	8	25.88
cssz-114z	Central and South America	289.9424	-55.1233	301.5	8	18.92
cssz-115a	Central and South America	290.7682	-55.8485	292.7	8	11.96
cssz-115b	Central and South America	290.4608	-56.2588	292.7	8	5
cssz-115x	Central and South America	291.6714	-54.6176	292.7	8	32.83
cssz-115y	Central and South America	291.3734	-55.0279	292.7	8	25.88
cssz-115z	Central and South America	291.0724	-55.4382	292.7	8	18.92

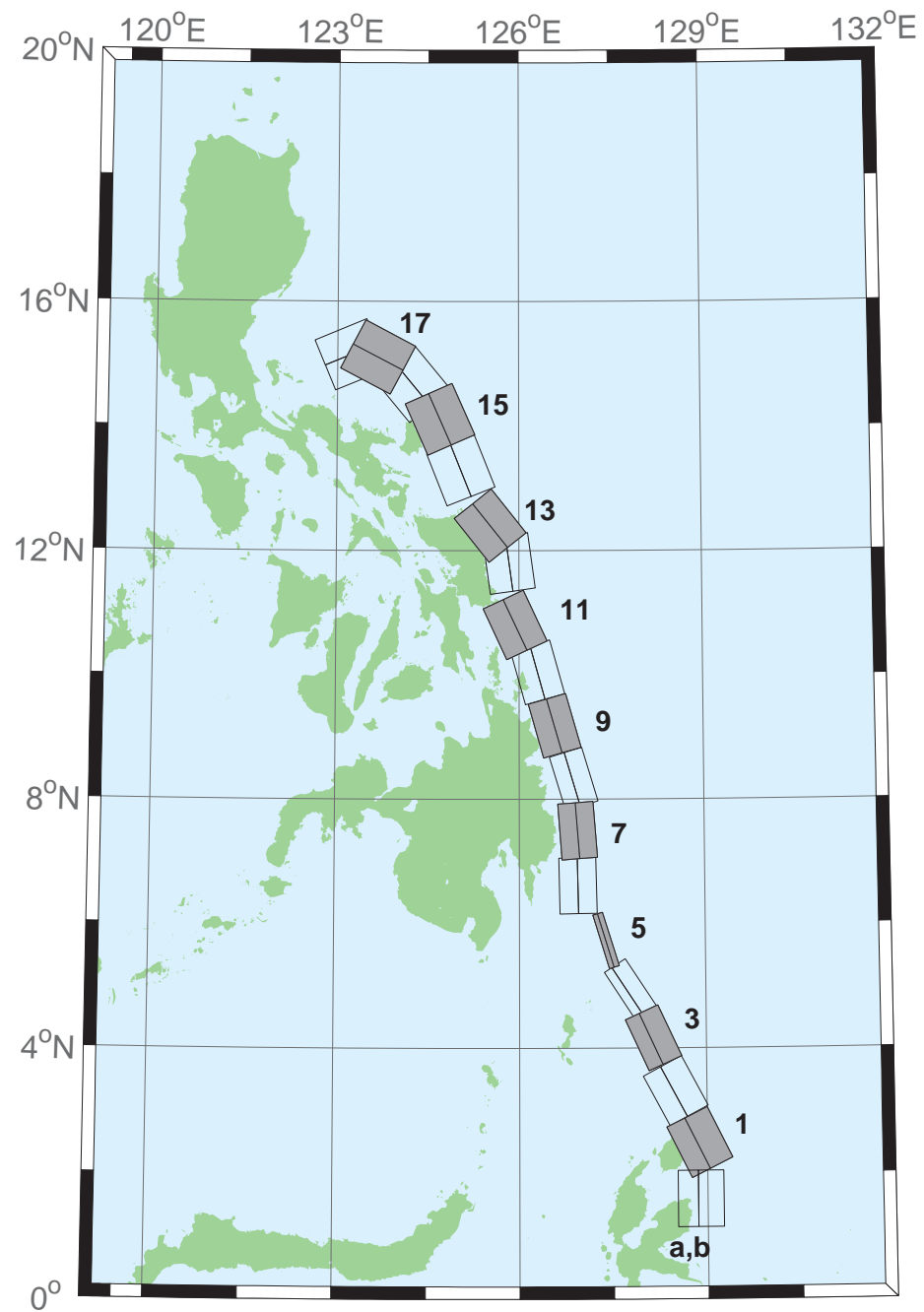


Figure B3: Eastern Philippines Subduction Zone unit sources.

Table B3: Earthquake parameters for Eastern Philippines Subduction Zone unit sources.

Segment	Description	Longitude (°E)	Latitude (°N)	Strike (°)	Dip (°)	Depth (km)
epsz-0a	Eastern Philippines	128.5264	1.5930	180	44	26.92
epsz-0b	Eastern Philippines	128.8496	1.5930	180	26	5
epsz-1a	Eastern Philippines	128.5521	2.3289	153.6	44.2	27.62
epsz-1b	Eastern Philippines	128.8408	2.4720	153.6	26.9	5
epsz-2a	Eastern Philippines	128.1943	3.1508	151.9	45.9	32.44
epsz-2b	Eastern Philippines	128.4706	3.2979	151.9	32.8	5.35
epsz-3a	Eastern Philippines	127.8899	4.0428	155.2	57.3	40.22
epsz-3b	Eastern Philippines	128.1108	4.1445	155.2	42.7	6.31
epsz-4a	Eastern Philippines	127.6120	4.8371	146.8	71.4	48.25
epsz-4b	Eastern Philippines	127.7324	4.9155	146.8	54.8	7.39
epsz-5a	Eastern Philippines	127.3173	5.7040	162.9	79.9	57.4
epsz-5b	Eastern Philippines	127.3930	5.7272	162.9	79.4	8.25
epsz-6a	Eastern Philippines	126.6488	6.6027	178.9	48.6	45.09
epsz-6b	Eastern Philippines	126.9478	6.6085	178.9	48.6	7.58
epsz-7a	Eastern Philippines	126.6578	7.4711	175.8	50.7	45.52
epsz-7b	Eastern Philippines	126.9439	7.4921	175.8	50.7	6.83
epsz-8a	Eastern Philippines	126.6227	8.2456	163.3	56.7	45.6
epsz-8b	Eastern Philippines	126.8614	8.3164	163.3	48.9	7.92
epsz-9a	Eastern Philippines	126.2751	9.0961	164.1	47	43.59
epsz-9b	Eastern Philippines	126.5735	9.1801	164.1	44.9	8.3
epsz-10a	Eastern Philippines	125.9798	9.9559	164.5	43.1	42.25
epsz-10b	Eastern Philippines	126.3007	10.0438	164.5	43.1	8.09
epsz-11a	Eastern Philippines	125.6079	10.6557	155	37.8	38.29
epsz-11b	Eastern Philippines	125.9353	10.8059	155	37.8	7.64
epsz-12a	Eastern Philippines	125.4697	11.7452	172.1	36	37.01
epsz-12b	Eastern Philippines	125.8374	11.7949	172.1	36	7.62
epsz-13a	Eastern Philippines	125.2238	12.1670	141.5	32.4	33.87
epsz-13b	Eastern Philippines	125.5278	12.4029	141.5	32.4	7.08
epsz-14a	Eastern Philippines	124.6476	13.1365	158.2	23	25.92
epsz-14b	Eastern Philippines	125.0421	13.2898	158.2	23	6.38
epsz-15a	Eastern Philippines	124.3107	13.9453	156.1	24.1	26.51
epsz-15b	Eastern Philippines	124.6973	14.1113	156.1	24.1	6.09
epsz-16a	Eastern Philippines	123.8998	14.4025	140.3	19.5	21.69
epsz-16b	Eastern Philippines	124.2366	14.6728	140.3	19.5	5
epsz-17a	Eastern Philippines	123.4604	14.7222	117.6	15.3	18.19
epsz-17b	Eastern Philippines	123.6682	15.1062	117.6	15.3	5
epsz-18a	Eastern Philippines	123.3946	14.7462	67.4	15	17.94
epsz-18b	Eastern Philippines	123.2219	15.1467	67.4	15	5

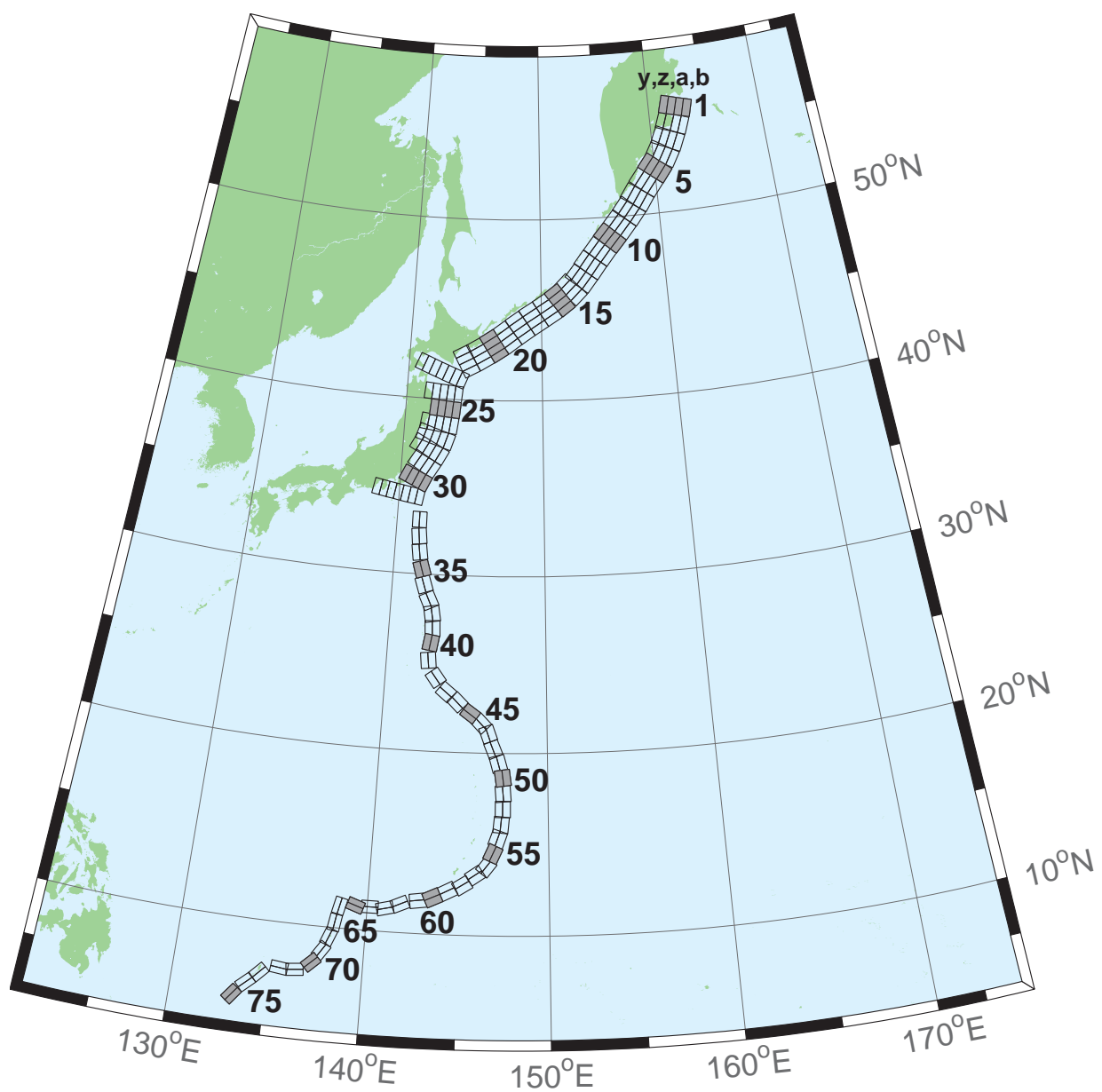


Figure B4: Kamchatka-Kuril-Japan-Izu-Mariana-Yap Subduction Zone unit sources.

Table B4: Earthquake parameters for Kamchatka-Kuril-Japan-Izu-Mariana-Yap Subduction Zone unit sources.

Segment	Description	Longitude (°E)	Latitude (°N)	Strike (°)	Dip (°)	Depth (km)
kisz-1a	Kamchatka-Kuril-Japan-Izu-Mariana-Yap	162.4318	55.5017	195	29	26.13
kisz-1b	Kamchatka-Kuril-Japan-Izu-Mariana-Yap	163.1000	55.4000	195	25	5
kisz-1y	Kamchatka-Kuril-Japan-Izu-Mariana-Yap	161.0884	55.7050	195	29	74.61
kisz-1z	Kamchatka-Kuril-Japan-Izu-Mariana-Yap	161.7610	55.6033	195	29	50.37
kisz-2a	Kamchatka-Kuril-Japan-Izu-Mariana-Yap	161.9883	54.6784	200	29	26.13
kisz-2b	Kamchatka-Kuril-Japan-Izu-Mariana-Yap	162.6247	54.5440	200	25	5
kisz-2y	Kamchatka-Kuril-Japan-Izu-Mariana-Yap	160.7072	54.9471	200	29	74.61
kisz-2z	Kamchatka-Kuril-Japan-Izu-Mariana-Yap	161.3488	54.8127	200	29	50.37
kisz-3a	Kamchatka-Kuril-Japan-Izu-Mariana-Yap	161.4385	53.8714	204	29	26.13
kisz-3b	Kamchatka-Kuril-Japan-Izu-Mariana-Yap	162.0449	53.7116	204	25	5
kisz-3y	Kamchatka-Kuril-Japan-Izu-Mariana-Yap	160.2164	54.1910	204	29	74.61
kisz-3z	Kamchatka-Kuril-Japan-Izu-Mariana-Yap	160.8286	54.0312	204	29	50.37
kisz-4a	Kamchatka-Kuril-Japan-Izu-Mariana-Yap	160.7926	53.1087	210	29	26.13
kisz-4b	Kamchatka-Kuril-Japan-Izu-Mariana-Yap	161.3568	52.9123	210	25	5
kisz-4y	Kamchatka-Kuril-Japan-Izu-Mariana-Yap	159.6539	53.5015	210	29	74.61
kisz-4z	Kamchatka-Kuril-Japan-Izu-Mariana-Yap	160.2246	53.3051	210	29	50.37
kisz-5a	Kamchatka-Kuril-Japan-Izu-Mariana-Yap	160.0211	52.4113	218	29	26.13
kisz-5b	Kamchatka-Kuril-Japan-Izu-Mariana-Yap	160.5258	52.1694	218	25	5
kisz-5y	Kamchatka-Kuril-Japan-Izu-Mariana-Yap	159.0005	52.8950	218	29	74.61
kisz-5z	Kamchatka-Kuril-Japan-Izu-Mariana-Yap	159.5122	52.6531	218	29	50.37
kisz-6a	Kamchatka-Kuril-Japan-Izu-Mariana-Yap	159.1272	51.7034	218	29	26.13
kisz-6b	Kamchatka-Kuril-Japan-Izu-Mariana-Yap	159.6241	51.4615	218	25	5
kisz-6y	Kamchatka-Kuril-Japan-Izu-Mariana-Yap	158.1228	52.1871	218	29	74.61
kisz-6z	Kamchatka-Kuril-Japan-Izu-Mariana-Yap	158.6263	51.9452	218	29	50.37
kisz-7a	Kamchatka-Kuril-Japan-Izu-Mariana-Yap	158.2625	50.9549	214	29	26.13
kisz-7b	Kamchatka-Kuril-Japan-Izu-Mariana-Yap	158.7771	50.7352	214	25	5
kisz-7y	Kamchatka-Kuril-Japan-Izu-Mariana-Yap	157.2236	51.3942	214	29	74.61
kisz-7z	Kamchatka-Kuril-Japan-Izu-Mariana-Yap	157.7443	51.1745	214	29	50.37
kisz-8a	Kamchatka-Kuril-Japan-Izu-Mariana-Yap	157.4712	50.2459	218	31	27.7
kisz-8b	Kamchatka-Kuril-Japan-Izu-Mariana-Yap	157.9433	50.0089	218	27	5
kisz-8y	Kamchatka-Kuril-Japan-Izu-Mariana-Yap	156.5176	50.7199	218	31	79.2
kisz-8z	Kamchatka-Kuril-Japan-Izu-Mariana-Yap	156.9956	50.4829	218	31	53.45
kisz-9a	Kamchatka-Kuril-Japan-Izu-Mariana-Yap	156.6114	49.5583	220	31	27.7
kisz-9b	Kamchatka-Kuril-Japan-Izu-Mariana-Yap	157.0638	49.3109	220	27	5
kisz-9y	Kamchatka-Kuril-Japan-Izu-Mariana-Yap	155.6974	50.0533	220	31	79.2
kisz-9z	Kamchatka-Kuril-Japan-Izu-Mariana-Yap	156.1556	49.8058	220	31	53.45
kisz-10a	Kamchatka-Kuril-Japan-Izu-Mariana-Yap	155.7294	48.8804	221	31	27.7
kisz-10b	Kamchatka-Kuril-Japan-Izu-Mariana-Yap	156.1690	48.6278	221	27	5
kisz-10y	Kamchatka-Kuril-Japan-Izu-Mariana-Yap	154.8413	49.3856	221	31	79.2
kisz-10z	Kamchatka-Kuril-Japan-Izu-Mariana-Yap	155.2865	49.1330	221	31	53.45
kisz-11a	Kamchatka-Kuril-Japan-Izu-Mariana-Yap	154.8489	48.1821	219	31	27.7
kisz-11b	Kamchatka-Kuril-Japan-Izu-Mariana-Yap	155.2955	47.9398	219	27	5
kisz-11y	Kamchatka-Kuril-Japan-Izu-Mariana-Yap	153.9472	48.6667	219	31	79.2
kisz-11z	Kamchatka-Kuril-Japan-Izu-Mariana-Yap	154.3991	48.4244	219	31	53.45
kisz-12a	Kamchatka-Kuril-Japan-Izu-Mariana-Yap	153.9994	47.4729	217	31	27.7
kisz-12b	Kamchatka-Kuril-Japan-Izu-Mariana-Yap	154.4701	47.2320	217	27	5
kisz-12y	Kamchatka-Kuril-Japan-Izu-Mariana-Yap	153.0856	47.9363	217	31	79.2
kisz-12z	Kamchatka-Kuril-Japan-Izu-Mariana-Yap	153.5435	47.7046	217	31	53.45
kisz-13a	Kamchatka-Kuril-Japan-Izu-Mariana-Yap	153.2239	46.7564	218	31	27.7
kisz-13b	Kamchatka-Kuril-Japan-Izu-Mariana-Yap	153.6648	46.5194	218	27	5
kisz-13y	Kamchatka-Kuril-Japan-Izu-Mariana-Yap	152.3343	47.2304	218	31	79.2
kisz-13z	Kamchatka-Kuril-Japan-Izu-Mariana-Yap	152.7801	46.9934	218	31	53.45
kisz-14a	Kamchatka-Kuril-Japan-Izu-Mariana-Yap	152.3657	46.1514	225	23	24.54
kisz-14b	Kamchatka-Kuril-Japan-Izu-Mariana-Yap	152.7855	45.8591	225	23	5

(continued on next page)

Table B4: (continued)

Segment	Description	Longitude (°E)	Latitude (°N)	Strike (°)	Dip (°)	Depth (km)
kisz-14y	Kamchatka-Kuril-Japan-Izu-Mariana-Yap	151.5172	46.7362	225	23	63.62
kisz-14z	Kamchatka-Kuril-Japan-Izu-Mariana-Yap	151.9426	46.4438	225	23	44.08
kisz-15a	Kamchatka-Kuril-Japan-Izu-Mariana-Yap	151.4663	45.5963	233	25	23.73
kisz-15b	Kamchatka-Kuril-Japan-Izu-Mariana-Yap	151.8144	45.2712	233	22	5
kisz-15y	Kamchatka-Kuril-Japan-Izu-Mariana-Yap	150.7619	46.2465	233	25	65.99
kisz-15z	Kamchatka-Kuril-Japan-Izu-Mariana-Yap	151.1151	45.9214	233	25	44.86
kisz-16a	Kamchatka-Kuril-Japan-Izu-Mariana-Yap	150.4572	45.0977	237	25	23.73
kisz-16b	Kamchatka-Kuril-Japan-Izu-Mariana-Yap	150.7694	44.7563	237	22	5
kisz-16y	Kamchatka-Kuril-Japan-Izu-Mariana-Yap	149.8253	45.7804	237	25	65.99
kisz-16z	Kamchatka-Kuril-Japan-Izu-Mariana-Yap	150.1422	45.4390	237	25	44.86
kisz-17a	Kamchatka-Kuril-Japan-Izu-Mariana-Yap	149.3989	44.6084	237	25	23.73
kisz-17b	Kamchatka-Kuril-Japan-Izu-Mariana-Yap	149.7085	44.2670	237	22	5
kisz-17y	Kamchatka-Kuril-Japan-Izu-Mariana-Yap	148.7723	45.2912	237	25	65.99
kisz-17z	Kamchatka-Kuril-Japan-Izu-Mariana-Yap	149.0865	44.9498	237	25	44.86
kisz-18a	Kamchatka-Kuril-Japan-Izu-Mariana-Yap	148.3454	44.0982	235	25	23.73
kisz-18b	Kamchatka-Kuril-Japan-Izu-Mariana-Yap	148.6687	43.7647	235	22	5
kisz-18y	Kamchatka-Kuril-Japan-Izu-Mariana-Yap	147.6915	44.7651	235	25	65.99
kisz-18z	Kamchatka-Kuril-Japan-Izu-Mariana-Yap	148.0194	44.4316	235	25	44.86
kisz-19a	Kamchatka-Kuril-Japan-Izu-Mariana-Yap	147.3262	43.5619	233	25	23.73
kisz-19b	Kamchatka-Kuril-Japan-Izu-Mariana-Yap	147.6625	43.2368	233	22	5
kisz-19y	Kamchatka-Kuril-Japan-Izu-Mariana-Yap	146.6463	44.2121	233	25	65.99
kisz-19z	Kamchatka-Kuril-Japan-Izu-Mariana-Yap	146.9872	43.8870	233	25	44.86
kisz-20a	Kamchatka-Kuril-Japan-Izu-Mariana-Yap	146.3513	43.0633	237	25	23.73
kisz-20b	Kamchatka-Kuril-Japan-Izu-Mariana-Yap	146.6531	42.7219	237	22	5
kisz-20y	Kamchatka-Kuril-Japan-Izu-Mariana-Yap	145.7410	43.7461	237	25	65.99
kisz-20z	Kamchatka-Kuril-Japan-Izu-Mariana-Yap	146.0470	43.4047	237	25	44.86
kisz-21a	Kamchatka-Kuril-Japan-Izu-Mariana-Yap	145.3331	42.5948	239	25	23.73
kisz-21b	Kamchatka-Kuril-Japan-Izu-Mariana-Yap	145.6163	42.2459	239	22	5
kisz-21y	Kamchatka-Kuril-Japan-Izu-Mariana-Yap	144.7603	43.2927	239	25	65.99
kisz-21z	Kamchatka-Kuril-Japan-Izu-Mariana-Yap	145.0475	42.9438	239	25	44.86
kisz-22a	Kamchatka-Kuril-Japan-Izu-Mariana-Yap	144.3041	42.1631	242	25	23.73
kisz-22b	Kamchatka-Kuril-Japan-Izu-Mariana-Yap	144.5605	41.8037	242	22	5
kisz-22y	Kamchatka-Kuril-Japan-Izu-Mariana-Yap	143.7854	42.8819	242	25	65.99
kisz-22z	Kamchatka-Kuril-Japan-Izu-Mariana-Yap	144.0455	42.5225	242	25	44.86
kisz-23a	Kamchatka-Kuril-Japan-Izu-Mariana-Yap	143.2863	41.3335	202	21	21.28
kisz-23b	Kamchatka-Kuril-Japan-Izu-Mariana-Yap	143.8028	41.1764	202	19	5
kisz-23v	Kamchatka-Kuril-Japan-Izu-Mariana-Yap	140.6816	42.1189	202	21	110.9
kisz-23w	Kamchatka-Kuril-Japan-Izu-Mariana-Yap	141.2050	41.9618	202	21	92.95
kisz-23x	Kamchatka-Kuril-Japan-Izu-Mariana-Yap	141.7273	41.8047	202	21	75.04
kisz-23y	Kamchatka-Kuril-Japan-Izu-Mariana-Yap	142.2482	41.6476	202	21	57.12
kisz-23z	Kamchatka-Kuril-Japan-Izu-Mariana-Yap	142.7679	41.4905	202	21	39.2
kisz-24a	Kamchatka-Kuril-Japan-Izu-Mariana-Yap	142.9795	40.3490	185	21	21.28
kisz-24b	Kamchatka-Kuril-Japan-Izu-Mariana-Yap	143.5273	40.3125	185	19	5
kisz-24x	Kamchatka-Kuril-Japan-Izu-Mariana-Yap	141.3339	40.4587	185	21	75.04
kisz-24y	Kamchatka-Kuril-Japan-Izu-Mariana-Yap	141.8827	40.4221	185	21	57.12
kisz-24z	Kamchatka-Kuril-Japan-Izu-Mariana-Yap	142.4312	40.3856	185	21	39.2
kisz-25a	Kamchatka-Kuril-Japan-Izu-Mariana-Yap	142.8839	39.4541	185	21	21.28
kisz-25b	Kamchatka-Kuril-Japan-Izu-Mariana-Yap	143.4246	39.4176	185	19	5
kisz-25y	Kamchatka-Kuril-Japan-Izu-Mariana-Yap	141.8012	39.5272	185	21	57.12
kisz-25z	Kamchatka-Kuril-Japan-Izu-Mariana-Yap	142.3426	39.4907	185	21	39.2
kisz-26a	Kamchatka-Kuril-Japan-Izu-Mariana-Yap	142.7622	38.5837	188	21	21.28
kisz-26b	Kamchatka-Kuril-Japan-Izu-Mariana-Yap	143.2930	38.5254	188	19	5
kisz-26x	Kamchatka-Kuril-Japan-Izu-Mariana-Yap	141.1667	38.7588	188	21	75.04
kisz-26y	Kamchatka-Kuril-Japan-Izu-Mariana-Yap	141.6990	38.7004	188	21	57.12
kisz-26z	Kamchatka-Kuril-Japan-Izu-Mariana-Yap	142.2308	38.6421	188	21	39.2

(continued on next page)

Table B4: (continued)

Segment	Description	Longitude (°E)	Latitude (°N)	Strike (°)	Dip (°)	Depth (km)
kisz-27a	Kamchatka-Kuril-Japan-Izu-Mariana-Yap	142.5320	37.7830	198	21	21.28
kisz-27b	Kamchatka-Kuril-Japan-Izu-Mariana-Yap	143.0357	37.6534	198	19	5
kisz-27x	Kamchatka-Kuril-Japan-Izu-Mariana-Yap	141.0142	38.1717	198	21	75.04
kisz-27y	Kamchatka-Kuril-Japan-Izu-Mariana-Yap	141.5210	38.0421	198	21	57.12
kisz-27z	Kamchatka-Kuril-Japan-Izu-Mariana-Yap	142.0269	37.9126	198	21	39.2
kisz-28a	Kamchatka-Kuril-Japan-Izu-Mariana-Yap	142.1315	37.0265	208	21	21.28
kisz-28b	Kamchatka-Kuril-Japan-Izu-Mariana-Yap	142.5941	36.8297	208	19	5
kisz-28x	Kamchatka-Kuril-Japan-Izu-Mariana-Yap	140.7348	37.6171	208	21	75.04
kisz-28y	Kamchatka-Kuril-Japan-Izu-Mariana-Yap	141.2016	37.4202	208	21	57.12
kisz-28z	Kamchatka-Kuril-Japan-Izu-Mariana-Yap	141.6671	37.2234	208	21	39.2
kisz-29a	Kamchatka-Kuril-Japan-Izu-Mariana-Yap	141.5970	36.2640	211	21	21.28
kisz-29b	Kamchatka-Kuril-Japan-Izu-Mariana-Yap	142.0416	36.0481	211	19	5
kisz-29y	Kamchatka-Kuril-Japan-Izu-Mariana-Yap	140.7029	36.6960	211	21	57.12
kisz-29z	Kamchatka-Kuril-Japan-Izu-Mariana-Yap	141.1506	36.4800	211	21	39.2
kisz-30a	Kamchatka-Kuril-Japan-Izu-Mariana-Yap	141.0553	35.4332	205	21	21.28
kisz-30b	Kamchatka-Kuril-Japan-Izu-Mariana-Yap	141.5207	35.2560	205	19	5
kisz-30y	Kamchatka-Kuril-Japan-Izu-Mariana-Yap	140.1204	35.7876	205	21	57.12
kisz-30z	Kamchatka-Kuril-Japan-Izu-Mariana-Yap	140.5883	35.6104	205	21	39.2
kisz-31a	Kamchatka-Kuril-Japan-Izu-Mariana-Yap	140.6956	34.4789	190	22	22.1
kisz-31b	Kamchatka-Kuril-Japan-Izu-Mariana-Yap	141.1927	34.4066	190	20	5
kisz-31v	Kamchatka-Kuril-Japan-Izu-Mariana-Yap	138.2025	34.8405	190	22	115.8
kisz-31w	Kamchatka-Kuril-Japan-Izu-Mariana-Yap	138.7021	34.7682	190	22	97.02
kisz-31x	Kamchatka-Kuril-Japan-Izu-Mariana-Yap	139.2012	34.6958	190	22	78.29
kisz-31y	Kamchatka-Kuril-Japan-Izu-Mariana-Yap	139.6997	34.6235	190	22	59.56
kisz-31z	Kamchatka-Kuril-Japan-Izu-Mariana-Yap	140.1979	34.5512	190	22	40.83
kisz-32a	Kamchatka-Kuril-Japan-Izu-Mariana-Yap	141.0551	33.0921	180	32	23.48
kisz-32b	Kamchatka-Kuril-Japan-Izu-Mariana-Yap	141.5098	33.0921	180	21.69	5
kisz-33a	Kamchatka-Kuril-Japan-Izu-Mariana-Yap	141.0924	32.1047	173.8	27.65	20.67
kisz-33b	Kamchatka-Kuril-Japan-Izu-Mariana-Yap	141.5596	32.1473	173.8	18.27	5
kisz-34a	Kamchatka-Kuril-Japan-Izu-Mariana-Yap	141.1869	31.1851	172.1	25	18.26
kisz-34b	Kamchatka-Kuril-Japan-Izu-Mariana-Yap	141.6585	31.2408	172.1	15.38	5
kisz-35a	Kamchatka-Kuril-Japan-Izu-Mariana-Yap	141.4154	30.1707	163	25	17.12
kisz-35b	Kamchatka-Kuril-Japan-Izu-Mariana-Yap	141.8662	30.2899	163	14.03	5
kisz-36a	Kamchatka-Kuril-Japan-Izu-Mariana-Yap	141.6261	29.2740	161.7	25.73	18.71
kisz-36b	Kamchatka-Kuril-Japan-Izu-Mariana-Yap	142.0670	29.4012	161.7	15.91	5
kisz-37a	Kamchatka-Kuril-Japan-Izu-Mariana-Yap	142.0120	28.3322	154.7	20	14.54
kisz-37b	Kamchatka-Kuril-Japan-Izu-Mariana-Yap	142.4463	28.5124	154.7	11	5
kisz-38a	Kamchatka-Kuril-Japan-Izu-Mariana-Yap	142.2254	27.6946	170.3	20	14.54
kisz-38b	Kamchatka-Kuril-Japan-Izu-Mariana-Yap	142.6955	27.7659	170.3	11	5
kisz-39a	Kamchatka-Kuril-Japan-Izu-Mariana-Yap	142.3085	26.9127	177.2	24.23	17.42
kisz-39b	Kamchatka-Kuril-Japan-Izu-Mariana-Yap	142.7674	26.9325	177.2	14.38	5
kisz-40a	Kamchatka-Kuril-Japan-Izu-Mariana-Yap	142.2673	26.1923	189.4	26.49	22.26
kisz-40b	Kamchatka-Kuril-Japan-Izu-Mariana-Yap	142.7090	26.1264	189.4	20.2	5
kisz-41a	Kamchatka-Kuril-Japan-Izu-Mariana-Yap	142.1595	25.0729	173.7	22.07	19.08
kisz-41b	Kamchatka-Kuril-Japan-Izu-Mariana-Yap	142.6165	25.1184	173.7	16.36	5
kisz-42a	Kamchatka-Kuril-Japan-Izu-Mariana-Yap	142.7641	23.8947	143.5	21.54	18.4
kisz-42b	Kamchatka-Kuril-Japan-Izu-Mariana-Yap	143.1321	24.1432	143.5	15.54	5
kisz-43a	Kamchatka-Kuril-Japan-Izu-Mariana-Yap	143.5281	23.0423	129.2	23.02	18.77
kisz-43b	Kamchatka-Kuril-Japan-Izu-Mariana-Yap	143.8128	23.3626	129.2	15.99	5
kisz-44a	Kamchatka-Kuril-Japan-Izu-Mariana-Yap	144.2230	22.5240	134.6	28.24	18.56
kisz-44b	Kamchatka-Kuril-Japan-Izu-Mariana-Yap	144.5246	22.8056	134.6	15.74	5
kisz-45a	Kamchatka-Kuril-Japan-Izu-Mariana-Yap	145.0895	21.8866	125.8	36.73	22.79
kisz-45b	Kamchatka-Kuril-Japan-Izu-Mariana-Yap	145.3171	22.1785	125.8	20.84	5
kisz-46a	Kamchatka-Kuril-Japan-Izu-Mariana-Yap	145.6972	21.3783	135.9	30.75	20.63
kisz-46b	Kamchatka-Kuril-Japan-Izu-Mariana-Yap	145.9954	21.6469	135.9	18.22	5

(continued on next page)

Table B4: (continued)

Segment	Description	Longitude (°E)	Latitude (°N)	Strike (°)	Dip (°)	Depth (km)
kisz-47a	Kamchatka-Kuril-Japan-Izu-Mariana-Yap	146.0406	20.9341	160.1	29.87	19.62
kisz-47b	Kamchatka-Kuril-Japan-Izu-Mariana-Yap	146.4330	21.0669	160.1	17	5
kisz-48a	Kamchatka-Kuril-Japan-Izu-Mariana-Yap	146.3836	20.0690	158	32.75	19.68
kisz-48b	Kamchatka-Kuril-Japan-Izu-Mariana-Yap	146.7567	20.2108	158	17.07	5
kisz-49a	Kamchatka-Kuril-Japan-Izu-Mariana-Yap	146.6689	19.3123	164.5	25.07	21.41
kisz-49b	Kamchatka-Kuril-Japan-Izu-Mariana-Yap	147.0846	19.4212	164.5	19.16	5
kisz-50a	Kamchatka-Kuril-Japan-Izu-Mariana-Yap	146.9297	18.5663	172.1	22	22.1
kisz-50b	Kamchatka-Kuril-Japan-Izu-Mariana-Yap	147.3650	18.6238	172.1	20	5
kisz-51a	Kamchatka-Kuril-Japan-Izu-Mariana-Yap	146.9495	17.7148	175.1	22.06	22.04
kisz-51b	Kamchatka-Kuril-Japan-Izu-Mariana-Yap	147.3850	17.7503	175.1	19.93	5
kisz-52a	Kamchatka-Kuril-Japan-Izu-Mariana-Yap	146.9447	16.8869	180	25.51	18.61
kisz-52b	Kamchatka-Kuril-Japan-Izu-Mariana-Yap	147.3683	16.8869	180	15.79	5
kisz-53a	Kamchatka-Kuril-Japan-Izu-Mariana-Yap	146.8626	16.0669	185.2	27.39	18.41
kisz-53b	Kamchatka-Kuril-Japan-Izu-Mariana-Yap	147.2758	16.0309	185.2	15.56	5
kisz-54a	Kamchatka-Kuril-Japan-Izu-Mariana-Yap	146.7068	15.3883	199.1	28.12	20.91
kisz-54b	Kamchatka-Kuril-Japan-Izu-Mariana-Yap	147.0949	15.2590	199.1	18.56	5
kisz-55a	Kamchatka-Kuril-Japan-Izu-Mariana-Yap	146.4717	14.6025	204.3	29.6	26.27
kisz-55b	Kamchatka-Kuril-Japan-Izu-Mariana-Yap	146.8391	14.4415	204.3	25.18	5
kisz-56a	Kamchatka-Kuril-Japan-Izu-Mariana-Yap	146.1678	13.9485	217.4	32.04	26.79
kisz-56b	Kamchatka-Kuril-Japan-Izu-Mariana-Yap	146.4789	13.7170	217.4	25.84	5
kisz-57a	Kamchatka-Kuril-Japan-Izu-Mariana-Yap	145.6515	13.5576	235.8	37	24.54
kisz-57b	Kamchatka-Kuril-Japan-Izu-Mariana-Yap	145.8586	13.2609	235.8	23	5
kisz-58a	Kamchatka-Kuril-Japan-Izu-Mariana-Yap	144.9648	12.9990	237.8	37.72	24.54
kisz-58b	Kamchatka-Kuril-Japan-Izu-Mariana-Yap	145.1589	12.6984	237.8	23	5
kisz-59a	Kamchatka-Kuril-Japan-Izu-Mariana-Yap	144.1799	12.6914	242.9	34.33	22.31
kisz-59b	Kamchatka-Kuril-Japan-Izu-Mariana-Yap	144.3531	12.3613	242.9	20.25	5
kisz-60a	Kamchatka-Kuril-Japan-Izu-Mariana-Yap	143.3687	12.3280	244.9	30.9	20.62
kisz-60b	Kamchatka-Kuril-Japan-Izu-Mariana-Yap	143.5355	11.9788	244.9	18.2	5
kisz-61a	Kamchatka-Kuril-Japan-Izu-Mariana-Yap	142.7051	12.1507	261.8	35.41	25.51
kisz-61b	Kamchatka-Kuril-Japan-Izu-Mariana-Yap	142.7582	11.7883	261.8	24.22	5
kisz-62a	Kamchatka-Kuril-Japan-Izu-Mariana-Yap	141.6301	11.8447	245.7	39.86	34.35
kisz-62b	Kamchatka-Kuril-Japan-Izu-Mariana-Yap	141.7750	11.5305	245.7	35.94	5
kisz-63a	Kamchatka-Kuril-Japan-Izu-Mariana-Yap	140.8923	11.5740	256.2	42	38.46
kisz-63b	Kamchatka-Kuril-Japan-Izu-Mariana-Yap	140.9735	11.2498	256.2	42	5
kisz-64a	Kamchatka-Kuril-Japan-Izu-Mariana-Yap	140.1387	11.6028	269.6	42.48	38.77
kisz-64b	Kamchatka-Kuril-Japan-Izu-Mariana-Yap	140.1410	11.2716	269.6	42.48	5
kisz-65a	Kamchatka-Kuril-Japan-Izu-Mariana-Yap	139.4595	11.5883	288.7	44.16	39.83
kisz-65b	Kamchatka-Kuril-Japan-Izu-Mariana-Yap	139.3541	11.2831	288.7	44.16	5
kisz-66a	Kamchatka-Kuril-Japan-Izu-Mariana-Yap	138.1823	11.2648	193.1	45	40.36
kisz-66b	Kamchatka-Kuril-Japan-Izu-Mariana-Yap	138.4977	11.1929	193.1	45	5
kisz-67a	Kamchatka-Kuril-Japan-Izu-Mariana-Yap	137.9923	10.3398	189.8	45	40.36
kisz-67b	Kamchatka-Kuril-Japan-Izu-Mariana-Yap	138.3104	10.2856	189.8	45	5
kisz-68a	Kamchatka-Kuril-Japan-Izu-Mariana-Yap	137.7607	9.6136	201.7	45	40.36
kisz-68b	Kamchatka-Kuril-Japan-Izu-Mariana-Yap	138.0599	9.4963	201.7	45	5
kisz-69a	Kamchatka-Kuril-Japan-Izu-Mariana-Yap	137.4537	8.8996	213.5	45	40.36
kisz-69b	Kamchatka-Kuril-Japan-Izu-Mariana-Yap	137.7215	8.7241	213.5	45	5
kisz-70a	Kamchatka-Kuril-Japan-Izu-Mariana-Yap	137.0191	8.2872	226.5	45	40.36
kisz-70b	Kamchatka-Kuril-Japan-Izu-Mariana-Yap	137.2400	8.0569	226.5	45	5
kisz-71a	Kamchatka-Kuril-Japan-Izu-Mariana-Yap	136.3863	7.9078	263.9	45	40.36
kisz-71b	Kamchatka-Kuril-Japan-Izu-Mariana-Yap	136.4202	7.5920	263.9	45	5
kisz-72a	Kamchatka-Kuril-Japan-Izu-Mariana-Yap	135.6310	7.9130	276.9	45	40.36
kisz-72b	Kamchatka-Kuril-Japan-Izu-Mariana-Yap	135.5926	7.5977	276.9	45	5
kisz-73a	Kamchatka-Kuril-Japan-Izu-Mariana-Yap	134.3296	7.4541	224	45	40.36
kisz-73b	Kamchatka-Kuril-Japan-Izu-Mariana-Yap	134.5600	7.2335	224	45	5
kisz-74a	Kamchatka-Kuril-Japan-Izu-Mariana-Yap	133.7125	6.8621	228.1	45	40.36

(continued on next page)

Table B4: (continued)

Segment	Description	Longitude (°E)	Latitude (°N)	Strike (°)	Dip (°)	Depth (km)
kisz-74b	Kamchatka-Kuril-Japan-Izu-Mariana-Yap	133.9263	6.6258	228.1	45	5
kisz-75a	Kamchatka-Kuril-Japan-Izu-Mariana-Yap	133.0224	6.1221	217.7	45	40.36
kisz-75b	Kamchatka-Kuril-Japan-Izu-Mariana-Yap	133.2751	5.9280	217.7	45	5

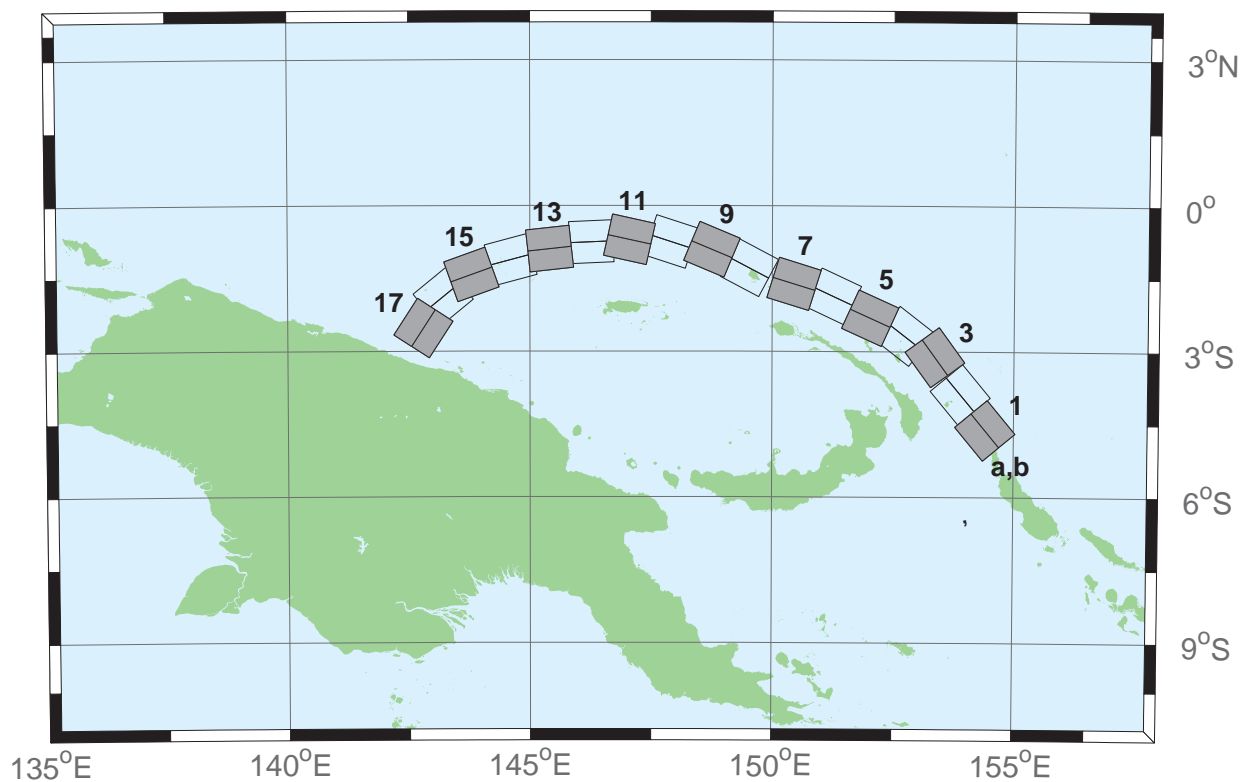


Figure B5: Manus-Oceanic Convergent Boundary Subduction Zone unit sources.

Table B5: Earthquake parameters for Manus-Oceanic Convergent Boundary Subduction Zone unit sources.

Segment	Description	Longitude ($^{\circ}$ E)	Latitude ($^{\circ}$ N)	Strike ($^{\circ}$)	Dip ($^{\circ}$)	Depth (km)
mosz-1a	Manus-Oceanic Convergent Boundary	154.0737	-4.8960	140.2	15	15.88
mosz-1b	Manus-Oceanic Convergent Boundary	154.4082	-4.6185	140.2	15	5
mosz-2a	Manus-Oceanic Convergent Boundary	153.5589	-4.1575	140.2	15	15.91
mosz-2b	Manus-Oceanic Convergent Boundary	153.8931	-3.8800	140.2	15	5.35
mosz-3a	Manus-Oceanic Convergent Boundary	153.0151	-3.3716	143.9	15	16.64
mosz-3b	Manus-Oceanic Convergent Boundary	153.3662	-3.1160	143.9	15	6.31
mosz-4a	Manus-Oceanic Convergent Boundary	152.4667	-3.0241	127.7	15	17.32
mosz-4b	Manus-Oceanic Convergent Boundary	152.7321	-2.6806	127.7	15	7.39
mosz-5a	Manus-Oceanic Convergent Boundary	151.8447	-2.7066	114.3	15	17.57
mosz-5b	Manus-Oceanic Convergent Boundary	152.0235	-2.3112	114.3	15	8.25
mosz-6a	Manus-Oceanic Convergent Boundary	151.0679	-2.2550	115	15	17.66
mosz-6b	Manus-Oceanic Convergent Boundary	151.2513	-1.8618	115	15	7.58
mosz-7a	Manus-Oceanic Convergent Boundary	150.3210	-2.0236	107.2	15	17.73
mosz-7b	Manus-Oceanic Convergent Boundary	150.4493	-1.6092	107.2	15	6.83
mosz-8a	Manus-Oceanic Convergent Boundary	149.3226	-1.6666	117.8	15	17.83
mosz-8b	Manus-Oceanic Convergent Boundary	149.5251	-1.2829	117.8	15	7.92
mosz-9a	Manus-Oceanic Convergent Boundary	148.5865	-1.3017	112.7	15	17.84
mosz-9b	Manus-Oceanic Convergent Boundary	148.7540	-0.9015	112.7	15	8.3
mosz-10a	Manus-Oceanic Convergent Boundary	147.7760	-1.1560	108	15	17.78
mosz-10b	Manus-Oceanic Convergent Boundary	147.9102	-0.7434	108	15	8.09
mosz-11a	Manus-Oceanic Convergent Boundary	146.9596	-1.1226	102.5	15	17.54
mosz-11b	Manus-Oceanic Convergent Boundary	147.0531	-0.6990	102.5	15	7.64
mosz-12a	Manus-Oceanic Convergent Boundary	146.2858	-1.1820	87.48	15	17.29
mosz-12b	Manus-Oceanic Convergent Boundary	146.2667	-0.7486	87.48	15	7.62
mosz-13a	Manus-Oceanic Convergent Boundary	145.4540	-1.3214	83.75	15	17.34
mosz-13b	Manus-Oceanic Convergent Boundary	145.4068	-0.8901	83.75	15	7.08
mosz-14a	Manus-Oceanic Convergent Boundary	144.7151	-1.5346	75.09	15	17.21
mosz-14b	Manus-Oceanic Convergent Boundary	144.6035	-1.1154	75.09	15	6.38
mosz-15a	Manus-Oceanic Convergent Boundary	143.9394	-1.8278	70.43	15	16.52
mosz-15b	Manus-Oceanic Convergent Boundary	143.7940	-1.4190	70.43	15	6.09
mosz-16a	Manus-Oceanic Convergent Boundary	143.4850	-2.2118	50.79	15	15.86
mosz-16b	Manus-Oceanic Convergent Boundary	143.2106	-1.8756	50.79	15	5
mosz-17a	Manus-Oceanic Convergent Boundary	143.1655	-2.7580	33	15	16.64
mosz-17b	Manus-Oceanic Convergent Boundary	142.8013	-2.5217	33	15	5

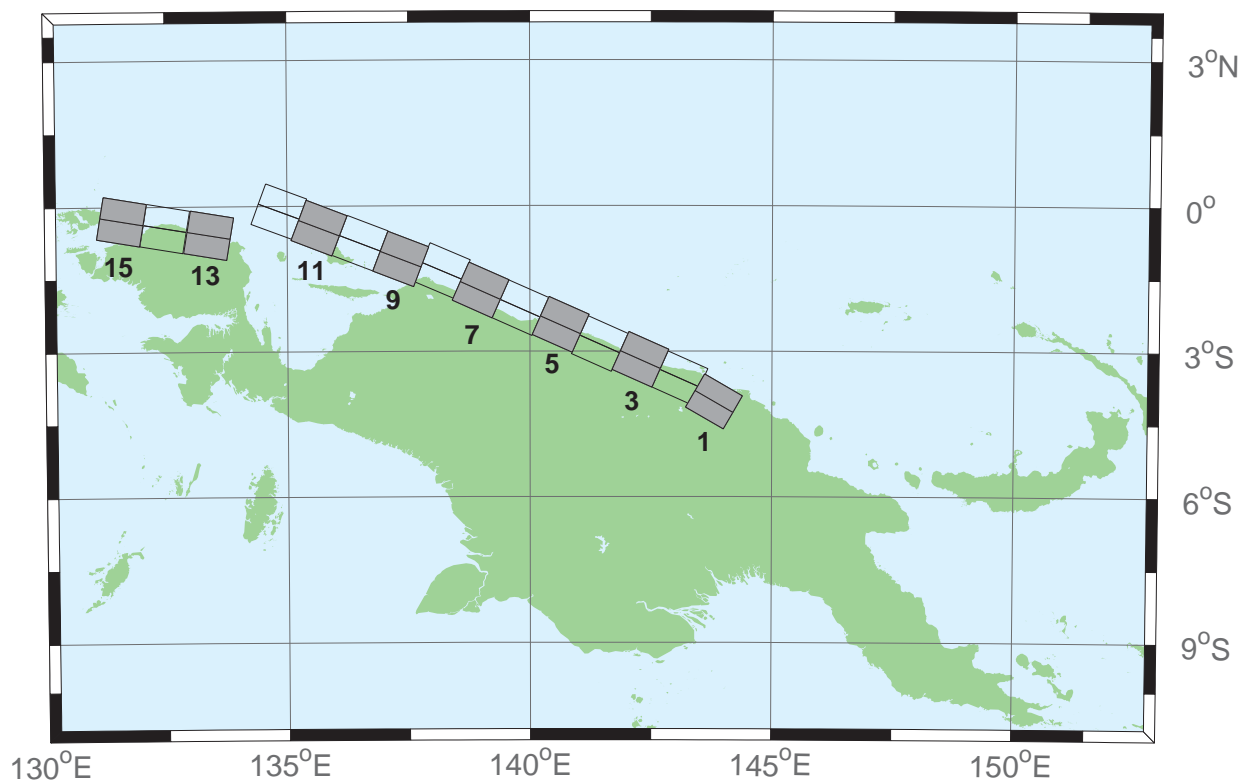


Figure B6: New Guinea Subduction Zone unit sources.

Table B6: Earthquake parameters for New Guinea Subduction Zone unit sources.

Segment	Description	Longitude (°E)	Latitude (°N)	Strike (°)	Dip (°)	Depth (km)
ngsz-1a	New Guinea	143.6063	-4.3804	120	29	25.64
ngsz-1b	New Guinea	143.8032	-4.0402	120	29	1.4
ngsz-2a	New Guinea	142.9310	-3.9263	114	27.63	20.1
ngsz-2b	New Guinea	143.0932	-3.5628	114	21.72	1.6
ngsz-3a	New Guinea	142.1076	-3.5632	114	20.06	18.73
ngsz-3b	New Guinea	142.2795	-3.1778	114	15.94	5
ngsz-4a	New Guinea	141.2681	-3.2376	114	21	17.76
ngsz-4b	New Guinea	141.4389	-2.8545	114	14.79	5
ngsz-5a	New Guinea	140.4592	-2.8429	114	21.26	16.14
ngsz-5b	New Guinea	140.6296	-2.4605	114	12.87	5
ngsz-6a	New Guinea	139.6288	-2.4960	114	22.72	15.4
ngsz-6b	New Guinea	139.7974	-2.1175	114	12	5
ngsz-7a	New Guinea	138.8074	-2.1312	114	21.39	15.4
ngsz-7b	New Guinea	138.9776	-1.7491	114	12	5
ngsz-8a	New Guinea	138.0185	-1.7353	113.1	18.79	15.14
ngsz-8b	New Guinea	138.1853	-1.3441	113.1	11.7	5
ngsz-9a	New Guinea	137.1805	-1.5037	111	15.24	13.23
ngsz-9b	New Guinea	137.3358	-1.0991	111	9.47	5
ngsz-10a	New Guinea	136.3418	-1.1774	111	13.51	11.09
ngsz-10b	New Guinea	136.4983	-0.7697	111	7	5
ngsz-11a	New Guinea	135.4984	-0.8641	111	11.38	12.49
ngsz-11b	New Guinea	135.6562	-0.4530	111	8.62	5
ngsz-12a	New Guinea	134.6759	-0.5216	110.5	10	13.68
ngsz-12b	New Guinea	134.8307	-0.1072	110.5	10	5
ngsz-13a	New Guinea	133.3065	-1.0298	99.5	10	13.68
ngsz-13b	New Guinea	133.3795	-0.5935	99.5	10	5
ngsz-14a	New Guinea	132.4048	-0.8816	99.5	10	13.68
ngsz-14b	New Guinea	132.4778	-0.4453	99.5	10	5
ngsz-15a	New Guinea	131.5141	-0.7353	99.5	10	13.68
ngsz-15b	New Guinea	131.5871	-0.2990	99.5	10	5

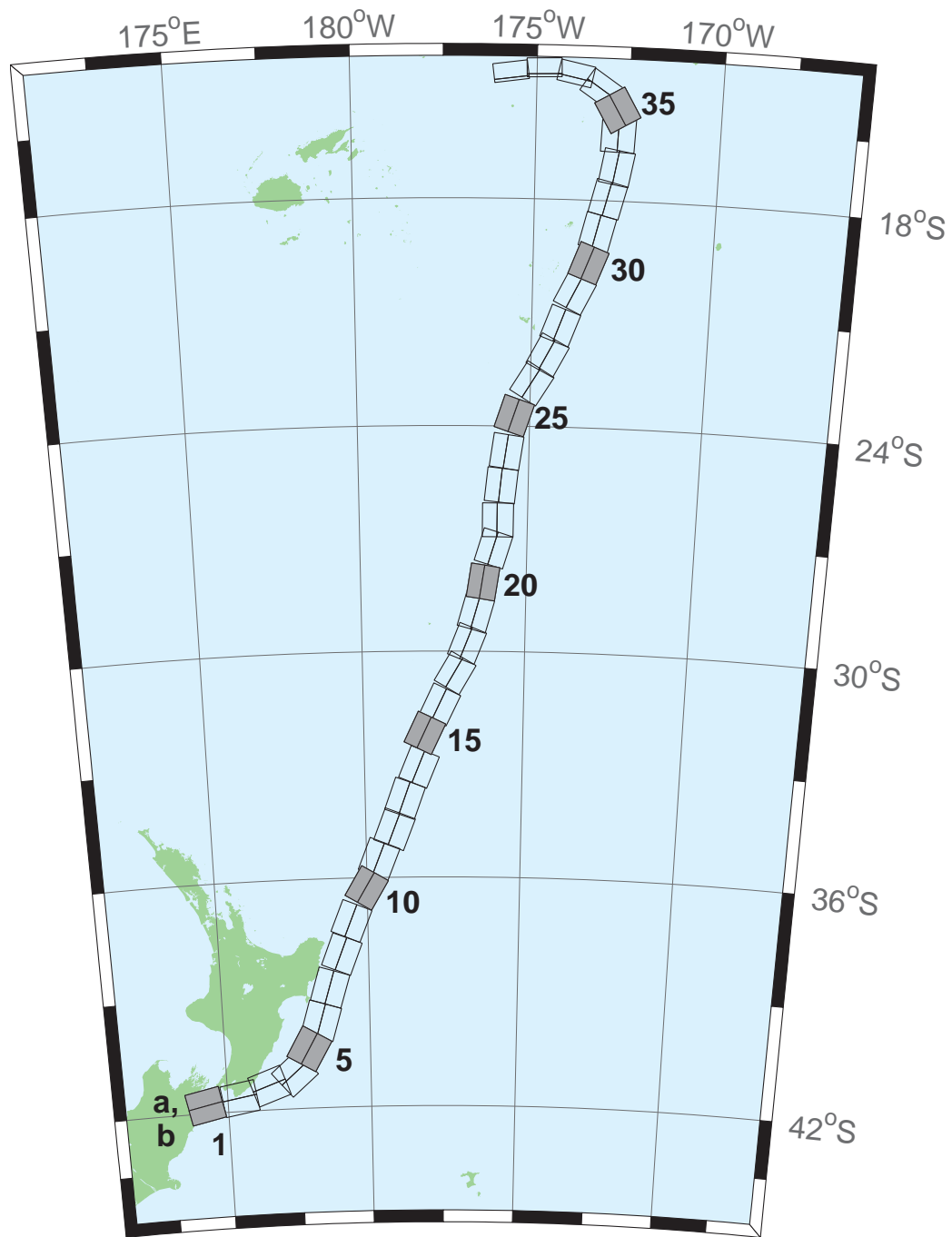


Figure B7: New Zealand-Kermadec-Tonga Subduction Zone unit sources.

Table B7: Earthquake parameters for New Zealand-Kermadec-Tonga Subduction Zone unit sources.

Segment	Description	Longitude (°E)	Latitude (°N)	Strike (°)	Dip (°)	Depth (km)
nts1-1a	New Zealand-Kermadec-Tonga	174.0985	-41.3951	258.6	24	25.34
nts1-1b	New Zealand-Kermadec-Tonga	174.2076	-41.7973	258.6	24	5
nts1-2a	New Zealand-Kermadec-Tonga	175.3289	-41.2592	260.6	29.38	23.17
nts1-2b	New Zealand-Kermadec-Tonga	175.4142	-41.6454	260.6	21.31	5
nts1-3a	New Zealand-Kermadec-Tonga	176.2855	-40.9950	250.7	29.54	21.74
nts1-3b	New Zealand-Kermadec-Tonga	176.4580	-41.3637	250.7	19.56	5
nts1-4a	New Zealand-Kermadec-Tonga	177.0023	-40.7679	229.4	24.43	18.87
nts1-4b	New Zealand-Kermadec-Tonga	177.3552	-41.0785	229.4	16.1	5
nts1-5a	New Zealand-Kermadec-Tonga	177.4114	-40.2396	210	18.8	19.29
nts1-5b	New Zealand-Kermadec-Tonga	177.8951	-40.4525	210	16.61	5
nts1-6a	New Zealand-Kermadec-Tonga	177.8036	-39.6085	196.7	18.17	15.8
nts1-6b	New Zealand-Kermadec-Tonga	178.3352	-39.7310	196.7	12.48	5
nts1-7a	New Zealand-Kermadec-Tonga	178.1676	-38.7480	197	28.1	17.85
nts1-7b	New Zealand-Kermadec-Tonga	178.6541	-38.8640	197	14.89	5
nts1-8a	New Zealand-Kermadec-Tonga	178.6263	-37.8501	201.4	31.47	18.78
nts1-8b	New Zealand-Kermadec-Tonga	179.0788	-37.9899	201.4	16	5
nts1-9a	New Zealand-Kermadec-Tonga	178.9833	-36.9770	202.2	29.58	20.02
nts1-9b	New Zealand-Kermadec-Tonga	179.4369	-37.1245	202.2	17.48	5
nts1-10a	New Zealand-Kermadec-Tonga	179.5534	-36.0655	210.6	32.1	20.72
nts1-10b	New Zealand-Kermadec-Tonga	179.9595	-36.2593	210.6	18.32	5
nts1-11a	New Zealand-Kermadec-Tonga	179.9267	-35.3538	201.7	25	16.09
nts1-11b	New Zealand-Kermadec-Tonga	180.3915	-35.5040	201.7	12.81	5
nts1-12a	New Zealand-Kermadec-Tonga	180.4433	-34.5759	201.2	25	15.46
nts1-12b	New Zealand-Kermadec-Tonga	180.9051	-34.7230	201.2	12.08	5
nts1-13a	New Zealand-Kermadec-Tonga	180.7990	-33.7707	199.8	25.87	19.06
nts1-13b	New Zealand-Kermadec-Tonga	181.2573	-33.9073	199.8	16.33	5
nts1-14a	New Zealand-Kermadec-Tonga	181.2828	-32.9288	202.4	31.28	22.73
nts1-14b	New Zealand-Kermadec-Tonga	181.7063	-33.0751	202.4	20.77	5
nts1-15a	New Zealand-Kermadec-Tonga	181.4918	-32.0035	205.4	32.33	22.64
nts1-15b	New Zealand-Kermadec-Tonga	181.8967	-32.1665	205.4	20.66	5
nts1-16a	New Zealand-Kermadec-Tonga	181.9781	-31.2535	205.5	34.29	23.59
nts1-16b	New Zealand-Kermadec-Tonga	182.3706	-31.4131	205.5	21.83	5
nts1-17a	New Zealand-Kermadec-Tonga	182.4819	-30.3859	210.3	37.6	25.58
nts1-17b	New Zealand-Kermadec-Tonga	182.8387	-30.5655	210.3	24.3	5
nts1-18a	New Zealand-Kermadec-Tonga	182.8176	-29.6545	201.6	37.65	26.13
nts1-18b	New Zealand-Kermadec-Tonga	183.1985	-29.7856	201.6	25	5
nts1-19a	New Zealand-Kermadec-Tonga	183.0622	-28.8739	195.7	34.41	26.13
nts1-19b	New Zealand-Kermadec-Tonga	183.4700	-28.9742	195.7	25	5
nts1-20a	New Zealand-Kermadec-Tonga	183.2724	-28.0967	188.8	38	26.13
nts1-20b	New Zealand-Kermadec-Tonga	183.6691	-28.1508	188.8	25	5
nts1-21a	New Zealand-Kermadec-Tonga	183.5747	-27.1402	197.1	32.29	24.83
nts1-21b	New Zealand-Kermadec-Tonga	183.9829	-27.2518	197.1	23.37	5
nts1-22a	New Zealand-Kermadec-Tonga	183.6608	-26.4975	180	29.56	18.63
nts1-22b	New Zealand-Kermadec-Tonga	184.0974	-26.4975	180	15.82	5
nts1-23a	New Zealand-Kermadec-Tonga	183.7599	-25.5371	185.8	32.42	20.56
nts1-23b	New Zealand-Kermadec-Tonga	184.1781	-25.5752	185.8	18.13	5
nts1-24a	New Zealand-Kermadec-Tonga	183.9139	-24.6201	188.2	33.31	23.73
nts1-24b	New Zealand-Kermadec-Tonga	184.3228	-24.6734	188.2	22	5
nts1-25a	New Zealand-Kermadec-Tonga	184.1266	-23.5922	198.5	29.34	19.64
nts1-25b	New Zealand-Kermadec-Tonga	184.5322	-23.7163	198.5	17.03	5
nts1-26a	New Zealand-Kermadec-Tonga	184.6613	-22.6460	211.7	30.26	19.43
nts1-26b	New Zealand-Kermadec-Tonga	185.0196	-22.8497	211.7	16.78	5
nts1-27a	New Zealand-Kermadec-Tonga	185.0879	-21.9139	207.9	31.73	20.67
nts1-27b	New Zealand-Kermadec-Tonga	185.4522	-22.0928	207.9	18.27	5
nts1-28a	New Zealand-Kermadec-Tonga	185.4037	-21.1758	200.5	32.44	21.76

(continued on next page)

Table B7: (continued)

Segment	Description	Longitude (°E)	Latitude (°N)	Strike (°)	Dip (°)	Depth (km)
nts2-28b	New Zealand-Kermadec-Tonga	185.7849	-21.3084	200.5	19.58	5
nts2-29a	New Zealand-Kermadec-Tonga	185.8087	-20.2629	206.4	32.47	20.4
nts2-29b	New Zealand-Kermadec-Tonga	186.1710	-20.4312	206.4	17.94	5
nts2-30a	New Zealand-Kermadec-Tonga	186.1499	-19.5087	200.9	32.98	22.46
nts2-30b	New Zealand-Kermadec-Tonga	186.5236	-19.6432	200.9	20.44	5
nts2-31a	New Zealand-Kermadec-Tonga	186.3538	-18.7332	193.9	34.41	21.19
nts2-31b	New Zealand-Kermadec-Tonga	186.7339	-18.8221	193.9	18.89	5
nts2-32a	New Zealand-Kermadec-Tonga	186.5949	-17.8587	194.1	30	19.12
nts2-32b	New Zealand-Kermadec-Tonga	186.9914	-17.9536	194.1	16.4	5
nts2-33a	New Zealand-Kermadec-Tonga	186.8172	-17.0581	190	33.15	23.34
nts2-33b	New Zealand-Kermadec-Tonga	187.2047	-17.1237	190	21.52	5
nts2-34a	New Zealand-Kermadec-Tonga	186.7814	-16.2598	182.1	15	13.41
nts2-34b	New Zealand-Kermadec-Tonga	187.2330	-16.2759	182.1	9.68	5
nts2-35a	New Zealand-Kermadec-Tonga	186.8000	-15.8563	149.8	15	12.17
nts2-35b	New Zealand-Kermadec-Tonga	187.1896	-15.6384	149.8	8.24	5
nts2-36a	New Zealand-Kermadec-Tonga	186.5406	-15.3862	123.9	40.44	36.72
nts2-36b	New Zealand-Kermadec-Tonga	186.7381	-15.1025	123.9	39.38	5
nts2-37a	New Zealand-Kermadec-Tonga	185.9883	-14.9861	102	68.94	30.99
nts2-37b	New Zealand-Kermadec-Tonga	186.0229	-14.8282	102	31.32	5
nts2-38a	New Zealand-Kermadec-Tonga	185.2067	-14.8259	88.4	80	26.13
nts2-38b	New Zealand-Kermadec-Tonga	185.2044	-14.7479	88.4	25	5
nts2-39a	New Zealand-Kermadec-Tonga	184.3412	-14.9409	82.55	80	26.13
nts2-39b	New Zealand-Kermadec-Tonga	184.3307	-14.8636	82.55	25	5

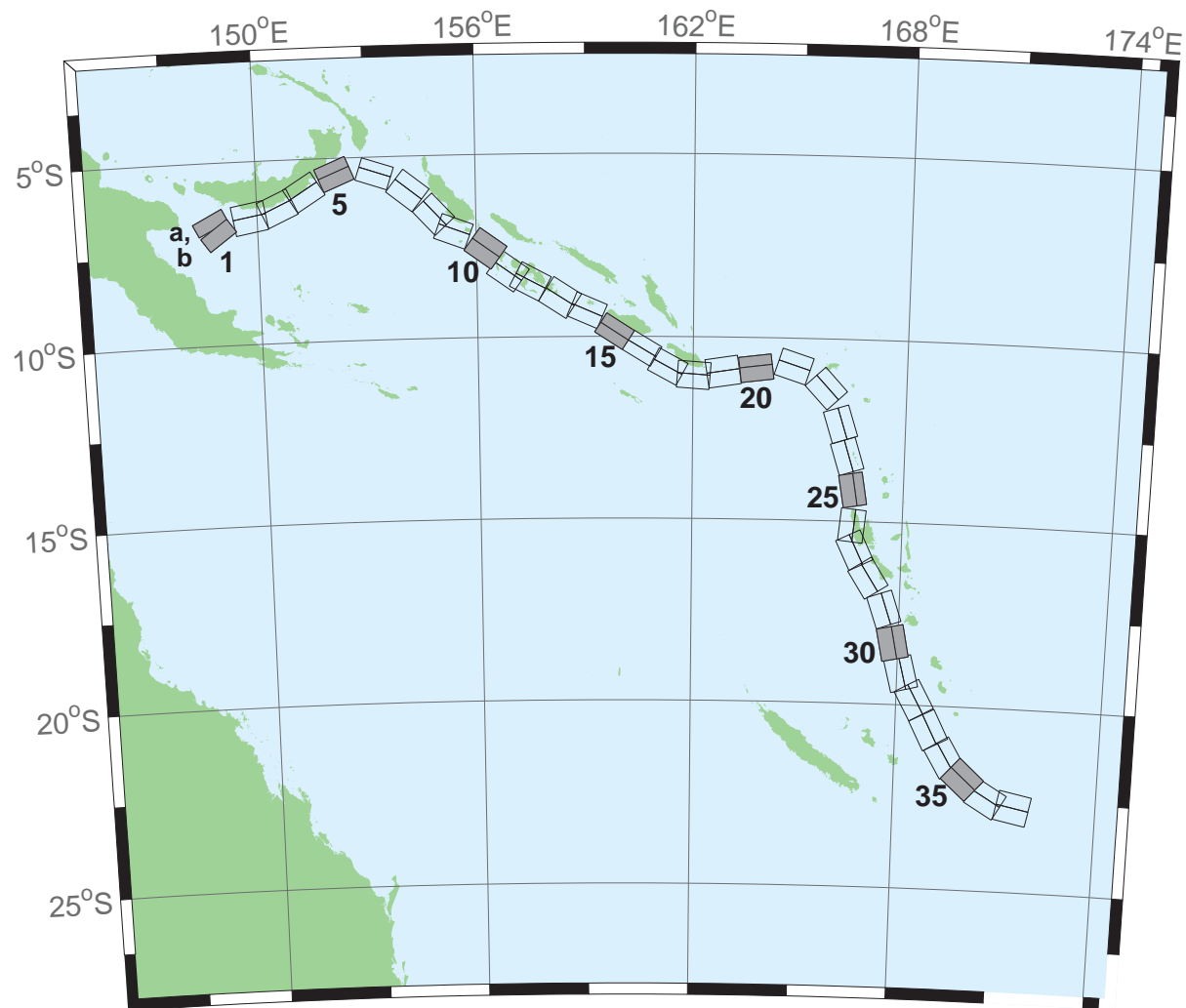


Figure B8: New Britain-Solomons-Vanuatu Subduction Zone unit sources.

Table B8: Earthquake parameters for New Britain-Solomons-Vanuatu Subduction Zone unit sources.

Segment	Description	Longitude (°E)	Latitude (°N)	Strike (°)	Dip (°)	Depth (km)
nvsz-1a	New Britain-Solomons-Vanuatu	148.6217	-6.4616	243.2	32.34	15.69
nvsz-1b	New Britain-Solomons-Vanuatu	148.7943	-6.8002	234.2	12.34	5
nvsz-2a	New Britain-Solomons-Vanuatu	149.7218	-6.1459	260.1	35.1	16.36
nvsz-2b	New Britain-Solomons-Vanuatu	149.7856	-6.5079	260.1	13.13	5
nvsz-3a	New Britain-Solomons-Vanuatu	150.4075	-5.9659	245.7	42.35	18.59
nvsz-3b	New Britain-Solomons-Vanuatu	150.5450	-6.2684	245.7	15.77	5
nvsz-4a	New Britain-Solomons-Vanuatu	151.1095	-5.5820	238.2	42.41	23.63
nvsz-4b	New Britain-Solomons-Vanuatu	151.2851	-5.8639	238.2	21.88	5
nvsz-5a	New Britain-Solomons-Vanuatu	152.0205	-5.1305	247.7	49.22	32.39
nvsz-5b	New Britain-Solomons-Vanuatu	152.1322	-5.4020	247.7	33.22	5
nvsz-6a	New Britain-Solomons-Vanuatu	153.3450	-5.1558	288.6	53.53	33.59
nvsz-6b	New Britain-Solomons-Vanuatu	153.2595	-5.4089	288.6	34.87	5
nvsz-7a	New Britain-Solomons-Vanuatu	154.3814	-5.6308	308.3	39.72	19.18
nvsz-7b	New Britain-Solomons-Vanuatu	154.1658	-5.9017	308.3	16.48	5
nvsz-8a	New Britain-Solomons-Vanuatu	155.1097	-6.3511	317.2	45.33	22.92
nvsz-8b	New Britain-Solomons-Vanuatu	154.8764	-6.5656	317.2	21	5
nvsz-9a	New Britain-Solomons-Vanuatu	155.5027	-6.7430	290.5	48.75	22.92
nvsz-9b	New Britain-Solomons-Vanuatu	155.3981	-7.0204	290.5	21	5
nvsz-10a	New Britain-Solomons-Vanuatu	156.4742	-7.2515	305.9	36.88	27.62
nvsz-10b	New Britain-Solomons-Vanuatu	156.2619	-7.5427	305.9	26.9	5
nvsz-11a	New Britain-Solomons-Vanuatu	157.0830	-7.8830	305.4	32.97	29.72
nvsz-11b	New Britain-Solomons-Vanuatu	156.8627	-8.1903	305.4	29.63	5
nvsz-12a	New Britain-Solomons-Vanuatu	157.6537	-8.1483	297.9	37.53	28.57
nvsz-12b	New Britain-Solomons-Vanuatu	157.4850	-8.4630	297.9	28.13	5
nvsz-13a	New Britain-Solomons-Vanuatu	158.5089	-8.5953	302.7	33.62	23.02
nvsz-13b	New Britain-Solomons-Vanuatu	158.3042	-8.9099	302.7	21.12	5
nvsz-14a	New Britain-Solomons-Vanuatu	159.1872	-8.9516	293.3	38.44	34.06
nvsz-14b	New Britain-Solomons-Vanuatu	159.0461	-9.2747	293.3	35.54	5
nvsz-15a	New Britain-Solomons-Vanuatu	159.9736	-9.5993	302.8	46.69	41.38
nvsz-15b	New Britain-Solomons-Vanuatu	159.8044	-9.8584	302.8	46.69	5
nvsz-16a	New Britain-Solomons-Vanuatu	160.7343	-10.0574	301	46.05	41
nvsz-16b	New Britain-Solomons-Vanuatu	160.5712	-10.3246	301	46.05	5
nvsz-17a	New Britain-Solomons-Vanuatu	161.4562	-10.5241	298.4	40.12	37.22
nvsz-17b	New Britain-Solomons-Vanuatu	161.2900	-10.8263	298.4	40.12	5
nvsz-18a	New Britain-Solomons-Vanuatu	162.0467	-10.6823	274.1	40.33	29.03
nvsz-18b	New Britain-Solomons-Vanuatu	162.0219	-11.0238	274.1	28.72	5
nvsz-19a	New Britain-Solomons-Vanuatu	162.7818	-10.5645	261.3	34.25	24.14
nvsz-19b	New Britain-Solomons-Vanuatu	162.8392	-10.9315	261.3	22.51	5
nvsz-20a	New Britain-Solomons-Vanuatu	163.7222	-10.5014	262.9	50.35	26.3
nvsz-20b	New Britain-Solomons-Vanuatu	163.7581	-10.7858	262.9	25.22	5
nvsz-21a	New Britain-Solomons-Vanuatu	164.9445	-10.4183	287.9	40.31	23.3
nvsz-21b	New Britain-Solomons-Vanuatu	164.8374	-10.7442	287.9	21.47	5
nvsz-22a	New Britain-Solomons-Vanuatu	166.0261	-11.1069	317.1	42.39	20.78
nvsz-22b	New Britain-Solomons-Vanuatu	165.7783	-11.3328	317.1	18.4	5
nvsz-23a	New Britain-Solomons-Vanuatu	166.5179	-12.2260	342.4	47.95	22.43
nvsz-23b	New Britain-Solomons-Vanuatu	166.2244	-12.3171	342.4	20.4	5
nvsz-24a	New Britain-Solomons-Vanuatu	166.7236	-13.1065	342.6	47.13	28.52
nvsz-24b	New Britain-Solomons-Vanuatu	166.4241	-13.1979	342.6	28.06	5
nvsz-25a	New Britain-Solomons-Vanuatu	166.8914	-14.0785	350.3	54.1	31.16
nvsz-25b	New Britain-Solomons-Vanuatu	166.6237	-14.1230	350.3	31.55	5
nvsz-26a	New Britain-Solomons-Vanuatu	166.9200	-15.1450	365.6	50.46	29.05
nvsz-26b	New Britain-Solomons-Vanuatu	166.6252	-15.1170	365.6	28.75	5
nvsz-27a	New Britain-Solomons-Vanuatu	167.0053	-15.6308	334.2	44.74	25.46
nvsz-27b	New Britain-Solomons-Vanuatu	166.7068	-15.7695	334.2	24.15	5
nvsz-28a	New Britain-Solomons-Vanuatu	167.4074	-16.3455	327.5	41.53	22.44

(continued on next page)

Table B8: (continued)

Segment	Description	Longitude (°E)	Latitude (°N)	Strike (°)	Dip (°)	Depth (km)
nvsz-28b	New Britain-Solomons-Vanuatu	167.1117	-16.5264	327.5	20.42	5
nvsz-29a	New Britain-Solomons-Vanuatu	167.9145	-17.2807	341.2	49.1	24.12
nvsz-29b	New Britain-Solomons-Vanuatu	167.6229	-17.3757	341.2	22.48	5
nvsz-30a	New Britain-Solomons-Vanuatu	168.2220	-18.2353	348.6	44.19	23.99
nvsz-30b	New Britain-Solomons-Vanuatu	167.8895	-18.2991	348.6	22.32	5
nvsz-31a	New Britain-Solomons-Vanuatu	168.5022	-19.0510	345.6	42.2	22.26
nvsz-31b	New Britain-Solomons-Vanuatu	168.1611	-19.1338	345.6	20.2	5
nvsz-32a	New Britain-Solomons-Vanuatu	168.8775	-19.6724	331.1	42.03	21.68
nvsz-32b	New Britain-Solomons-Vanuatu	168.5671	-19.8338	331.1	19.49	5
nvsz-33a	New Britain-Solomons-Vanuatu	169.3422	-20.4892	332.9	40.25	22.4
nvsz-33b	New Britain-Solomons-Vanuatu	169.0161	-20.6453	332.9	20.37	5
nvsz-34a	New Britain-Solomons-Vanuatu	169.8304	-21.2121	329.1	39	22.73
nvsz-34b	New Britain-Solomons-Vanuatu	169.5086	-21.3911	329.1	20.77	5
nvsz-35a	New Britain-Solomons-Vanuatu	170.3119	-21.6945	311.9	39	22.13
nvsz-35b	New Britain-Solomons-Vanuatu	170.0606	-21.9543	311.9	20.03	5
nvsz-36a	New Britain-Solomons-Vanuatu	170.9487	-22.1585	300.4	39.42	23.5
nvsz-36b	New Britain-Solomons-Vanuatu	170.7585	-22.4577	300.4	21.71	5
nvsz-37a	New Britain-Solomons-Vanuatu	171.6335	-22.3087	281.3	30	22.1
nvsz-37b	New Britain-Solomons-Vanuatu	171.5512	-22.6902	281.3	20	5

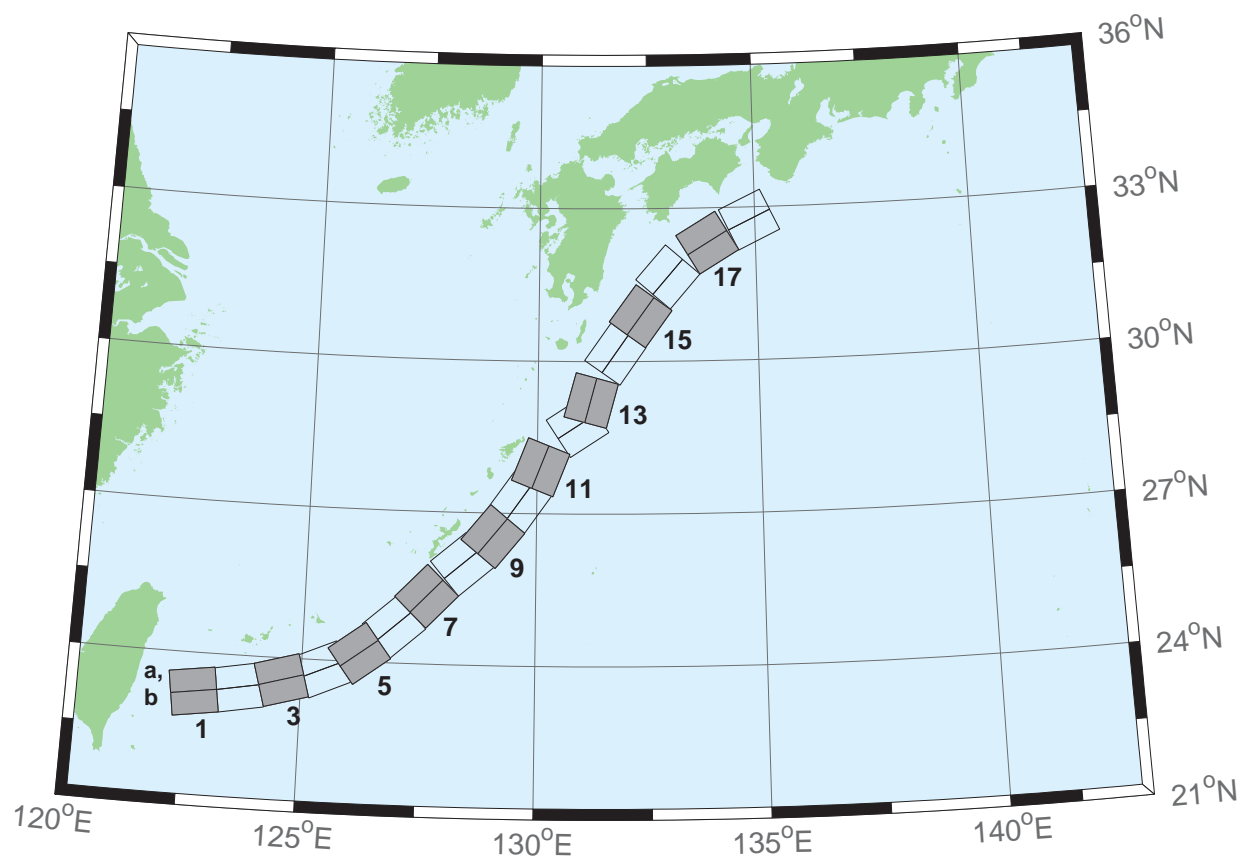


Figure B9: Ryukyu-Kyushu-Nankai Subduction Zone unit sources.

Table B9: Earthquake parameters for Ryukyu-Kyushu-Nankai Subduction Zone unit sources.

Segment	Description	Longitude (°E)	Latitude (°N)	Strike (°)	Dip (°)	Depth (km)
rnsz-1a	Ryukyu-Kyushu-Nankai	122.6672	23.6696	262	14	11.88
rnsz-1b	Ryukyu-Kyushu-Nankai	122.7332	23.2380	262	10	3.2
rnsz-2a	Ryukyu-Kyushu-Nankai	123.5939	23.7929	259.9	18.11	12.28
rnsz-2b	Ryukyu-Kyushu-Nankai	123.6751	23.3725	259.9	10	3.6
rnsz-3a	Ryukyu-Kyushu-Nankai	124.4604	23.9777	254.6	19.27	14.65
rnsz-3b	Ryukyu-Kyushu-Nankai	124.5830	23.5689	254.6	12.18	4.1
rnsz-4a	Ryukyu-Kyushu-Nankai	125.2720	24.2102	246.8	18	20.38
rnsz-4b	Ryukyu-Kyushu-Nankai	125.4563	23.8177	246.8	16	6.6
rnsz-5a	Ryukyu-Kyushu-Nankai	125.9465	24.5085	233.6	18	20.21
rnsz-5b	Ryukyu-Kyushu-Nankai	126.2241	24.1645	233.6	16	6.43
rnsz-6a	Ryukyu-Kyushu-Nankai	126.6349	25.0402	228.7	17.16	19.55
rnsz-6b	Ryukyu-Kyushu-Nankai	126.9465	24.7176	228.7	15.16	6.47
rnsz-7a	Ryukyu-Kyushu-Nankai	127.2867	25.6343	224	15.85	17.98
rnsz-7b	Ryukyu-Kyushu-Nankai	127.6303	25.3339	224	13.56	6.26
rnsz-8a	Ryukyu-Kyushu-Nankai	128.0725	26.3146	229.7	14.55	14.31
rnsz-8b	Ryukyu-Kyushu-Nankai	128.3854	25.9831	229.7	9.64	5.94
rnsz-9a	Ryukyu-Kyushu-Nankai	128.6642	26.8177	219.2	15.4	12.62
rnsz-9b	Ryukyu-Kyushu-Nankai	129.0391	26.5438	219.2	8	5.66
rnsz-10a	Ryukyu-Kyushu-Nankai	129.2286	27.4879	215.2	17	12.55
rnsz-10b	Ryukyu-Kyushu-Nankai	129.6233	27.2402	215.2	8.16	5.45
rnsz-11a	Ryukyu-Kyushu-Nankai	129.6169	28.0741	201.3	17	12.91
rnsz-11b	Ryukyu-Kyushu-Nankai	130.0698	27.9181	201.3	8.8	5.26
rnsz-12a	Ryukyu-Kyushu-Nankai	130.6175	29.0900	236.7	16.42	13.05
rnsz-12b	Ryukyu-Kyushu-Nankai	130.8873	28.7299	236.7	9.57	4.74
rnsz-13a	Ryukyu-Kyushu-Nankai	130.7223	29.3465	195.2	20.25	15.89
rnsz-13b	Ryukyu-Kyushu-Nankai	131.1884	29.2362	195.2	12.98	4.66
rnsz-14a	Ryukyu-Kyushu-Nankai	131.3467	30.3899	215.1	22.16	19.73
rnsz-14b	Ryukyu-Kyushu-Nankai	131.7402	30.1507	215.1	17.48	4.71
rnsz-15a	Ryukyu-Kyushu-Nankai	131.9149	31.1450	216	15.11	16.12
rnsz-15b	Ryukyu-Kyushu-Nankai	132.3235	30.8899	216	13.46	4.48
rnsz-16a	Ryukyu-Kyushu-Nankai	132.5628	31.9468	220.9	10.81	10.88
rnsz-16b	Ryukyu-Kyushu-Nankai	132.9546	31.6579	220.9	7.19	4.62
rnsz-17a	Ryukyu-Kyushu-Nankai	133.6125	32.6956	239	10.14	12.01
rnsz-17b	Ryukyu-Kyushu-Nankai	133.8823	32.3168	239	8.41	4.7
rnsz-18a	Ryukyu-Kyushu-Nankai	134.6416	33.1488	244.7	10.99	14.21
rnsz-18b	Ryukyu-Kyushu-Nankai	134.8656	32.7502	244.5	10.97	4.7

Appendix C. Synthetic Testing Report: Kahului, Hawaii

Author: Lindsey Wright

1.0 PURPOSE

Forecast models are tested with synthetic tsunami events covering a range of tsunami source locations and magnitudes ranging from mega-events to micro-events. Testing is also done with selected historical tsunami events when available.

The purpose of forecast model testing is three-fold. The first objective is to assure that the results obtained with the Short-term Inundation Forecasting of Tsunamis (SIFT) forecast software, which has been released to the Tsunami Warning Centers for operational use, are identical or close to those obtained by the researcher during the development of the forecast model. The second objective is to test the forecast model for consistency, accuracy, time efficiency, and quality of results over a range of possible tsunami locations and magnitudes. The third objective is to identify bugs and issues in need of resolution by the researcher who developed the Forecast Model or by the SIFT software development team before the next version release to NOAA's two Tsunami Warning Centers.

Local hardware and software applications, and tools familiar to the researcher(s), are used to run the Method of Splitting Tsunamis (MOST) model during the forecast model development. The test results presented in this report lend confidence that the model performs as developed and produces the same results when initiated within the SIFT application in an operational setting as those produced by the researcher during the forecast model development. The test results assure those who rely on the Kahului tsunami forecast model that consistent results are produced irrespective of system.

2.0 TESTING PROCEDURE

The general procedure for forecast model testing is to run a set of synthetic tsunami scenarios and a selected set of historical tsunami events through the SIFT application and compare the results with those obtained by the researcher during the forecast model development and presented in the Tsunami Forecast Model Report. Specific steps taken to test the model include:

1. Identification of testing scenarios, including the standard set of synthetic events, appropriate historical events, and customized synthetic scenarios that may have been used by the researcher(s) in developing the forecast model.
2. Creation of new SIFT events to represent customized synthetic scenarios used by the researcher(s) in developing the forecast model, if any.
3. Submission of test model runs with SIFT, and export of the results from A, B, and C grids, along with time series.
4. Recording applicable metadata, including the specific SIFT version used for testing.
5. Examination of SIFT forecast model results for instabilities in both time series and plot results.
6. Comparison of forecast model results obtained through SIFT with those obtained during the forecast model development.
7. Summarization of results with specific mention of quality, consistency, and time efficiency.
8. Reporting of issues identified to modeler and SIFT software development team.

Retesting the forecast models in SIFT when reported issues have been addressed or explained.

Synthetic model runs were tested on a DELL PowerEdge R510 computer equipped with two Xeon E5670 processors at 2.93 Ghz, each with 12 MBytes of cache and 32GB memory. The processors are hex core and support hyperthreading, resulting in the computer performing as a 24 processor core machine. Additionally, the testing computer supports 10 Gigabit Ethernet for fast network connections. This computer configuration is similar or the same as the configurations of the computers installed at the Tsunami Warning Centers so the compute times should only vary slightly.

Results

The Kahului forecast model was tested with SIFT version 3.1, the current version installed at the NOAA Tsunami Warning Centers.

The Kahului, Hawaii forecast model was tested with twenty seven synthetic scenarios and two historical tsunami events. Test results from SIFT and comparisons with results obtained during the forecast model development are shown numerically in Table 1 and graphically in Figures 1 to 4. The results show that the forecast model is stable and robust, with consistent and high quality results across geographically distributed tsunami sources and tsunami magnitudes from micro-events to mega-events. The model run time (wall clock time) was 15.37 minutes for 7.98 hours of simulation time, and 7.68 minutes for 4.0 hours. This run time is within the 10 minute run time for 4 hours of simulation time and satisfies time efficiency requirements.

The standard suite of synthetic events was run on the Kahului forecast model. The modeled scenarios were stable for all cases tested, with no instabilities or ringing. Results show that the largest modeled height was 837 centimeters (cm) and originated in the Kamchatka-Yap-Mariana-Izu-Bonin (KISZ 1-10) source. Additionally, a 737cm wave amplitude was seen using the Aleutian-Alaska-Cascadia (ACSZ 16-25) source. Amplitudes greater than 300 cm were recorded at the Aleutian-Alaska-Cascadia (ACSZ 22-31), the Kamchatka-Yap-Mariana-Izu-Bonin (KISZ 32-41), and using the Manus OCB (MOSZ 1-10) source. In all of the mega-tsunami cases run, wave heights at the warning point were greater than 100 cm, with the smallest signal of 144 cm recorded with the Central and South American (CSSZ 1-10) source. Small scale events ($M_w = 7.5$) and the micro events tested were also stable. Direct comparisons of SIFT output with development results of both the historical events and synthetic events demonstrated that the wave pattern obtained during SIFT software testing were similar in shape to what the modeler produced during forecast model development of Kahului (Figs. C1-C4). The resulting maximum wave amplitudes from the M_w 9.3 tsunamis tended to be higher in the developmental results. One reason is the different versions of propagation database used. The Kahului forecast model was first developed in 2006. The boundary conditions for the M_w 9.3 tsunamis (velocity and amplitude) were extracted from propagation database 1.0 during the development. The current SIFT testing used database 3.1. For the historical and small tsunamis, the SIFT outputs agree well with the results obtained during model development.

Table 1. Table of maximum and minimum amplitudes (cm) at the Kahului, Hawaii warning point for synthetic and historical events tested using SIFT 3.1 and obtained during development.

Scenario Name	Source Zone	Tsunami Source	α [m]	SIFT Max (cm)	Development Max (cm)	SIFT Min (cm)	Development Min (cm)
Mega-tsunami Scenarios							
KISZ 1-10	Kamchatka-Yap-Mariana-Izu-Bonin	A1-A10, B1-B10	25	837.3	n/a	-208.0	n/a
KISZ 22-31	Kamchatka-Yap-Mariana-Izu-Bonin	A22-A31, B22-B31	25	287.8	n/a	-208.4	n/a
KISZ 32-41	Kamchatka-Yap-Mariana-Izu-Bonin	A32-A41, B32-B41	25	326.2	n/a	-209.1	n/a
KISZ 56-65	Kamchatka-Yap-Mariana-Izu-Bonin	A56-A65, B56-B65	25	176.1	n/a	-197.7	n/a
ACSZ 6-15	Aleutian-Alaska-Cascadia	A6-A15, B6-B15	25	292.4	n/a	-211.1	n/a
ASCZ 16-25	Aleutian-Alaska-Cascadia	A16-A25, B16-B25	25	737.1	n/a	-206.7	n/a
ASCZ 22-31	Aleutian-Alaska-Cascadia	A22-A31, B22-B31	25	365.8	n/a	-196.7	n/a
ASCZ 50-59	Aleutian-Alaska-Cascadia	A50-A59, B50-B59	25	607.7	n/a	-208.0	n/a
ASCZ 56-65	Aleutian-Alaska-Cascadia	A56-A65, B56-B65	25	208.5	n/a	-208.5	n/a
CSSZ 1-10	Central and South America	A1-A10, B1-B10	25	143.9	n/a	-197.4	n/a
CSSZ 37-46	Central and South America	A37-A46, B37-B46	25	152.2	n/a	-208.0	n/a
CSSZ 89-98	Central and South America	A89-A98, B89-B98	25	217.3	n/a	-194.2	n/a
CSSZ 102-111	Central and South America	A102-A111, B102-B111	25	274.2	n/a	-197.4	n/a
NTSZ 30-39	New Zealand-Kermadec-Tonga	A30-A39, B30-B39	25	191.6	n/a	-197.6	n/a
NVSZ 28-37	New Britain-Solomons-Vanuatu	A28-A37, B28-B37	25	233.6	n/a	-196.9	n/a
MOSZ 1-10	ManusOCB	A1-A10, B1-B10	25	339.0	n/a	-211.1	n/a
NGSZ 3-12	North New Guinea	A3-A12, B3-B12	25	170.1	n/a	-196.9	n/a
EPSZ 6-15	East Philippines	A6-A15, B6-B15	25	271.0	n/a	-197.1	n/a
RNSZ 12-21	Ryukus-Kyushu-Nankai	A12-A21, B12-B21	25	265.4	n/a	-197.3	n/a
KISZ 22-31	Kamchatka-Yap-Mariana-Izu-Bonin	A22-A31, B22-B31	29	329.8	285.6	-208.1	-197.8
ACSZ 22-31	Aleutian-Alaska-Cascadia	A22-A31, B22-B31	29	410.3	470.5	-197.2	-197.7
NTSZ 30-39	New Zealand-Kermadec-Tonga	A30-A39, B30-B39	29	193.1	205.5	-196.7	-197.1
EPSZ 6-15	East Philippines	A6-A15, B6-B15	29	304.6	350.5	-196.5	-197.9
Mw 7.5 Scenarios							
NTSZ B36	New Zealand-Kermadec-Tonga	B36	1	9.0	8.9	-10.5	-10.5
Micro-tsunami Scenarios							
EPS B19	East Philippines	B19	0.02	0.05	0.05	-0.05	-0.05
RNSZ B14	Ryukus-Kyushu-Nankai	B14	0.03	0.16	n/a	-0.17	n/a
ACSZ B6	Aleutian-Alaska-Cascadia	B6	0.02	0.11	0.12	-0.13	-0.14
Historical Events							
2006 Tonga	New Zealand-Kermadec-Tonga	6.6xb29	n/a	43.7	38.5	-41.9	-32.23
2006 Kuril	Kamchatka-Yap-Mariana-Izu-Bonin	4a12+5 b12+2a13+1.5b13	n/a	63.9	57.3	-62.3	-73.0

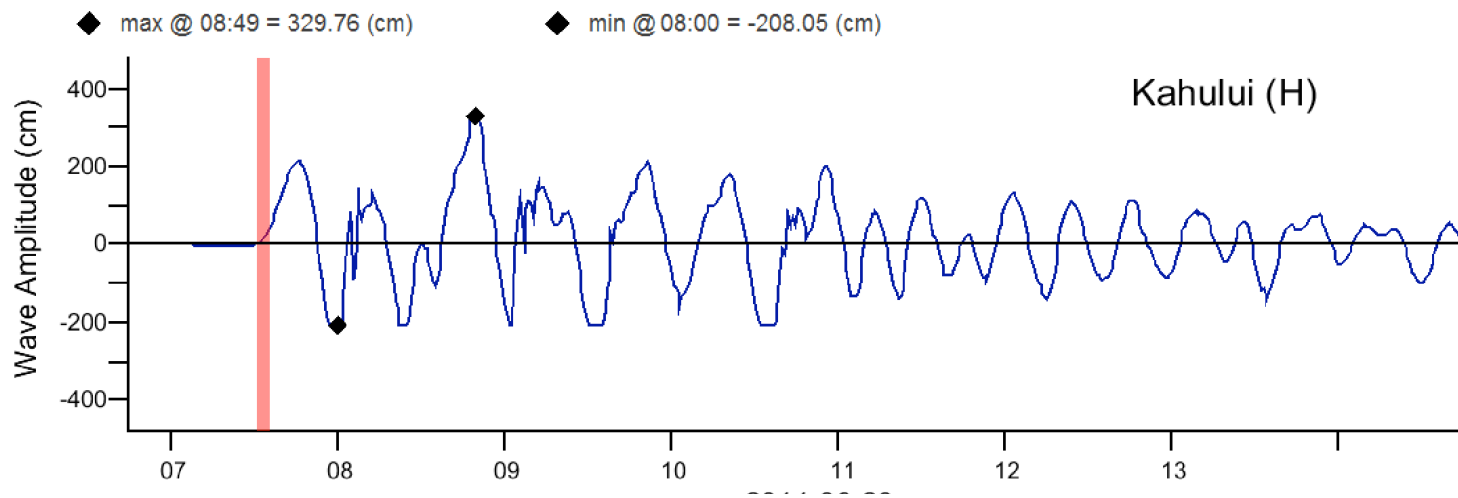
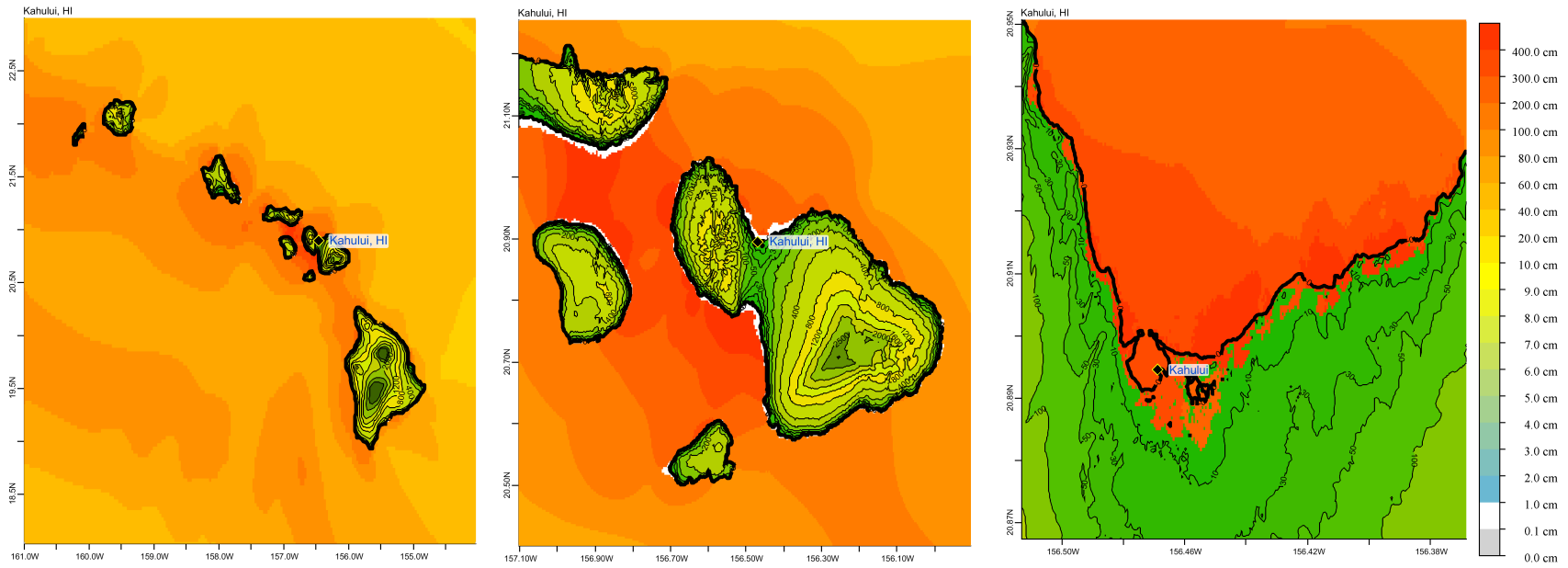


Figure C1: Response of the Kahului forecast model to synthetic scenario KISZ 32-41 ($\alpha=29$). Maximum sea surface elevation for (a) A-grid, b) B-grid, c) C-grid. Sea surface elevation time series at the C-grid warning point. (d) Sea surface elevation time series at the C-grid warning point.

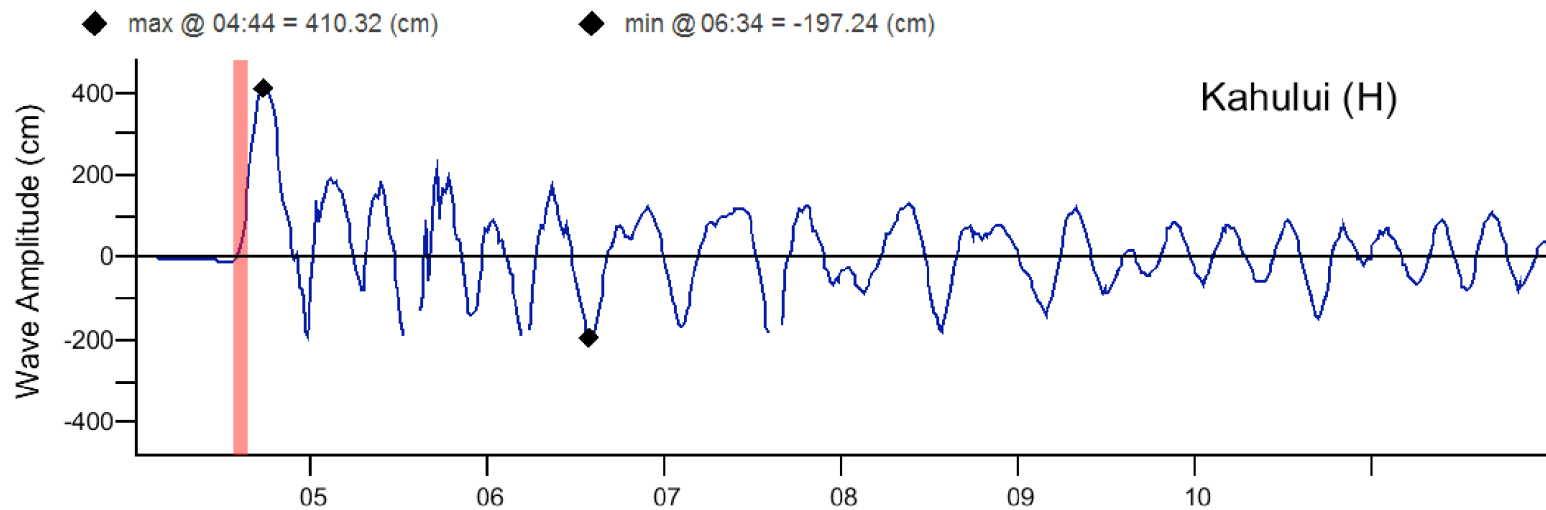
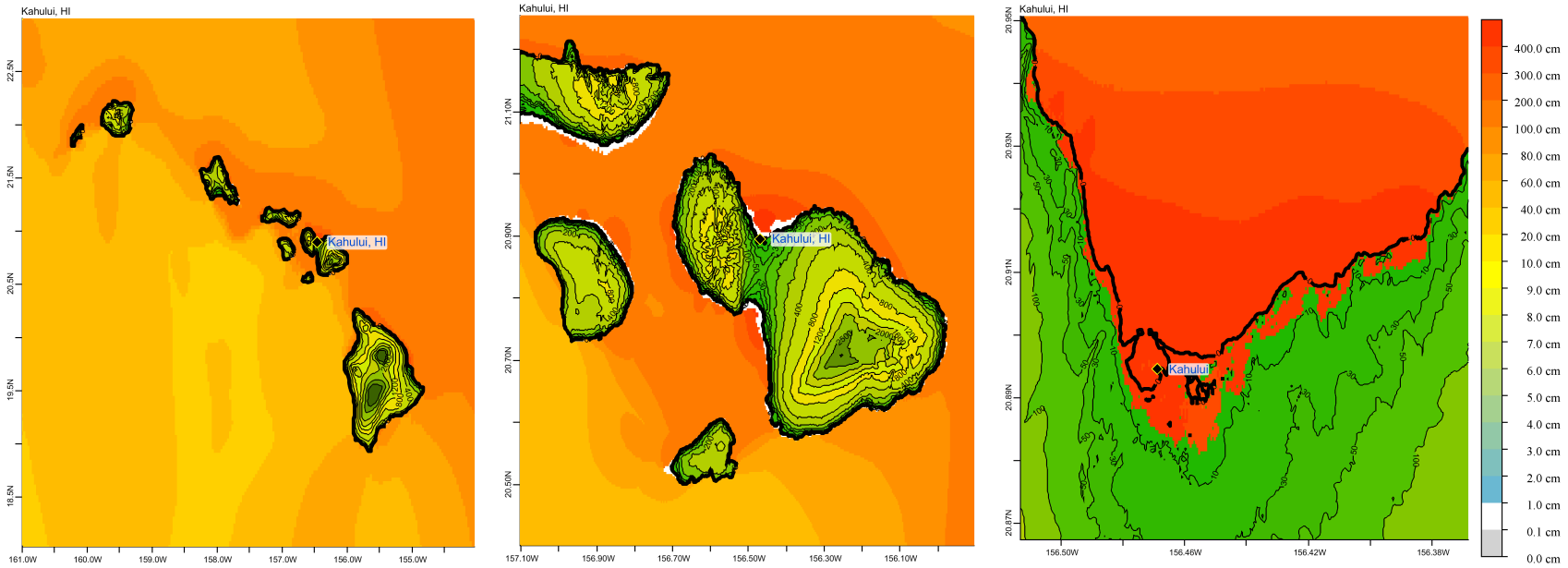


Figure C2: Response of the Kahului forecast model to synthetic scenario ACSZ 22-31 ($\alpha=29$). Maximum sea surface elevation for (a) A-grid, b) B-grid, c) C-grid. (d) Sea surface elevation time series at the C-grid warning point.

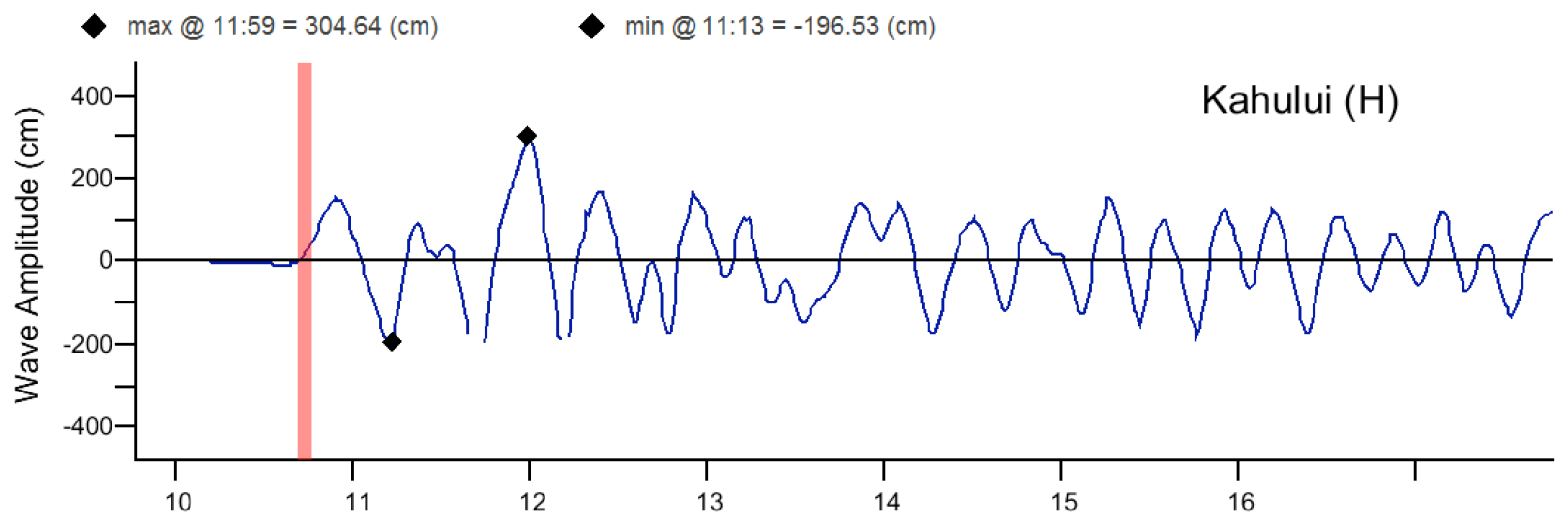
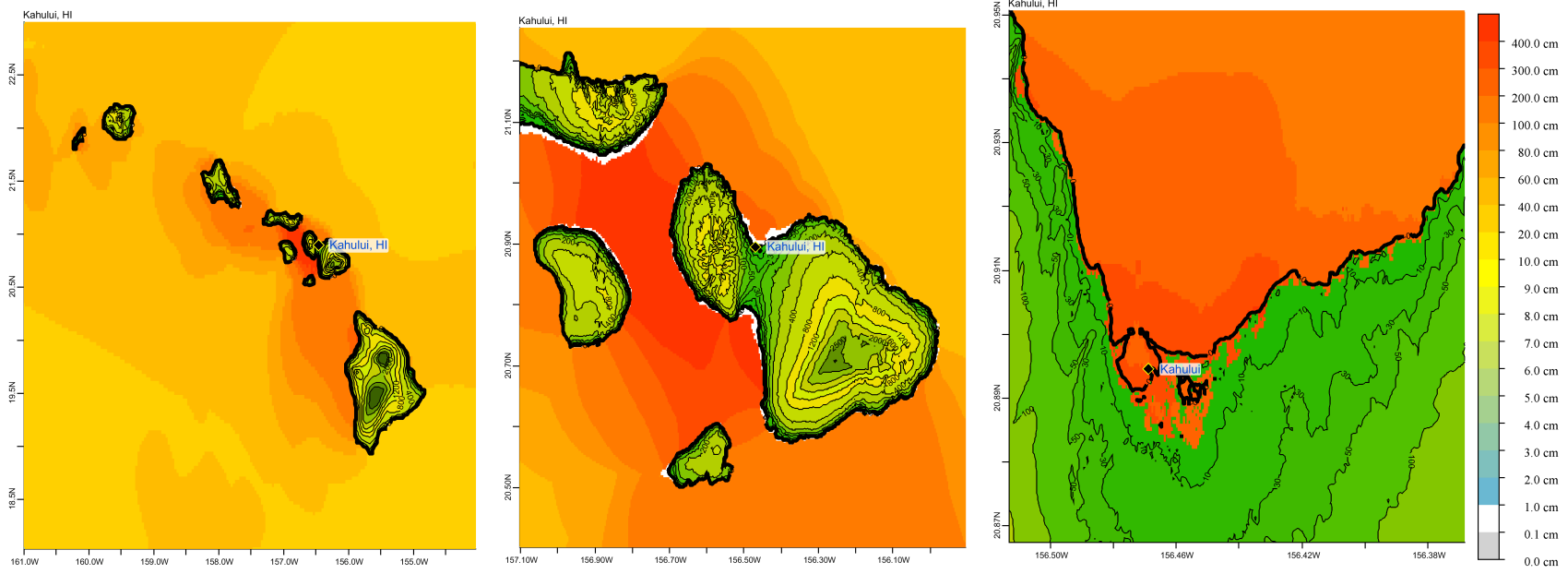


Figure C3: Response of the Kahului forecast model to synthetic scenario EPSZ 6-15 ($\alpha=29$). Maximum sea surface elevation for (a) A-grid, b) B-grid, c) C-grid. Sea surface elevation time series at the C-grid warning point (d).

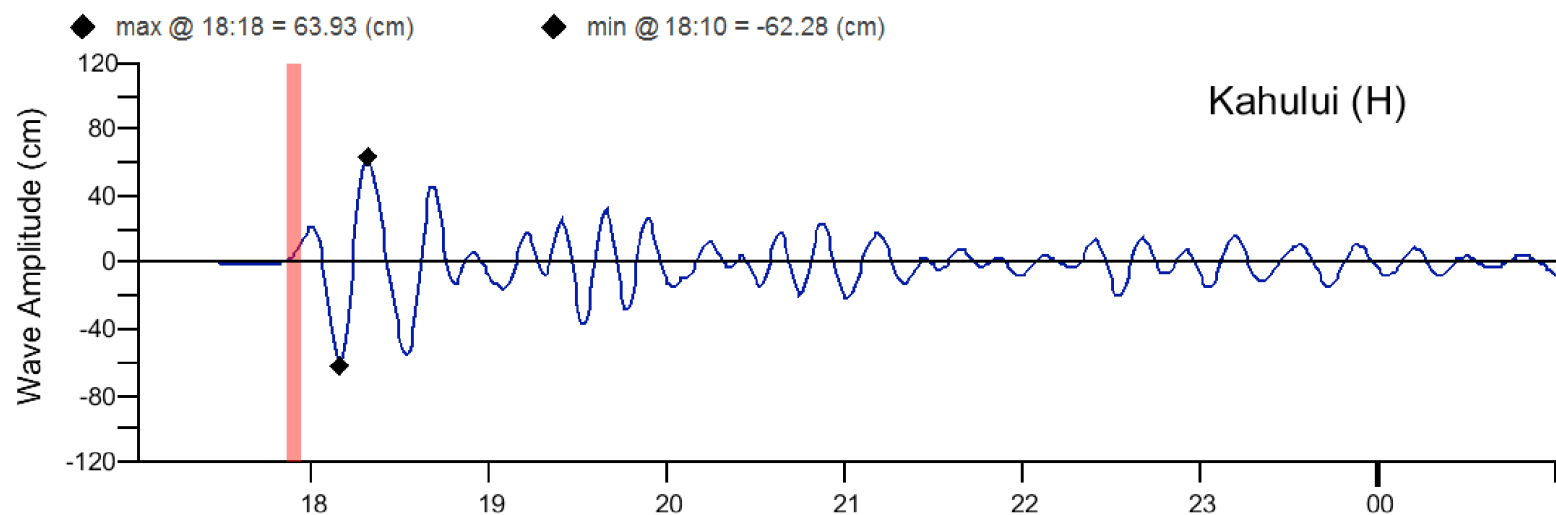
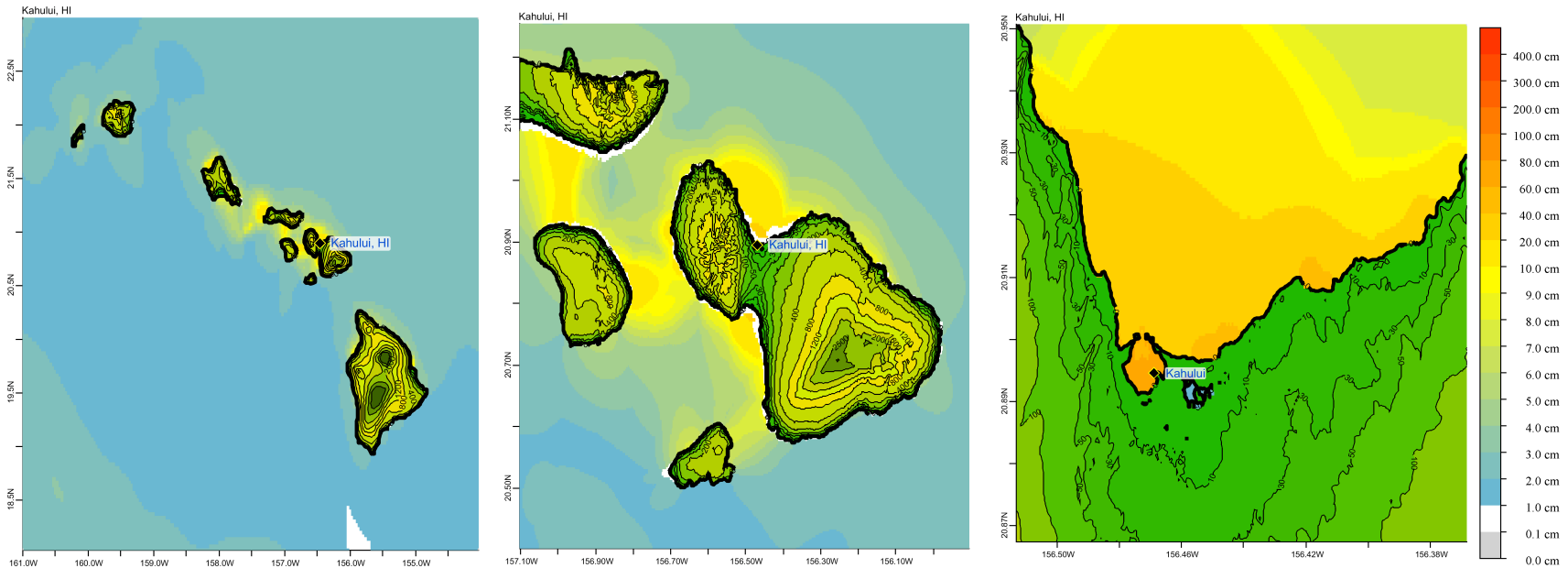


Figure C4: Response of the Kahului forecast model to the 2006 Kuril tsunami. Maximum sea surface elevation for (a) A-grid, b) B-grid, c) C-grid. Sea surface elevation time series at the C-grid warning point (d).